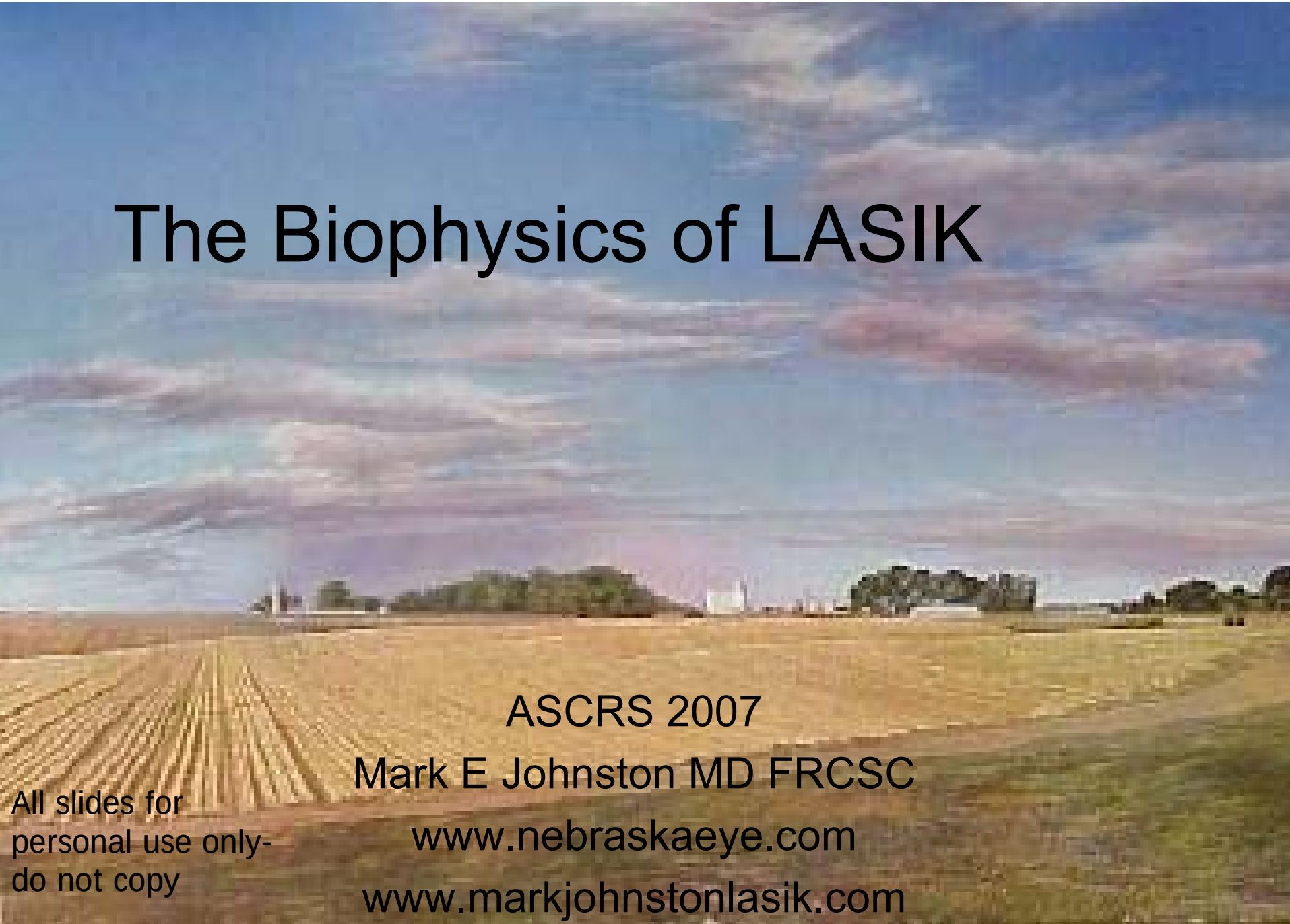

The Biophysics of LASIK

ASCRS 2007

Mark E Johnston MD FRCSC

www.nebraskaeye.com

www.markjohnstonlasik.com

PRK: Stromal cells

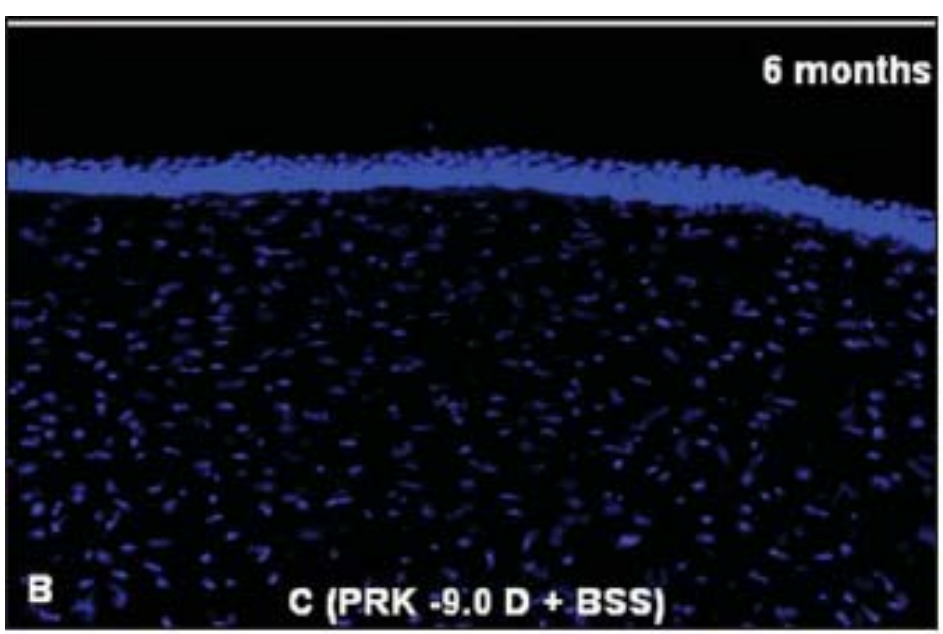

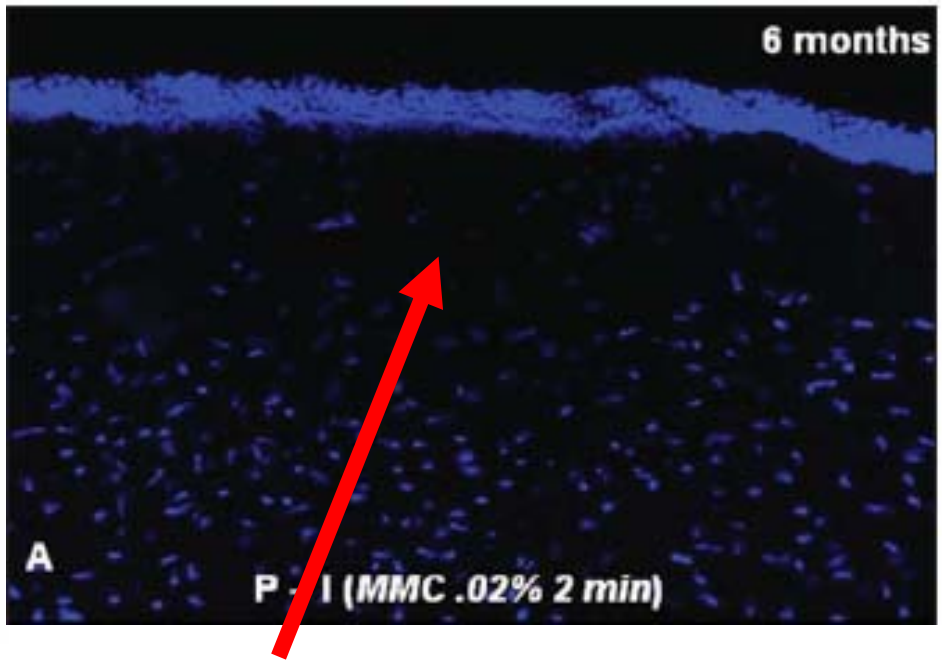

Without mitomycin

Cell death with mitomycin

Stromal cell culture: contact and contact inhibition

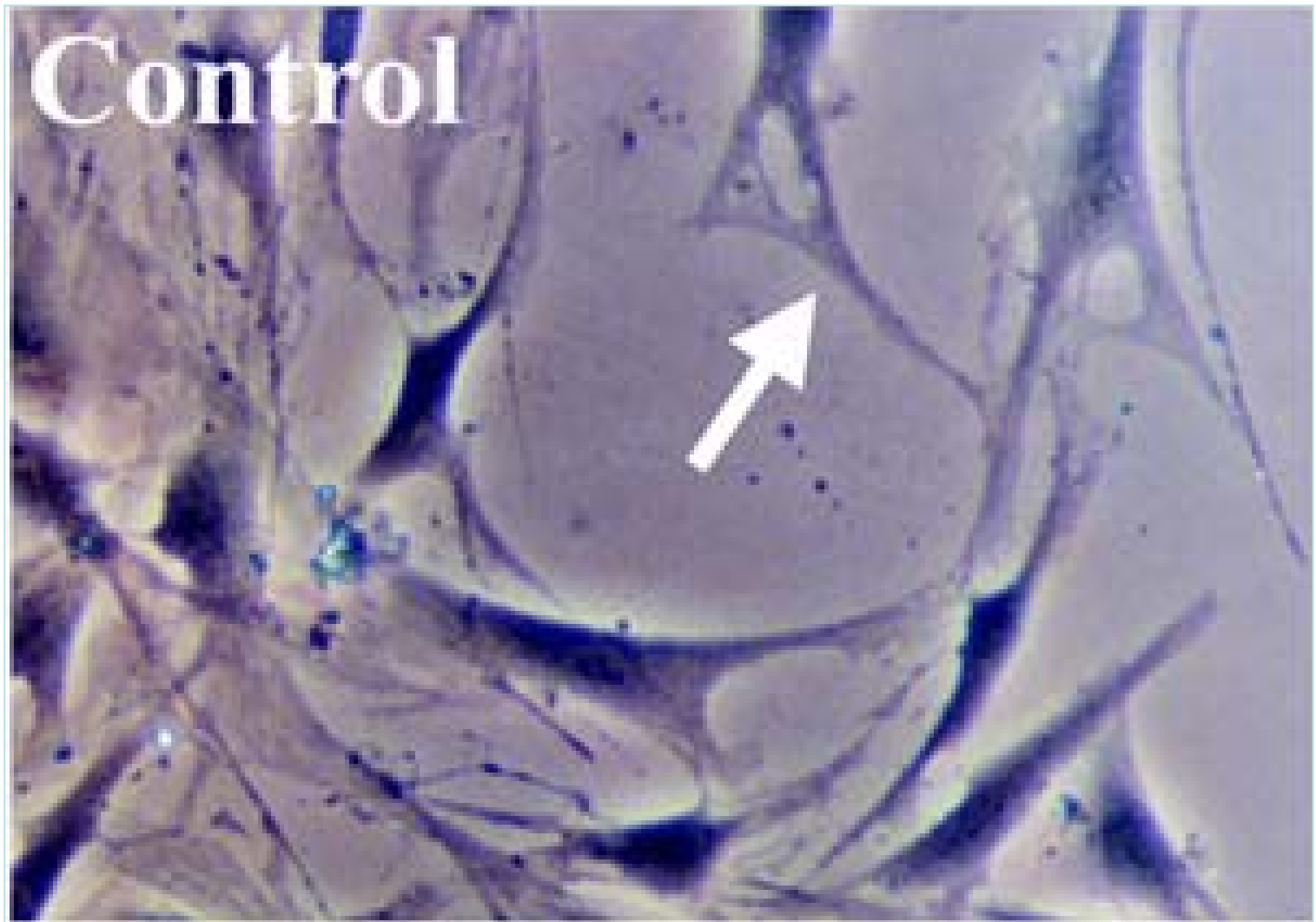

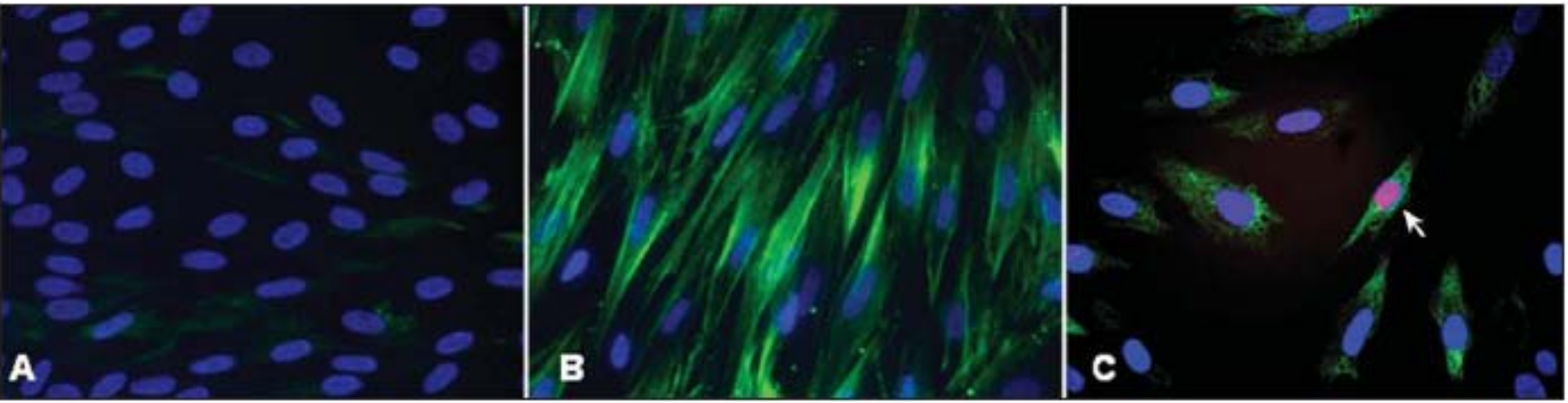

Figure 12. Mitomycin C-induced apoptosis of myofibroblasts in vitro. **A)** Keratocytes cultured in the absence of TGFβ1. Nuclei stain with DAPI, with no detectible α-smooth muscle actin-positive cells. **B)** Myofibroblasts generated in the presence of TGFβ1 stain green for α-smooth muscle actin, with nuclei staining with DAPI. **C)** After treatment of myofibroblasts with 0.02% mitomycin C for 2 minutes, cells undergo triple staining—immunohistochemistry for α-smooth muscle actin, TUNEL assay, and DAPI staining. Cells are shrunken and the nucleus of one cell (arrow) is stained with the TUNEL assay.

A. Normal keratocytes
B. Myofibroblasts- (can be induced by PRK)
C. Mitomycin treated

(Intra) Lasik induced interface fibrosis

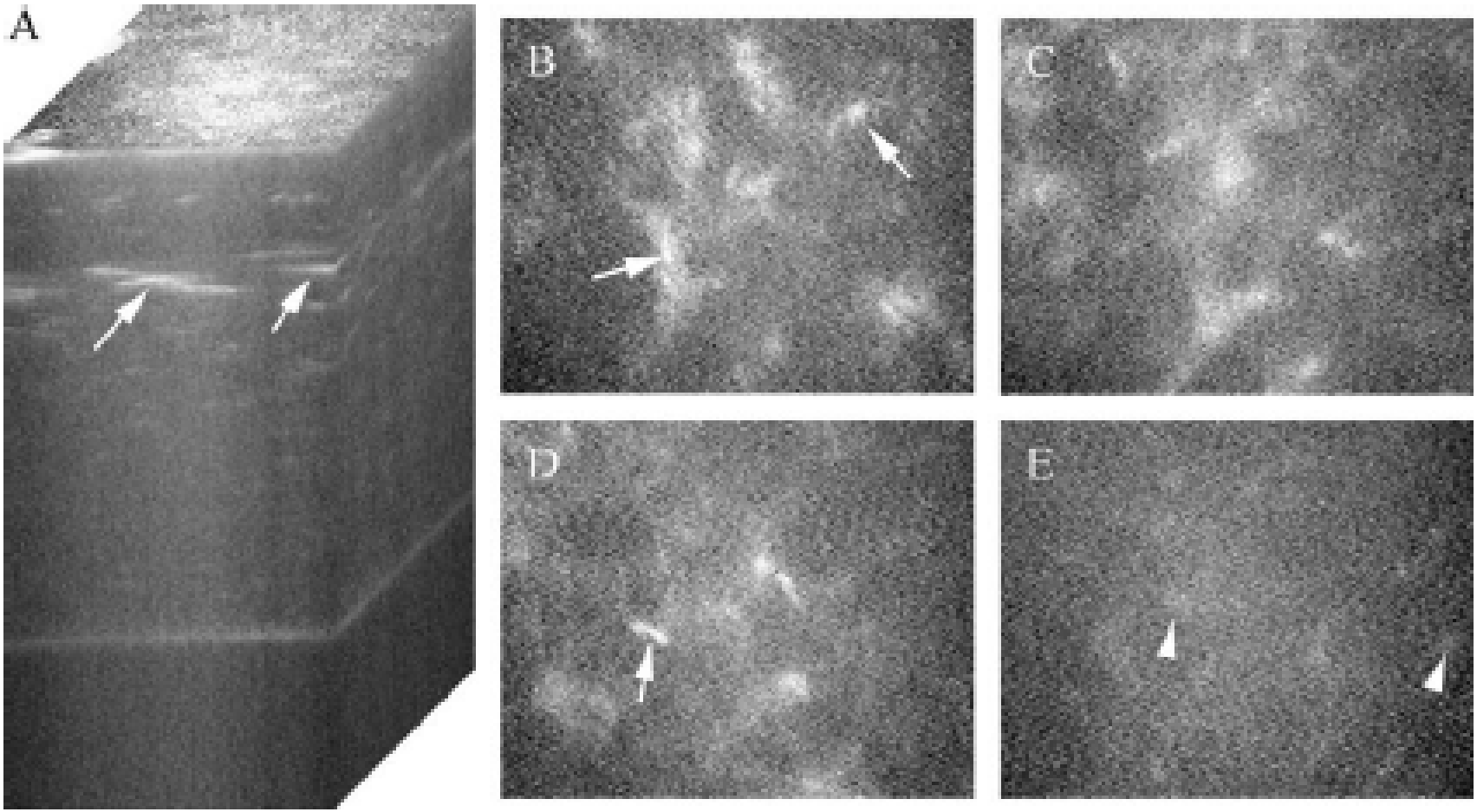

Cornea edema results in posterior corneal folds

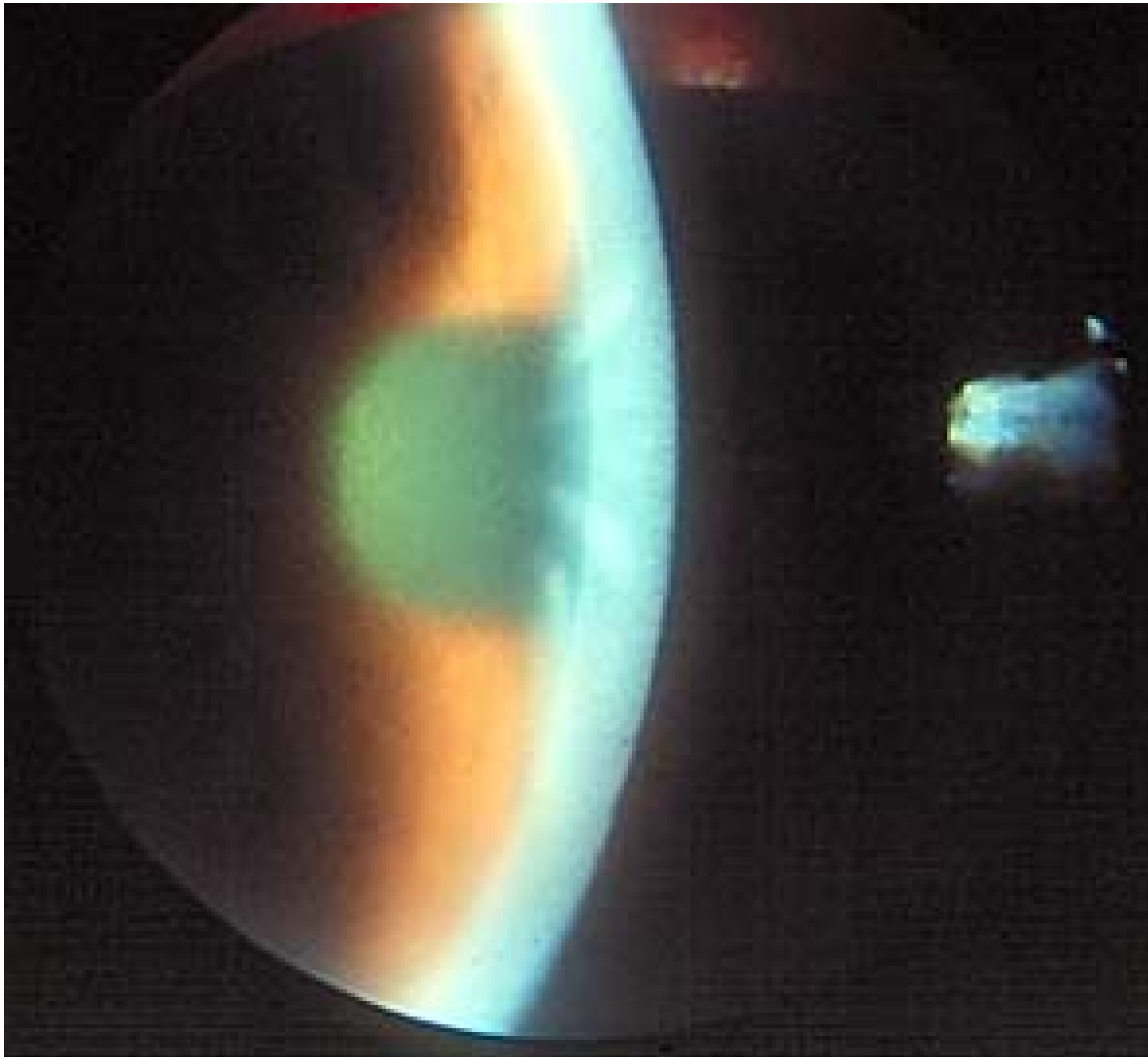

Epithelial/Bowman's barrier

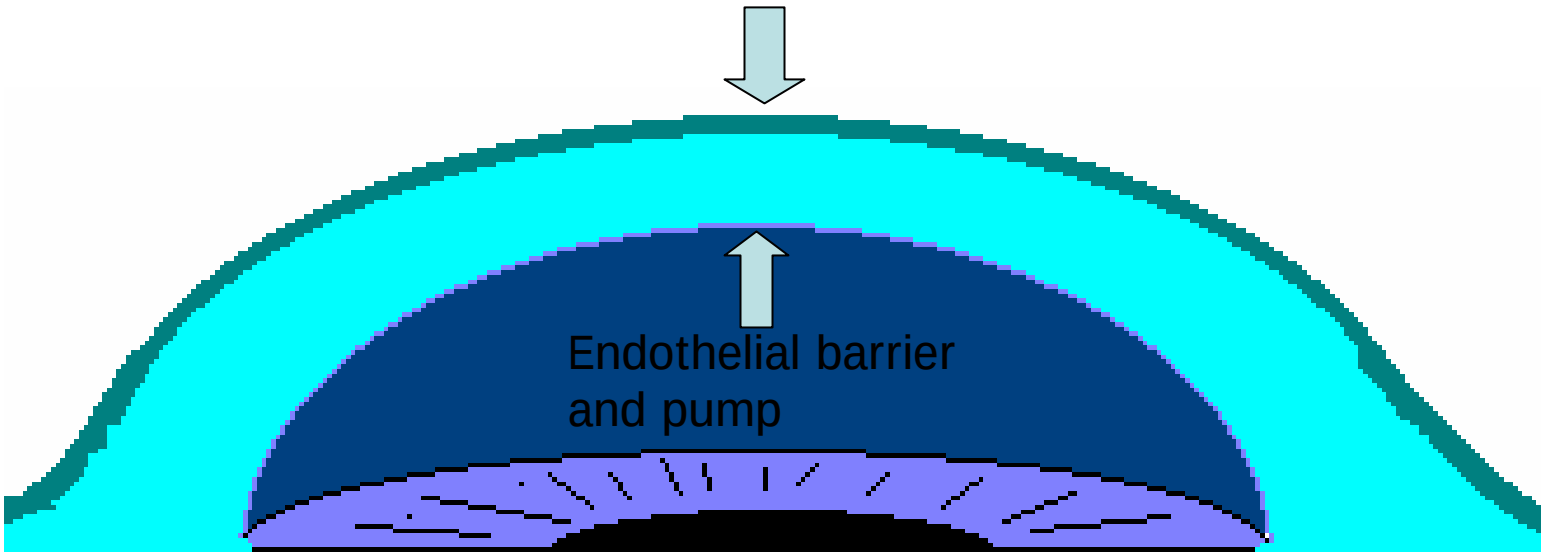

The normal cornea exists in a dehydrated state maintained by the epithelium and endothelium

Bowman's Membrane

- Resistant to swelling
  - Minimal corneal edema even with an epithelial defect
- Can be flattened over a LASIK bed
- **Cannot be steepened** (except by keratoconus)
  - Limits risk of significant ectasia

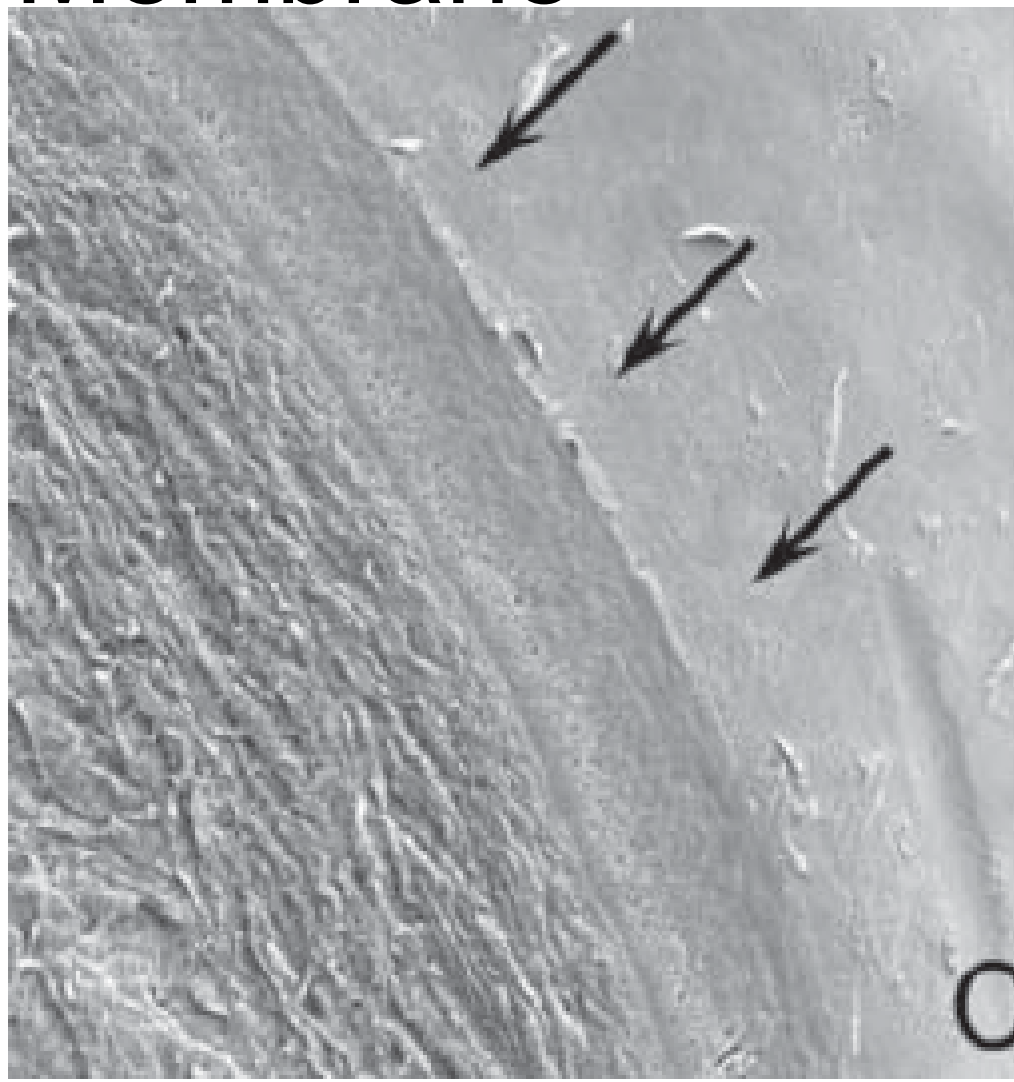

Collagen fibers
Light transmission made possible by regular arrangement

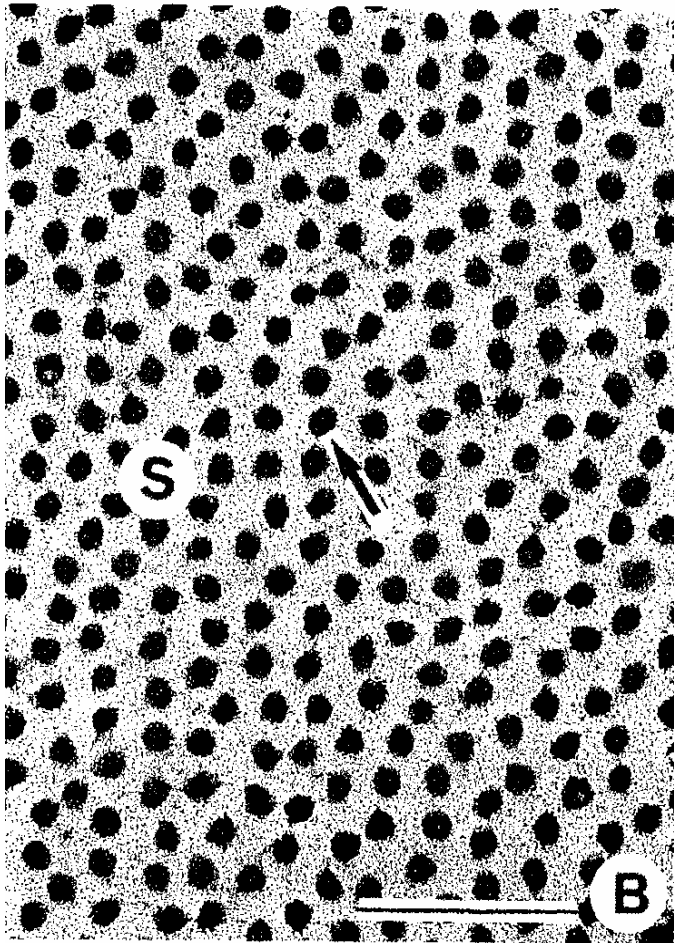

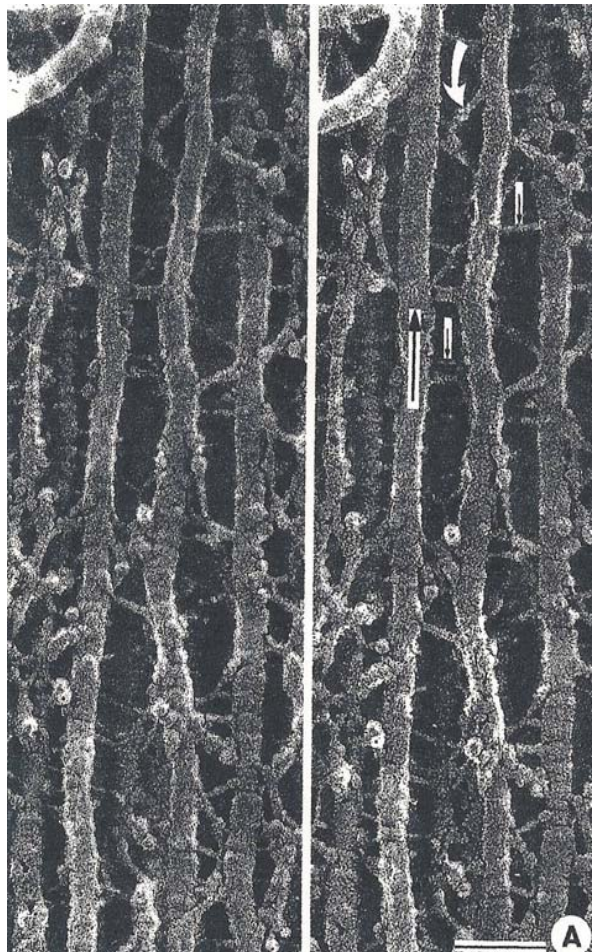

Stereo view: loose posterior cornea

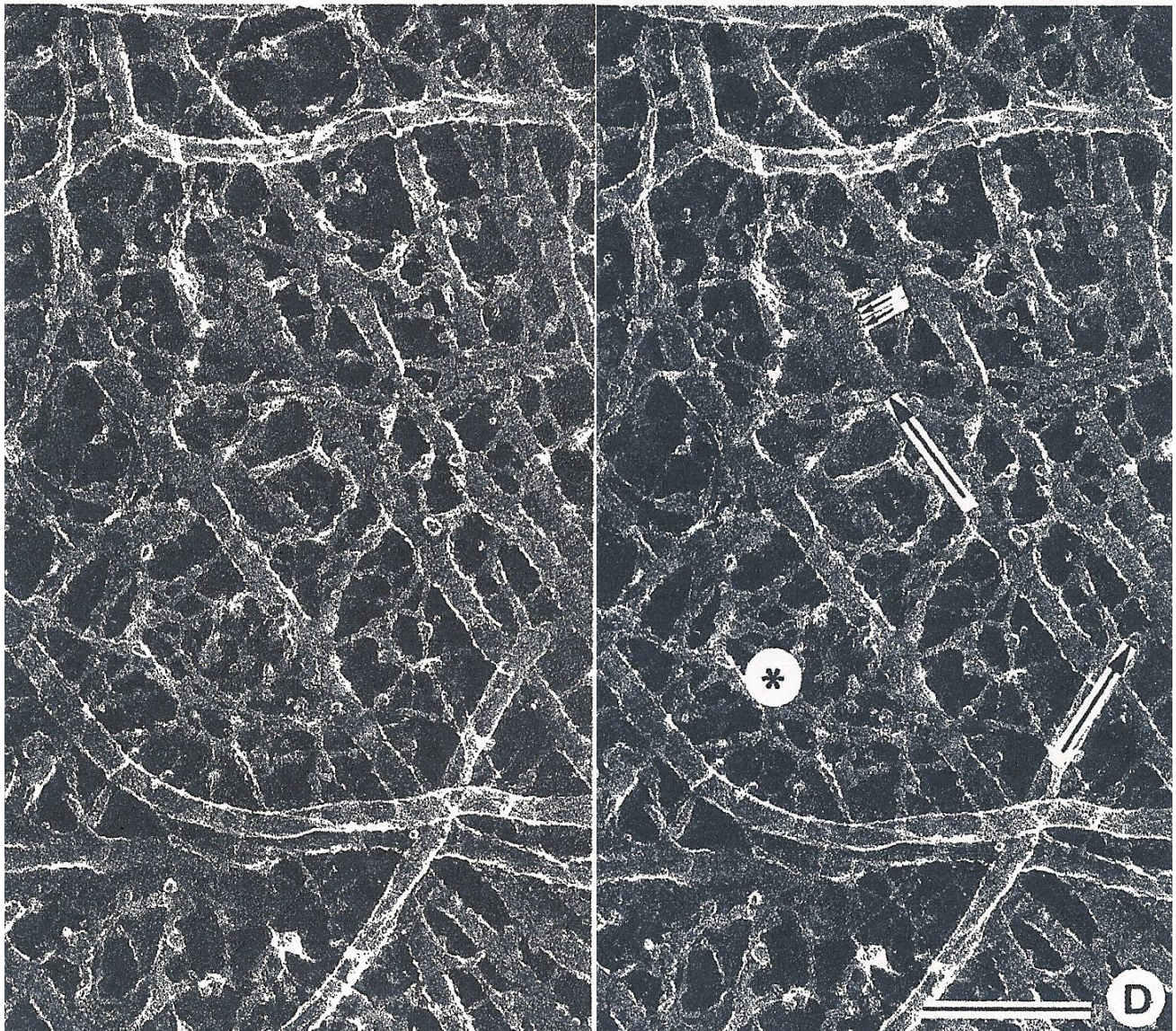

Examples of OCT light-backscattering two-dimensional images of the central cornea (1.13 mm) **before and after contact lens wear**

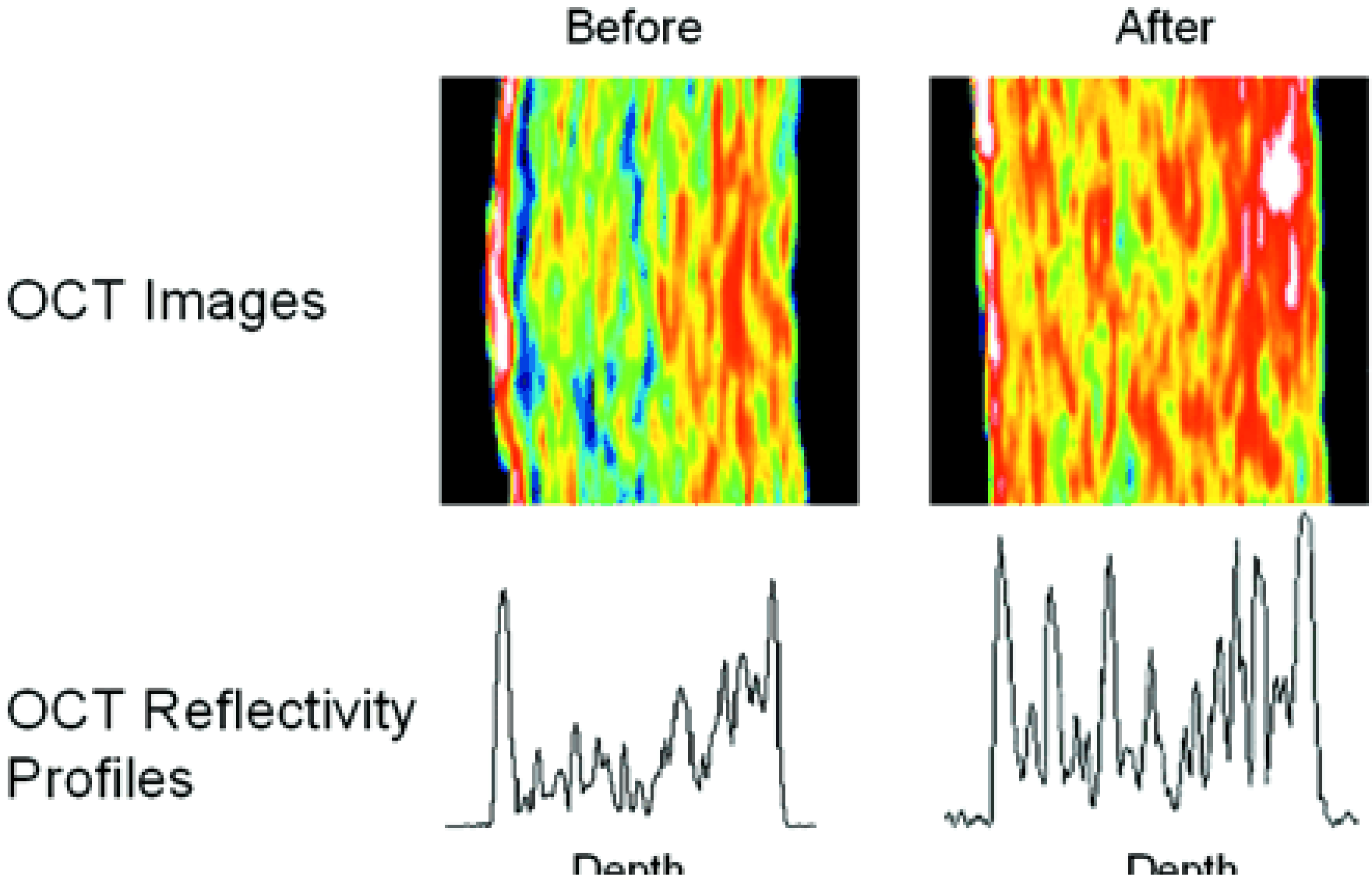

Central island

Central fluid pushed up by broad-beam laser

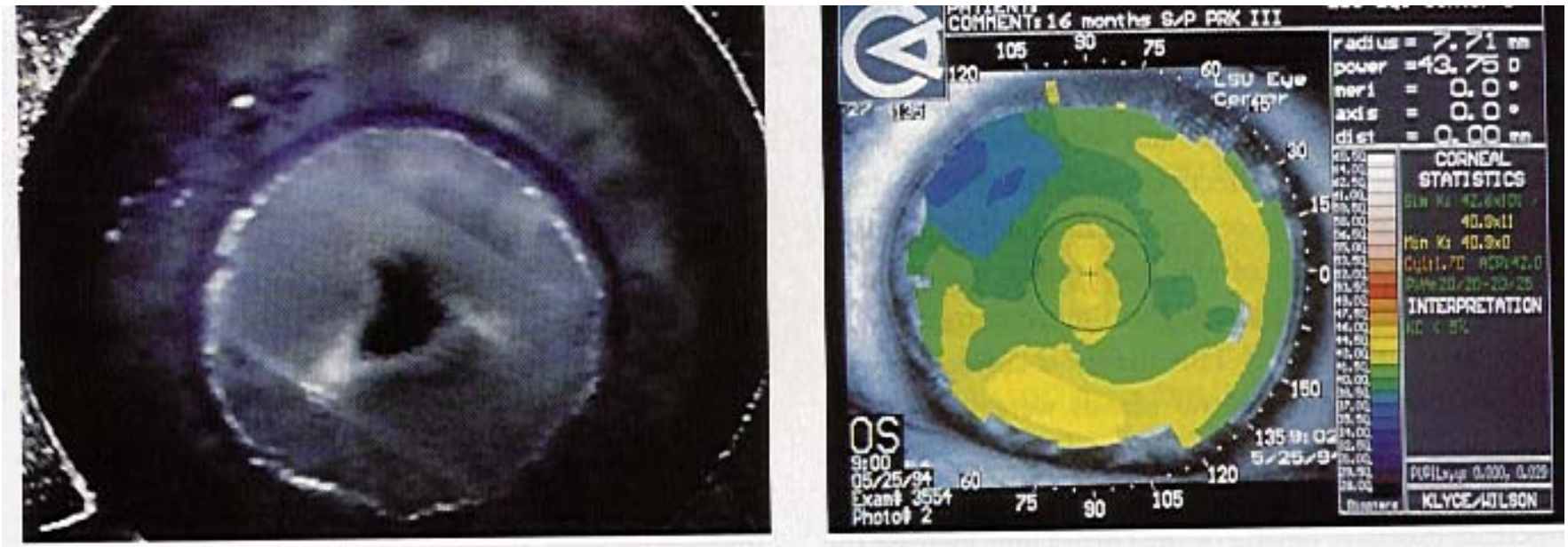

Post-op Central Island

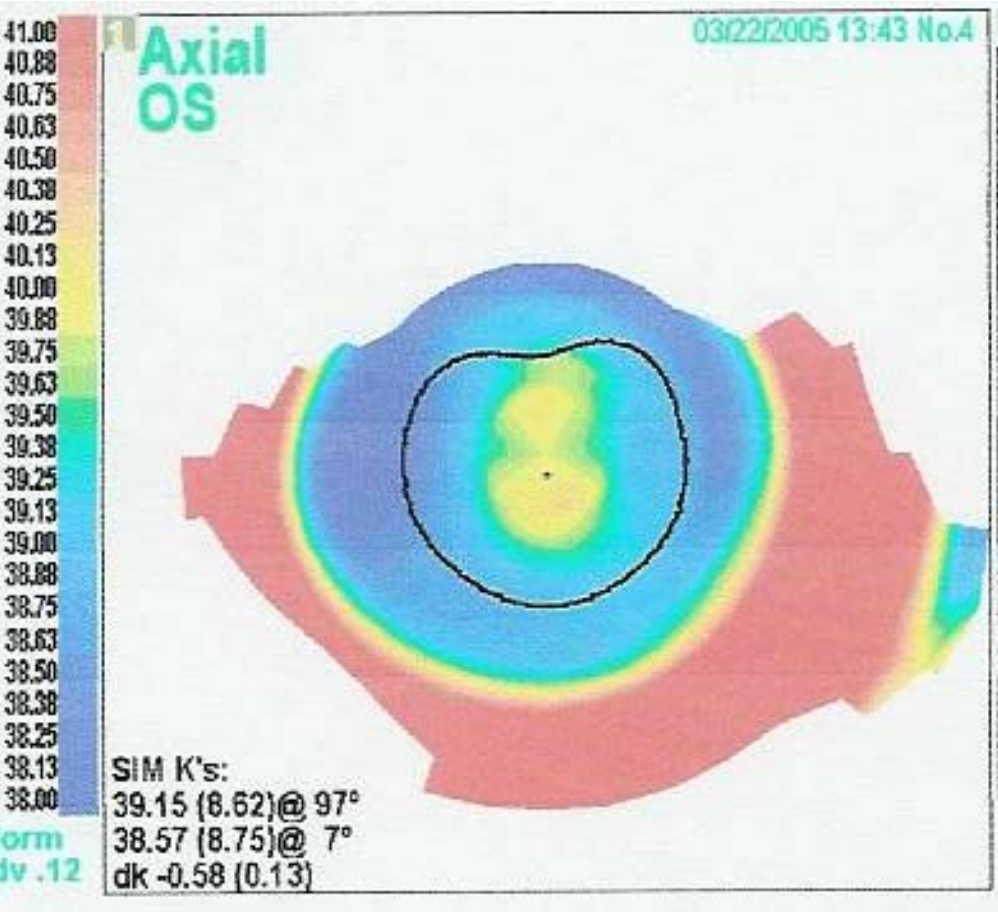

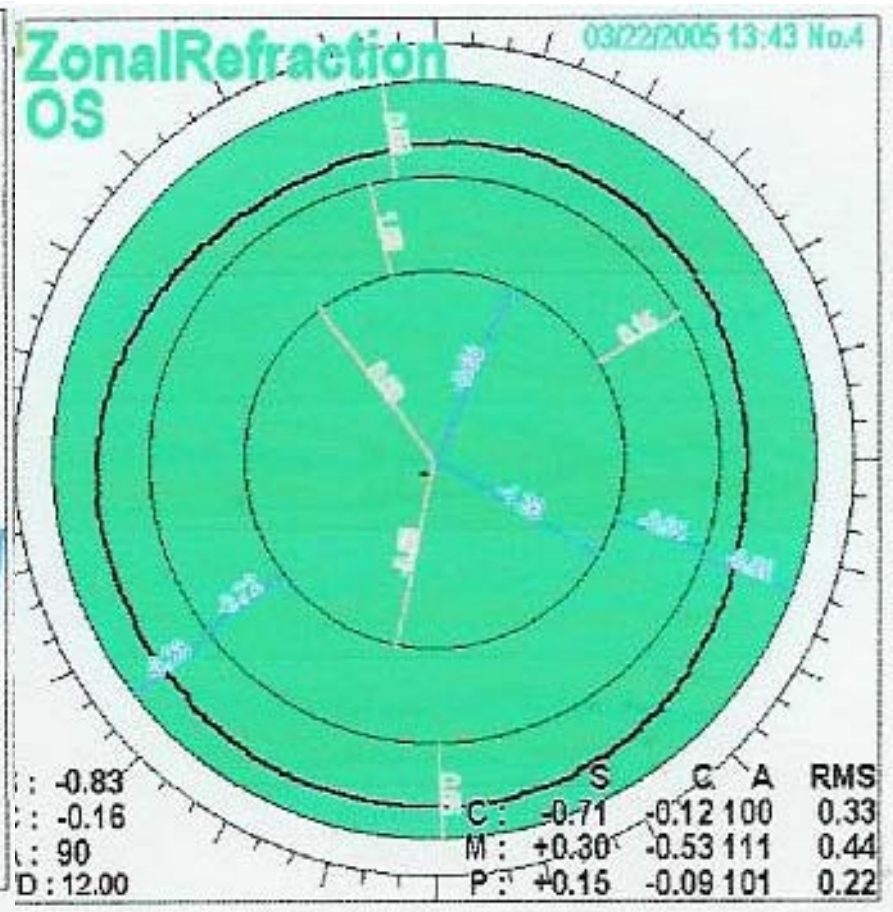

Central Island

Undercorrection with negative spherical aberration

- **Manifest is the average height over the center of the island:**
  - **Water level is like the average wavefront**
  - **Minus spherical aberration is like the height of the island compared to depth of the lagoon**

Soil Swelling

Weight of overlying soil prevents swelling

Corneal stromal swelling in isotonic solution is time dependent: unfolding of proteins

Doughty MJ.Biochim Biophys Acta 1999 Oct 18;1472(1-2):99-106

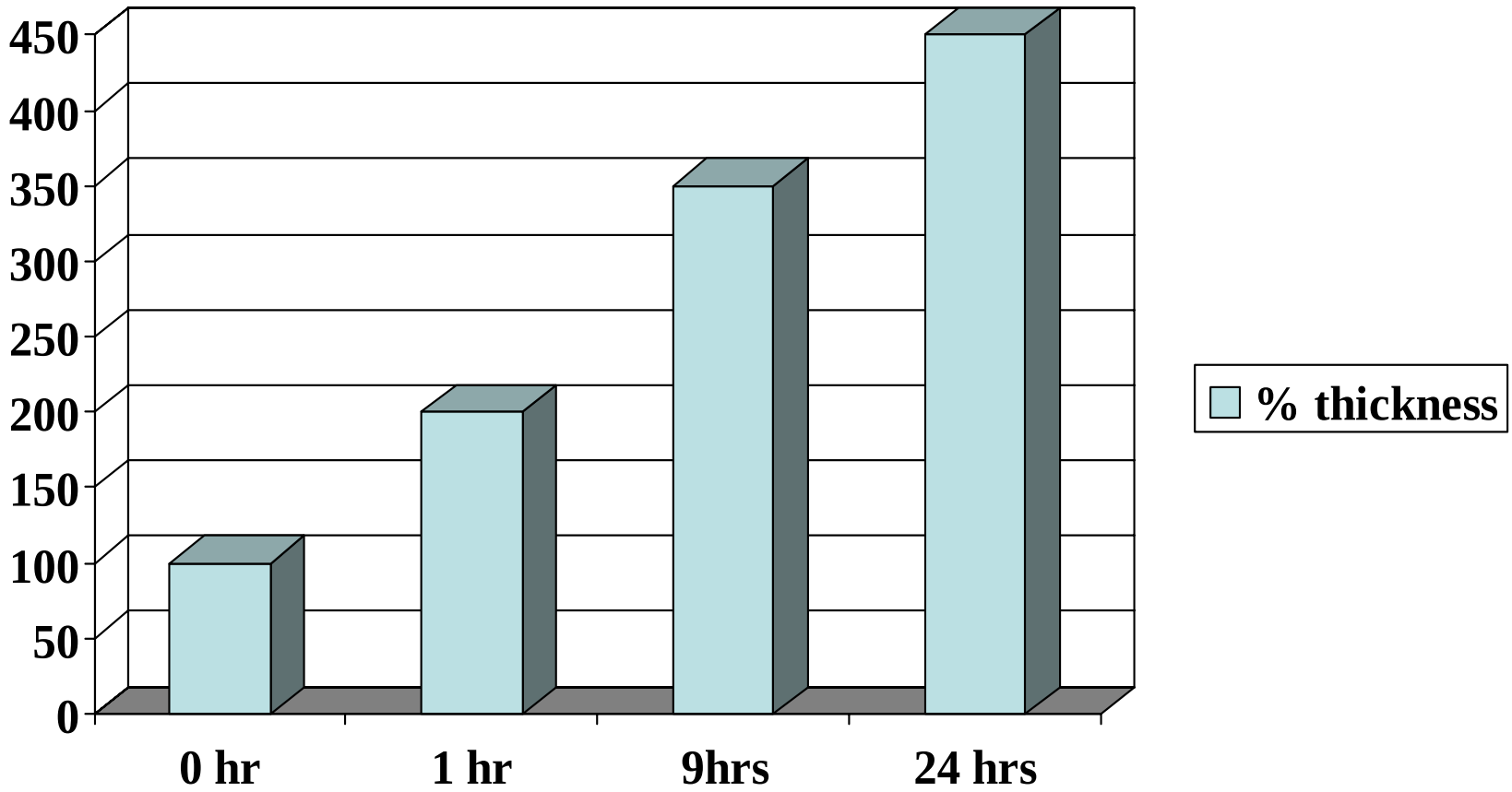

Measuring Swelling Pressure

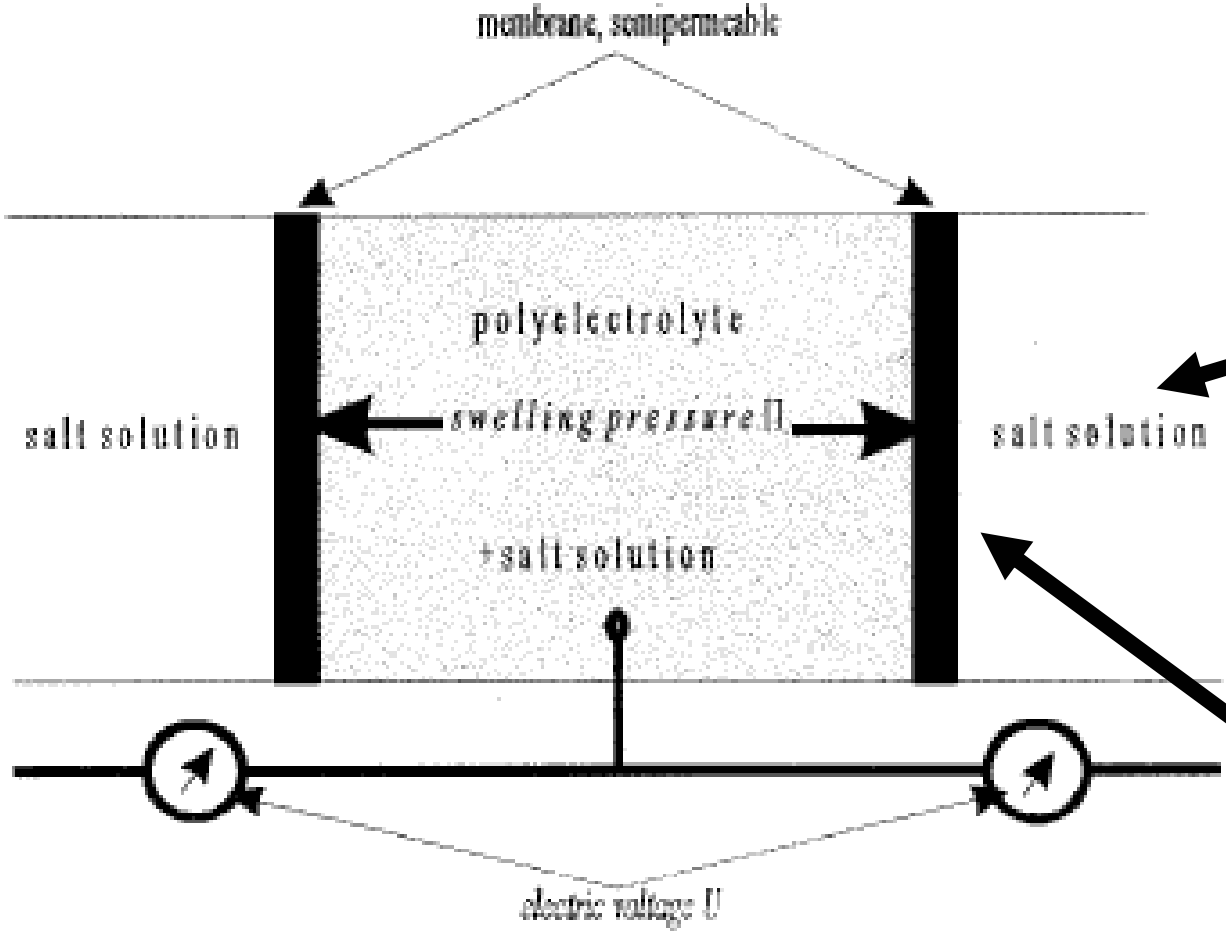

FIG. 1. Macroscopic Donnan model of a charged medium (polyelectrolyte concentration n_p) in a large reservoir with the salt concentration n. Membranes are permeable to water and salt but not to polyelectrolyte molecules. Due to the unequal ion distribution, osmotic and swelling pressure and potential difference (voltage) between the two phases exist.

Salt solution the same in all chambers

Membrane permeable to salt and fluid

Gel Pressure

- That portion of the internal osmotic pressure that can only be offset by external non-penetrating solutes (such as dextran and chondrotin)
- Generated by the potential energy developed by the mutual repulsion of fixed matrix charges on macromolecules (crowding)

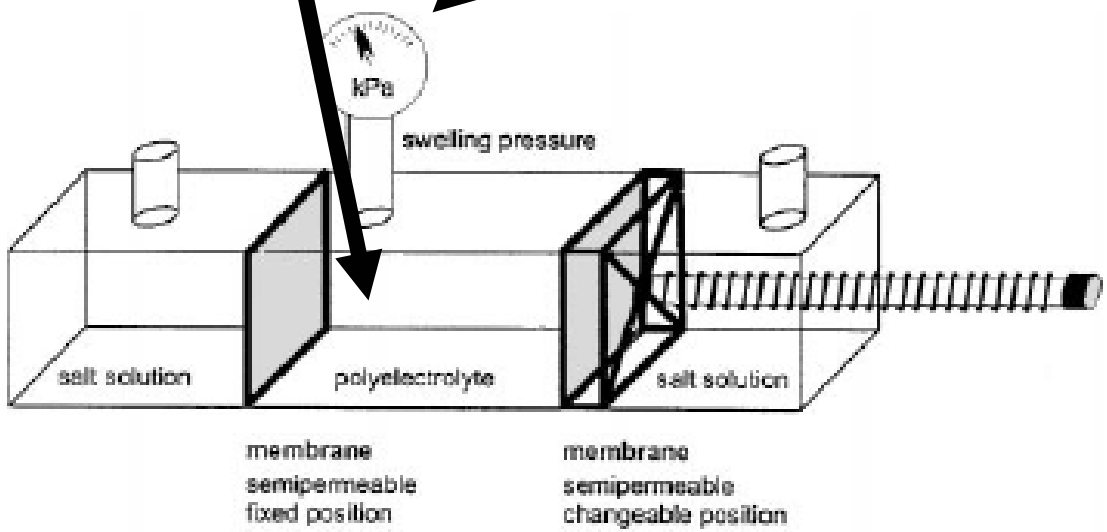

FIG. 3. Between a semipermeable membrane permeable for water and salt ions a polyelectrolyte solution is confined containing 150 mmol of fixed ions. The salt concentration in the sufficiently large outer space is 150 mM. The external space is under atmospheric pressure. By moving the right membrane pressure can be regulated and a certain pressure is achieved.

Stromal swelling at 3 hour is minimal with dextran (non-penetrating solute)

Kohlhaas M.Ophthalmologe 1995Aug;92(4):410-3

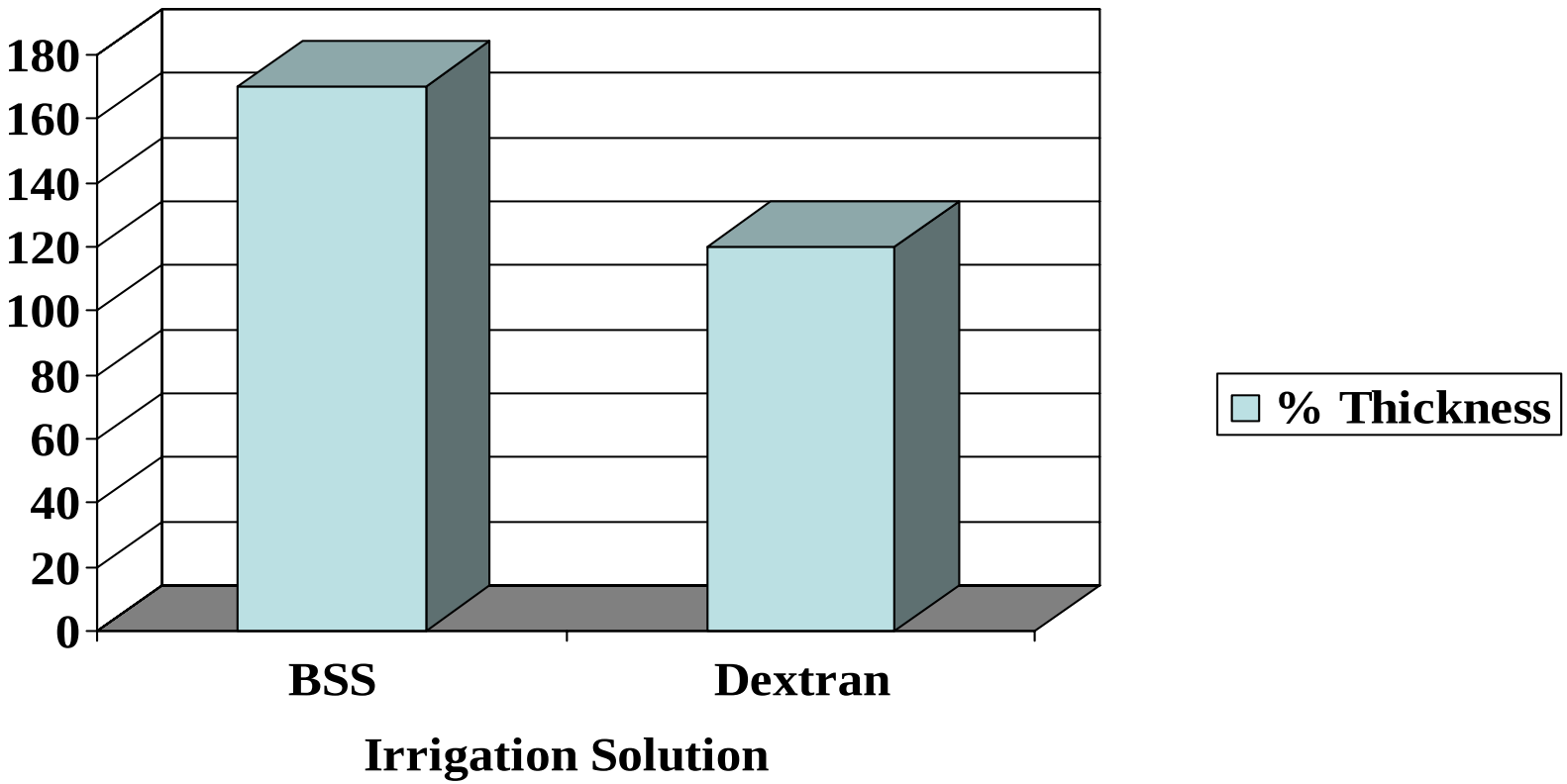

Optisol GS (Chiron)

- **Corneal Storage media**
- **Non-penetrating solute/colloidal**
- **Contains Chondrotin sulfate and dextran**

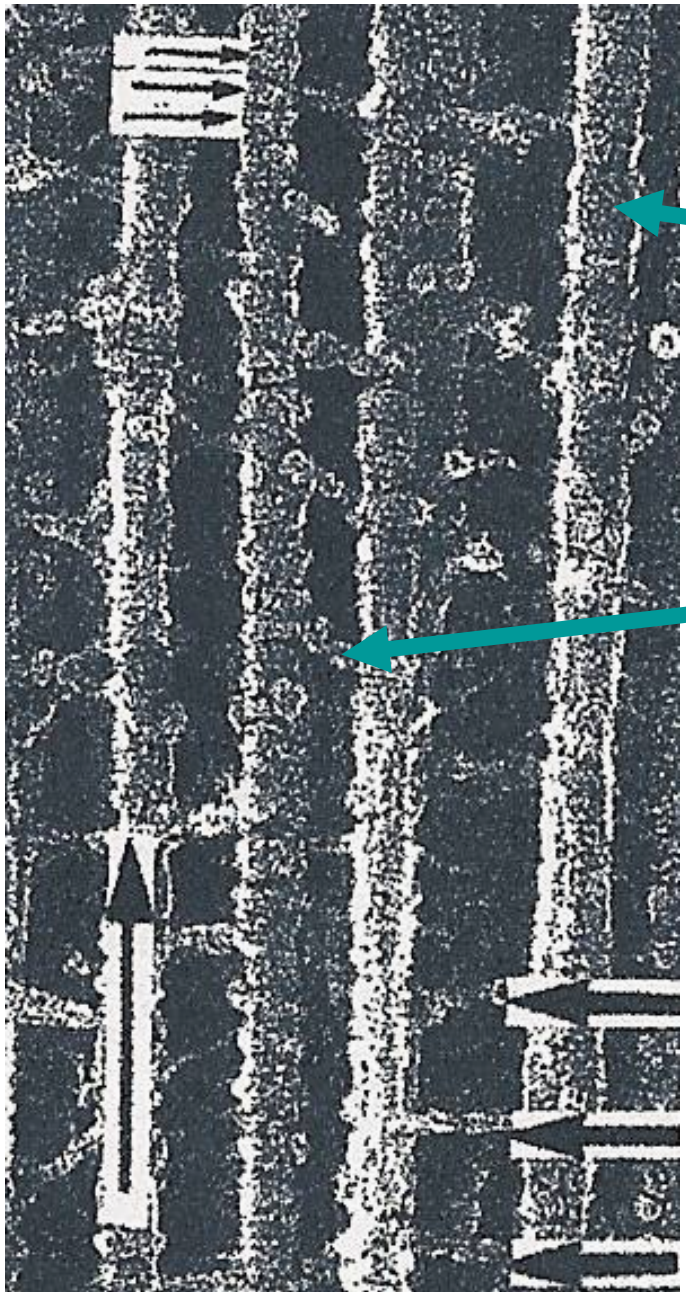

Collagen fibrils

- Banding pattern
- Minimal swelling

Proteoglycans

- **Interfibrillary bridging structures with attached globular domain**
- **Create gel pressure that controls collagen spacing**

- **Use viscoelastics/ glucosaminoglycans during cataract surgery to hold the chamber open**
  - **Healon**
  - **Vitrex**
  - **OcuVisc**
- **Adsorbs water easily**
- **Have a gel consistency**

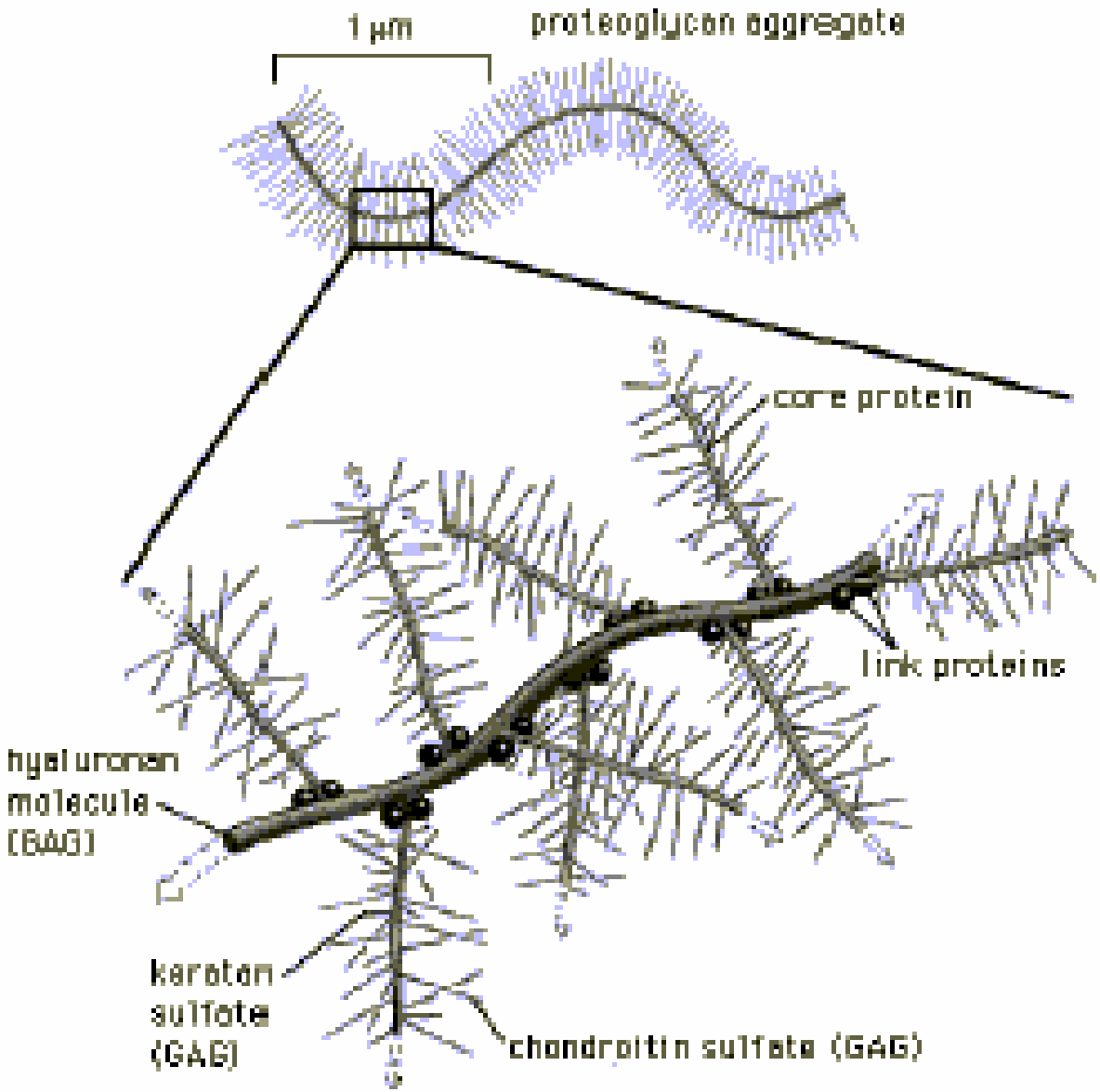

- Bullous keratopathy
  - Anterior epithelium has tight junctions
  - post epithelium can swell

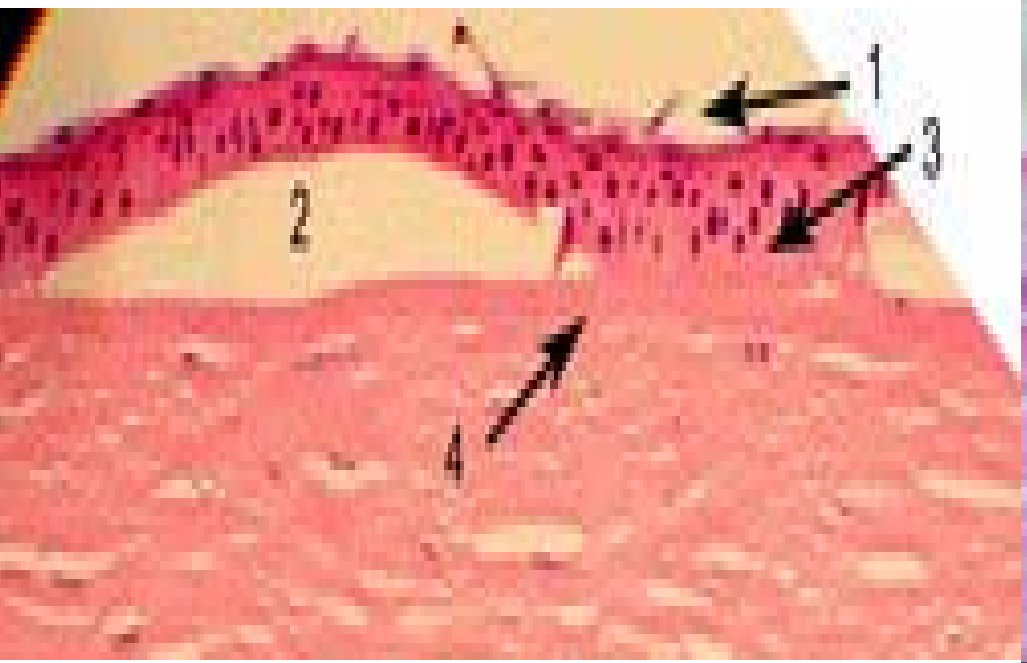

Epithelial swelling &Anterior Cell Damage: Worse with BSS

Doughty MJ.Ophthalmic Physiol Opt 1995 Nov;15(6):585-99

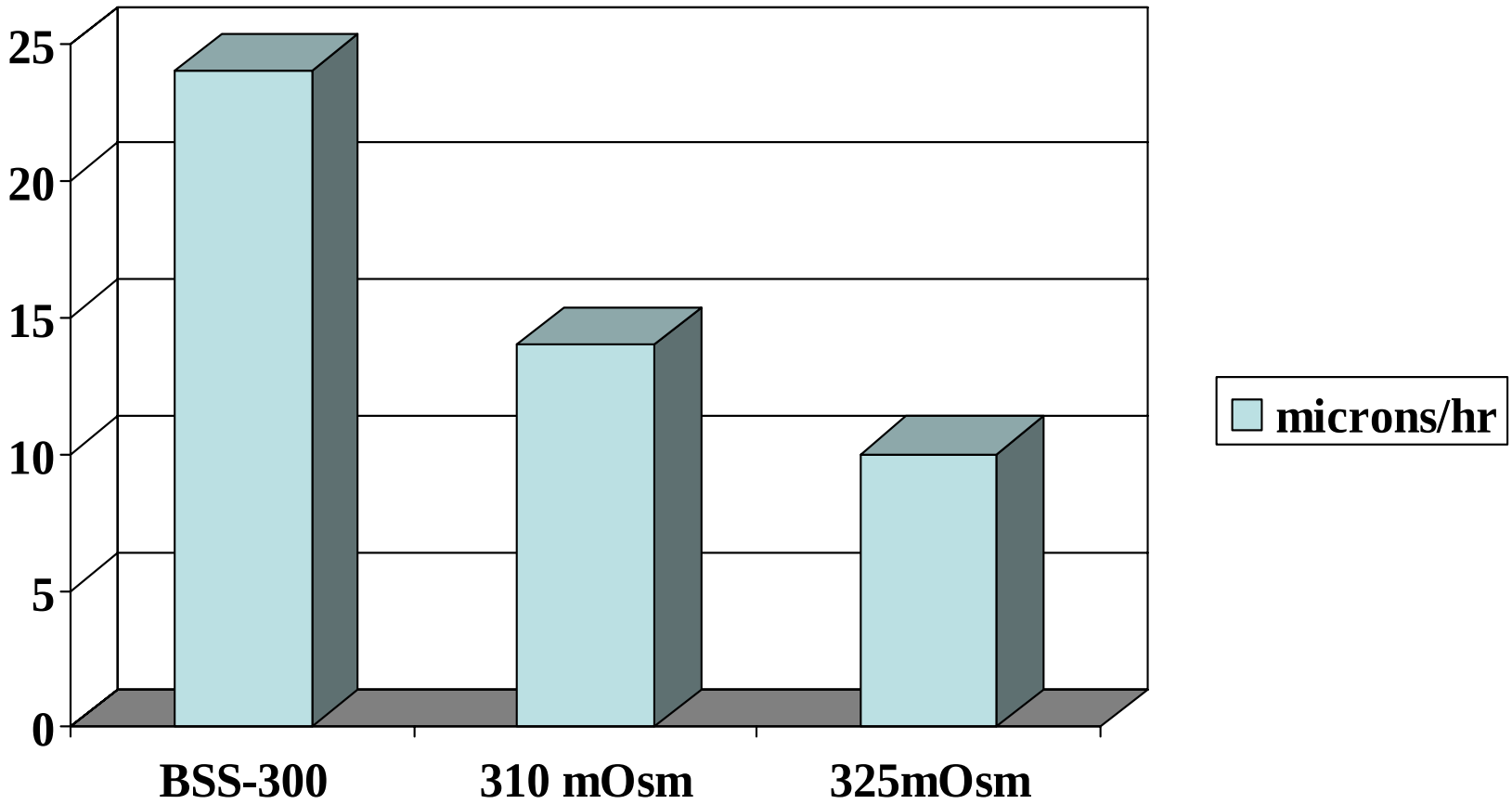

Sterile water is adsorbed through the stroma and causes epithelial edema and swelling

Case shown is being treated for slipped flap and microstriae

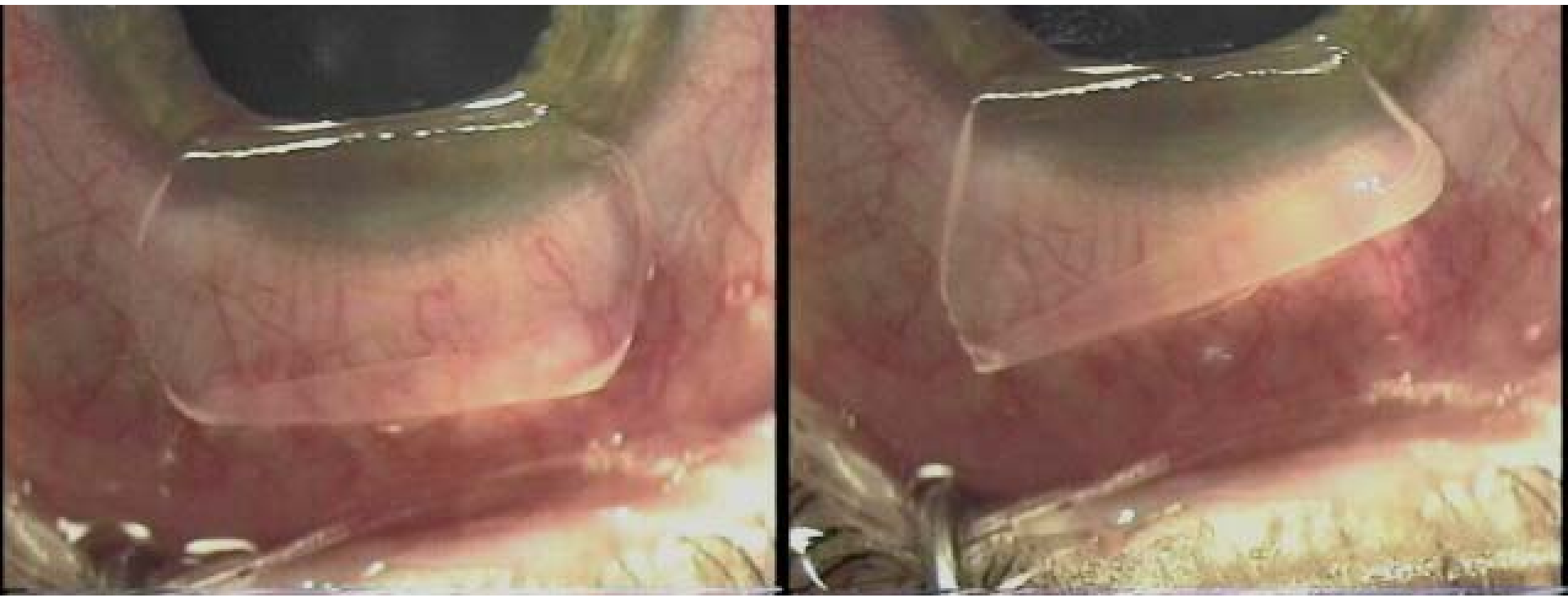

The Cornea is not a sponge , MEJ / ASCRS 2001

Case 2:Large inferior epithelial tear with Hansatome

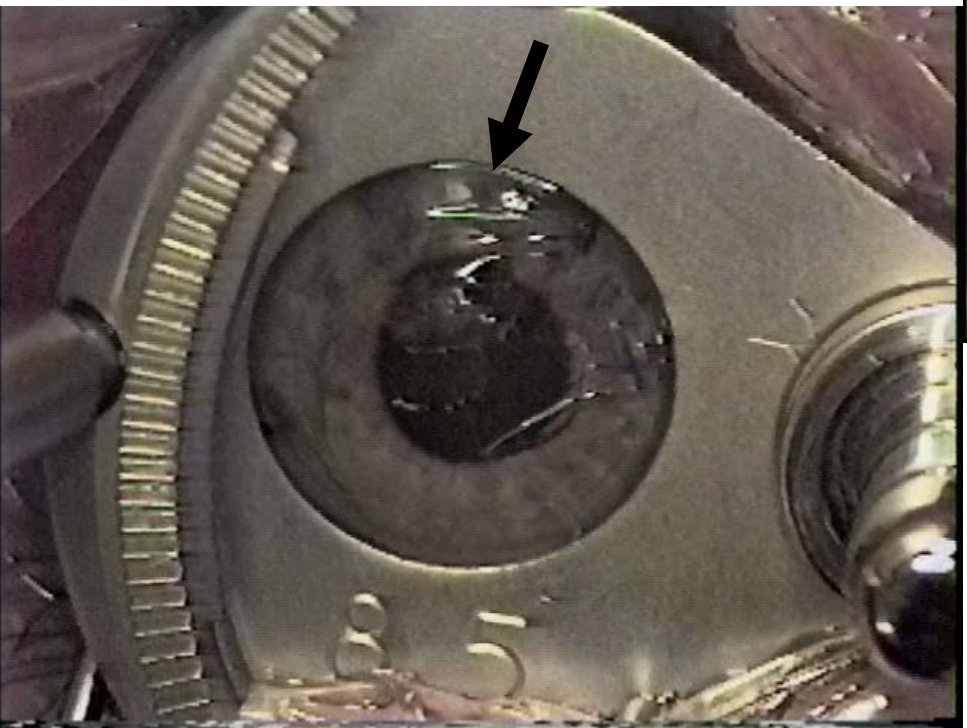

Widened gutter

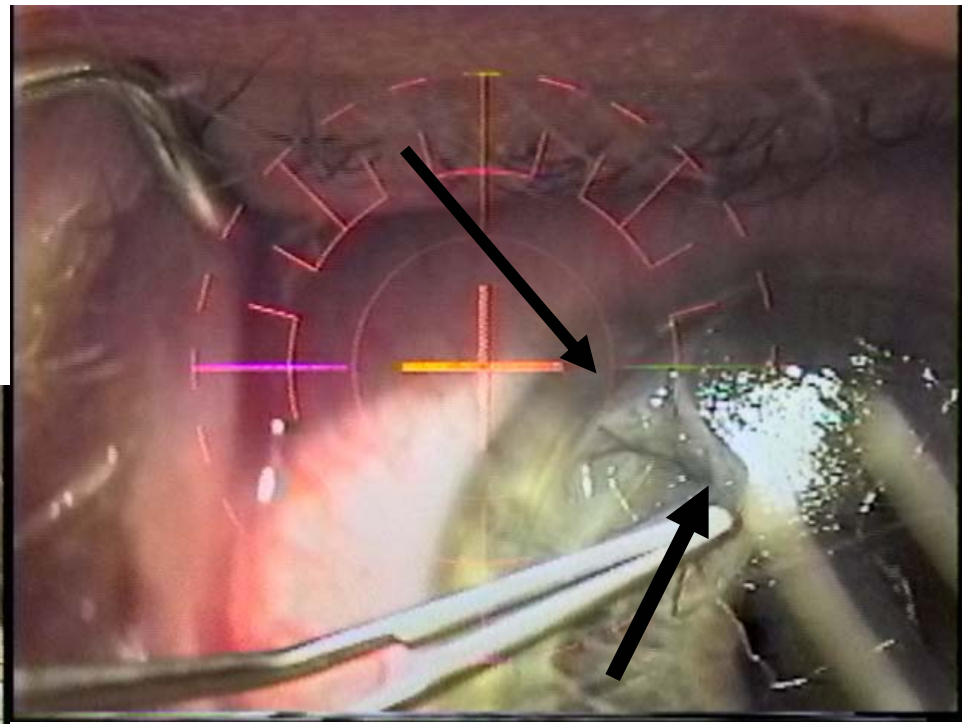

BSS used: Edematous epithelium removed

Important to replace the liquid in the contact case with steroid and antibiotic drops before transferring to the eye

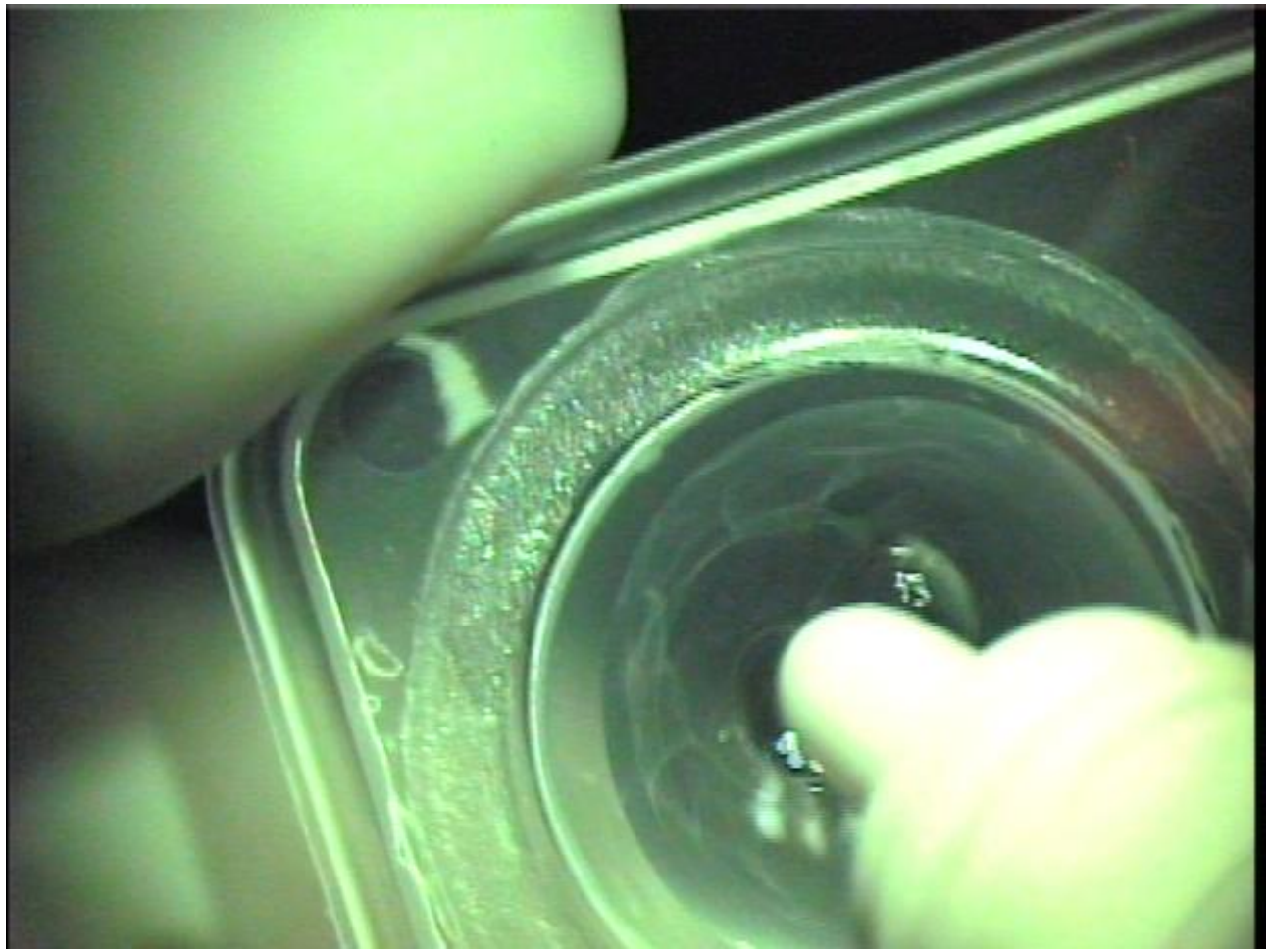

Epithelial Defect

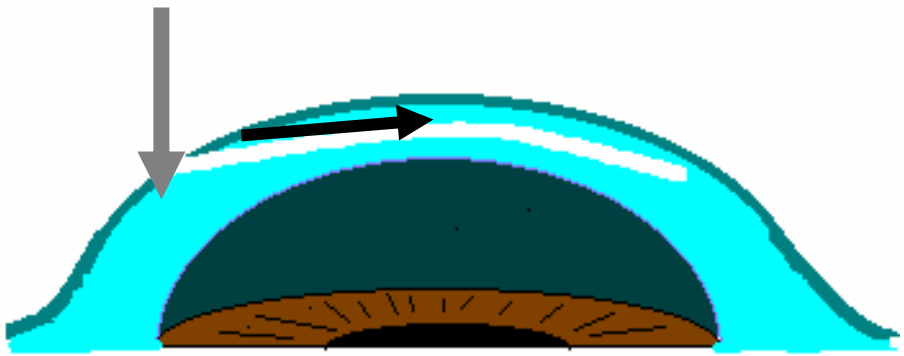

- Lasik creates a circular epithelial defect (gutter) confluent with the **potential space** in the Lasik interface

“Stromal Suction Model”

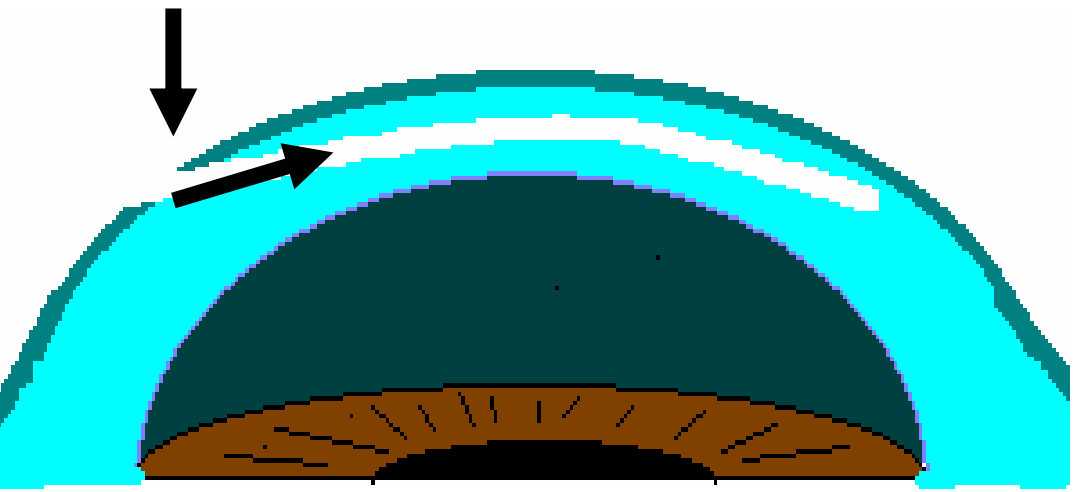

- **Fluid and debris is actively aspirated into the LASIK interface and corneal stroma after LASIK surgery until the epithelial barrier is intact**
- **Important to etiology of DLK, interface debris and topographic abnormalities**

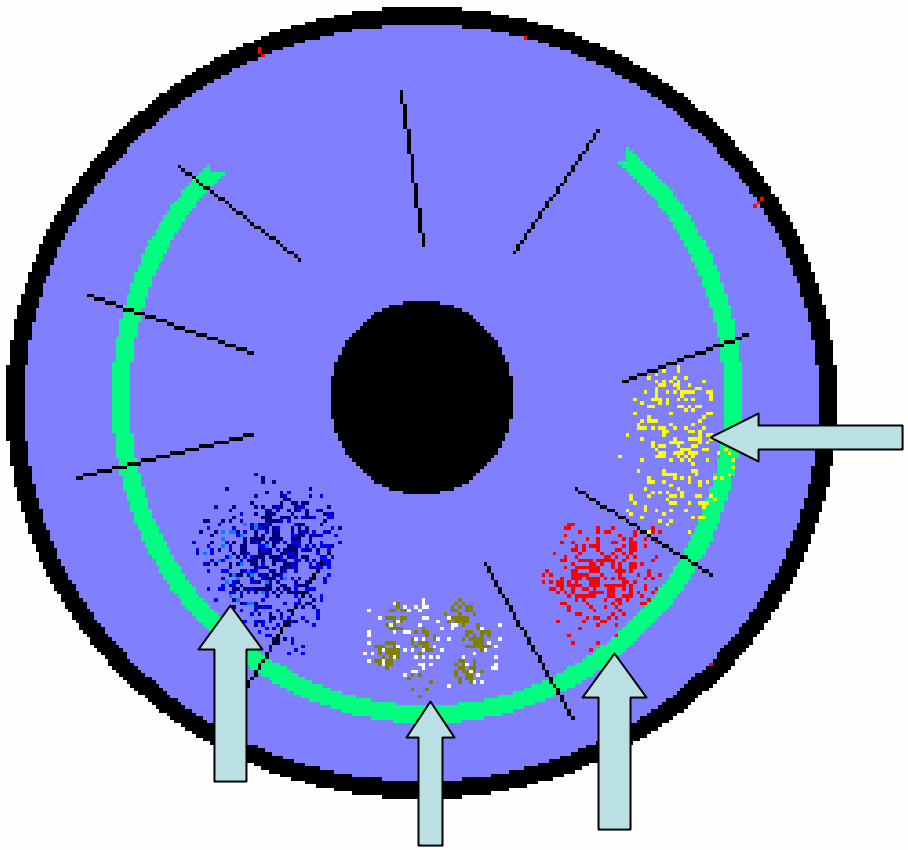

Until the epithelium is intact debris and fluid are actively aspirated into LASIK gutter and the potential space in the LASIK interface

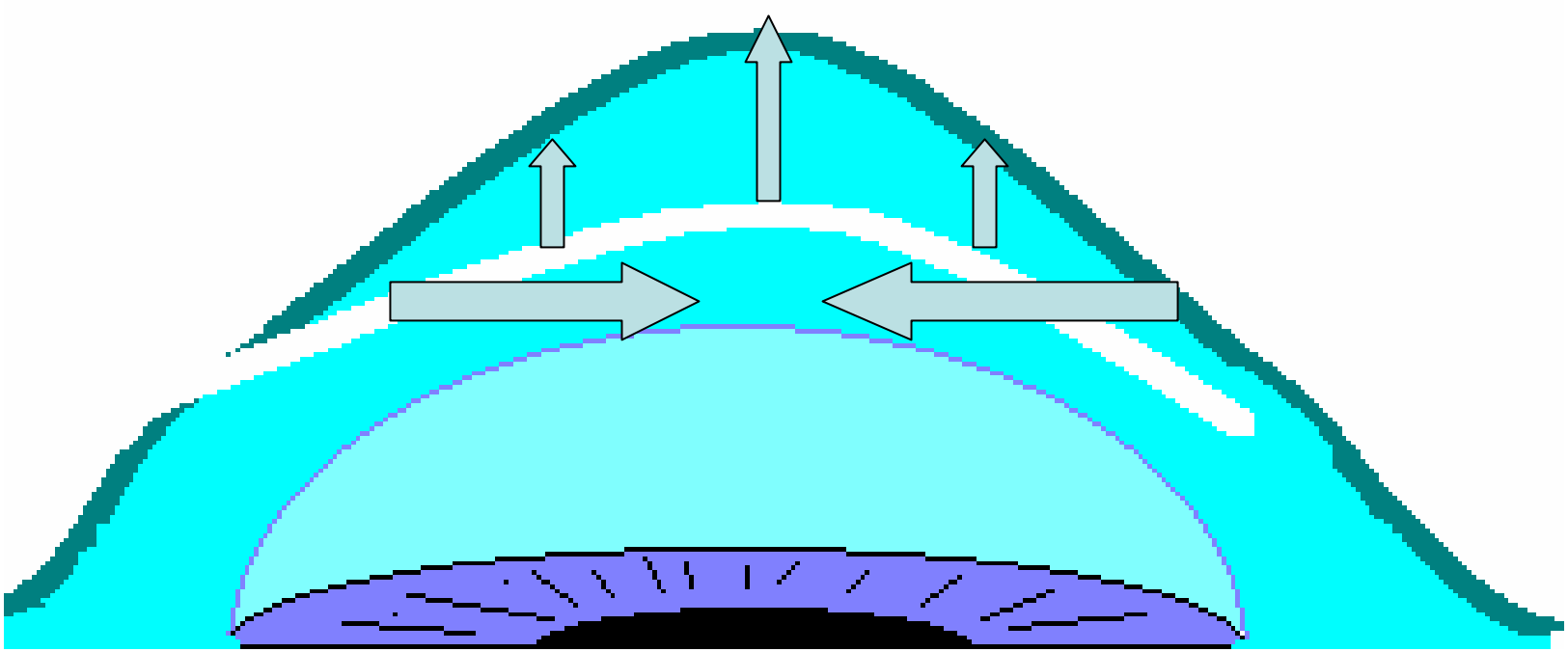

Figure 4
The corneal swelling pressure draws fluid and debris into the Lasik interface. The negative swelling pressure is greatest centrally and draws fluid and debris into the central cornea (thereby creating central islands).

Widening of the Gutter

M E Johnston, ASCRS 1999

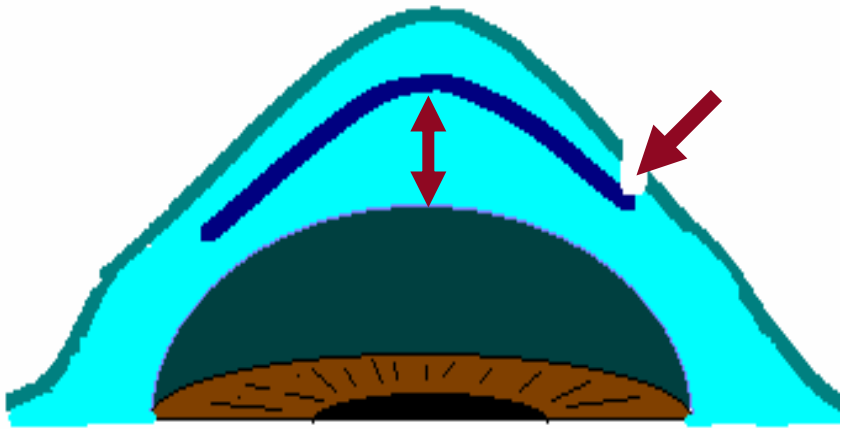

- **Related to excessive corneal swelling**
- **Significant swelling allows the flap to “lift away”**
- **Anterior cornea integrity prevents significant anterior swelling**

Epithelium with 5% NaCl

note the gutter and whitening (denaturation) of epithelium

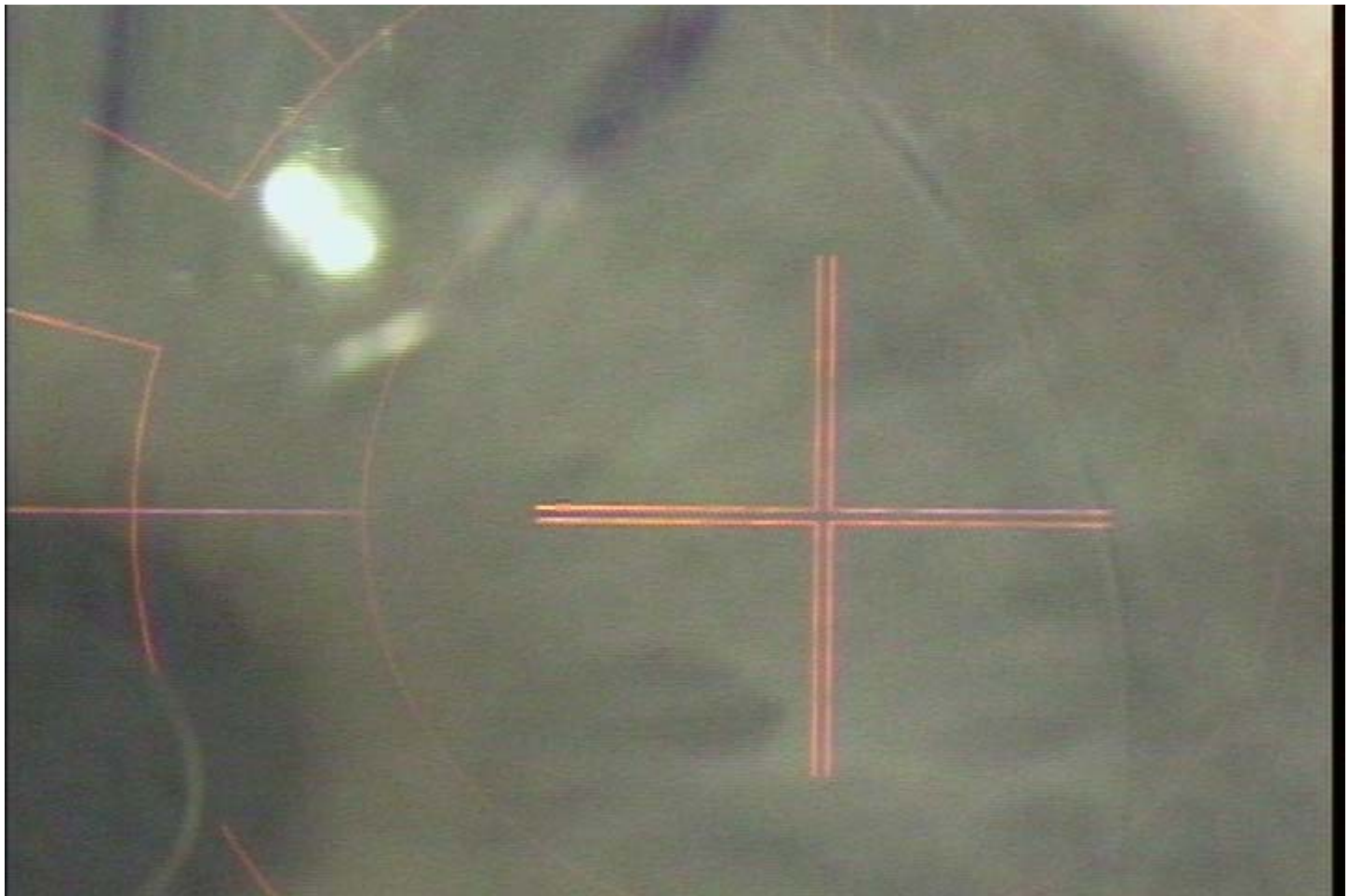

Case 3: Inferior horizontal horseshoe tear epithelium

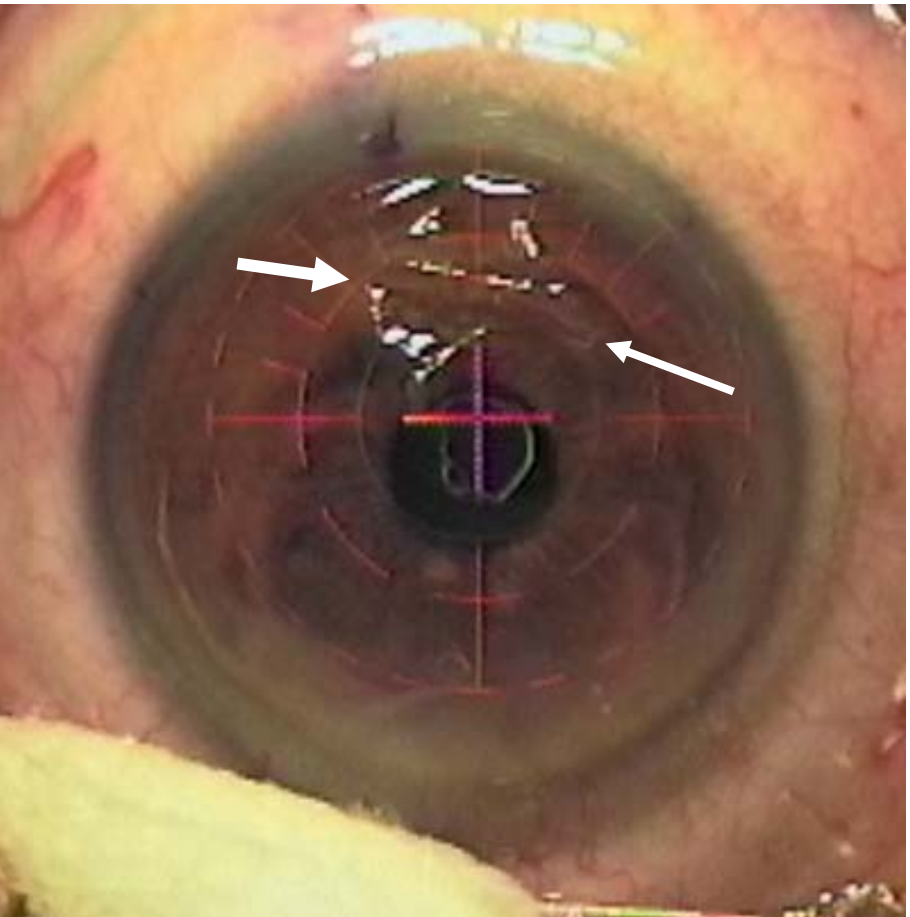

Residual Epithelial irregularity,edema and widened gutter after re-float with BSS

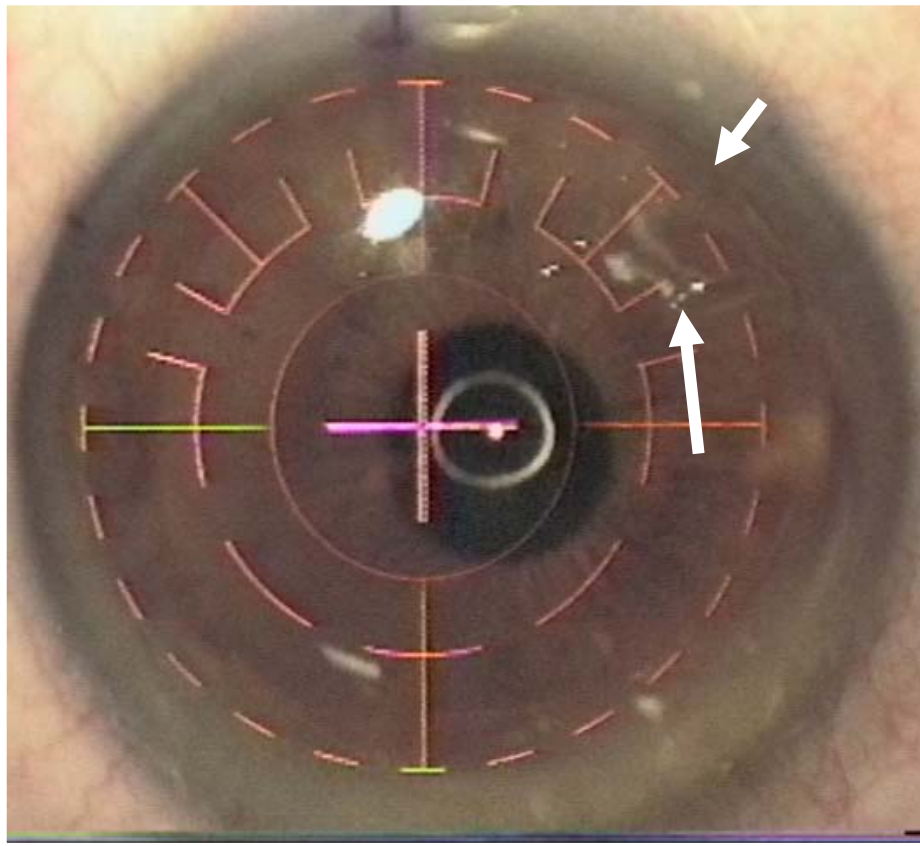

Patient developed Grade I DLK

Case 1:Flap slippage with removal drapes

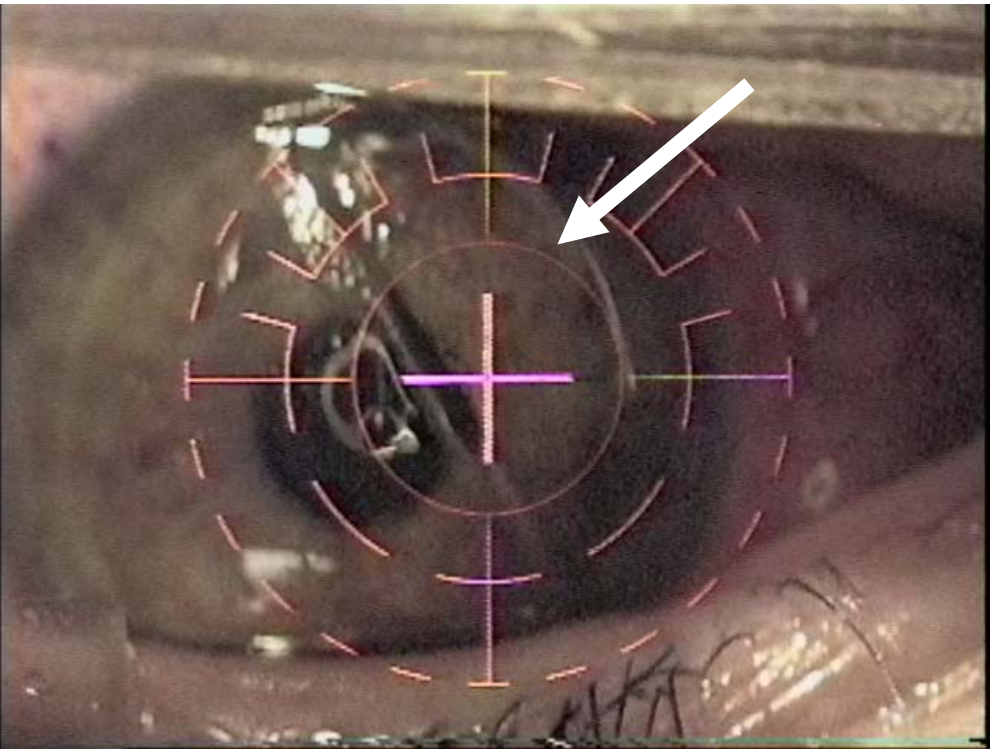

Refloated with copious BSS

Widened gutter

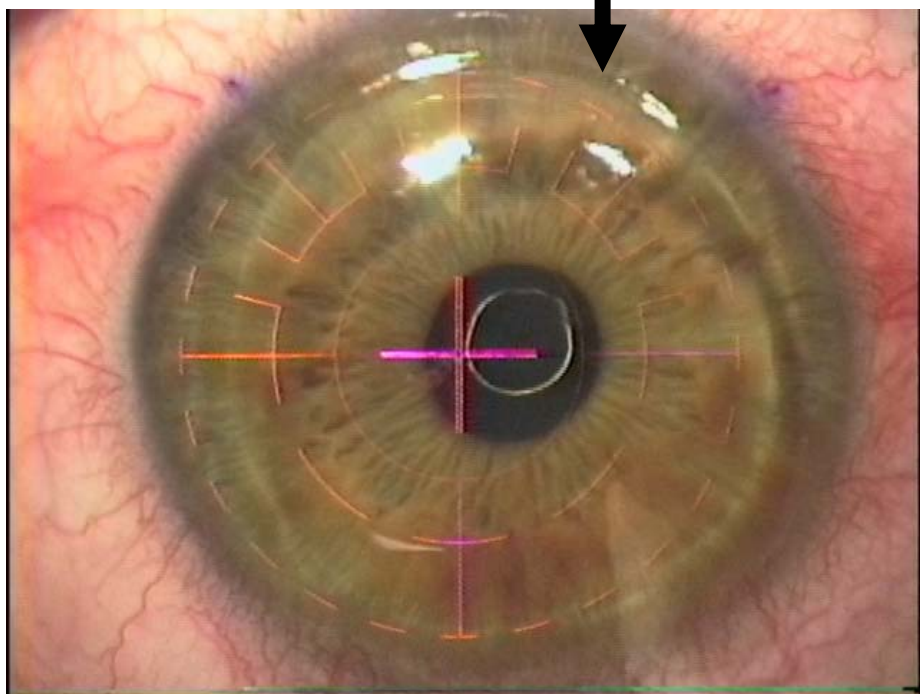

A. Interface fluid syndrome
B. Infectious keratitis
C. DLK

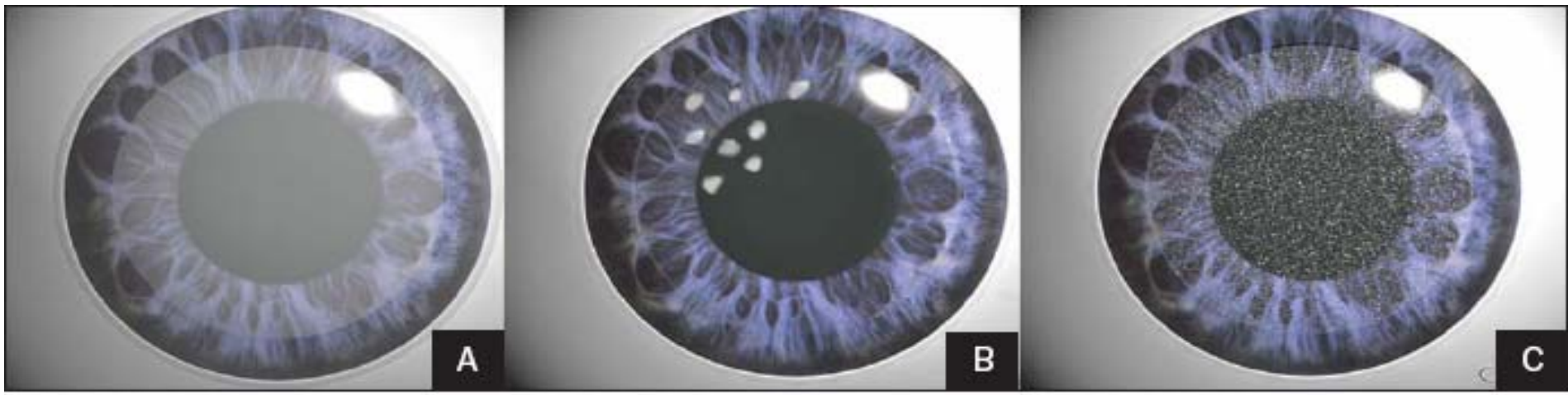

Interface fluid

Elevated IOP creates central islands

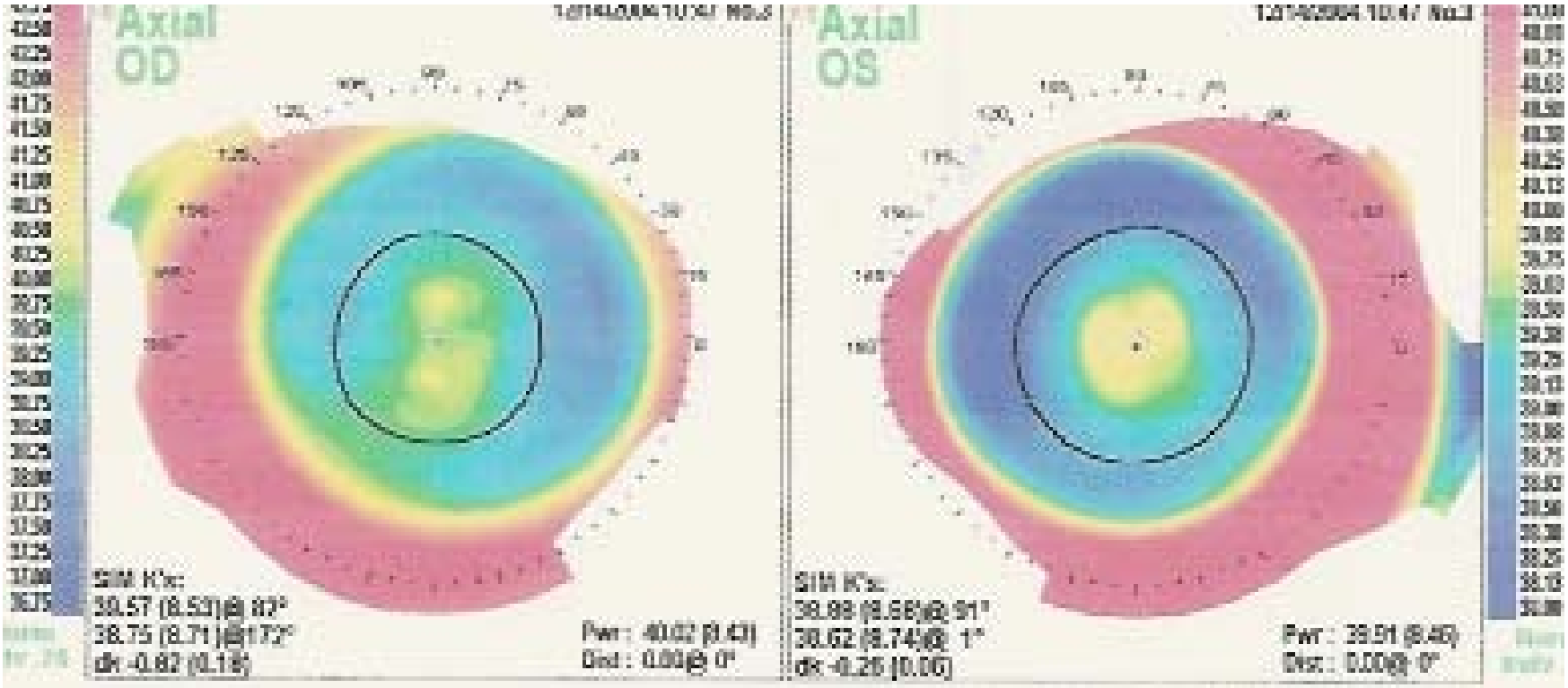

DLK Endotoxin

- Endotoxin
  - Derives from a Gram negative (anaerobic) cell membrane component
  - The source is usually the steam chamber in an autoclave or humidifier
    - Use dry heat to autoclave LASIK instruments
  - Triggers a breakdown of the endothelial barrier of the conjunctival blood vessels
    - Large out-pouring of neutrophils into the tear film

Immunologic modulators carry the message to the nucleus

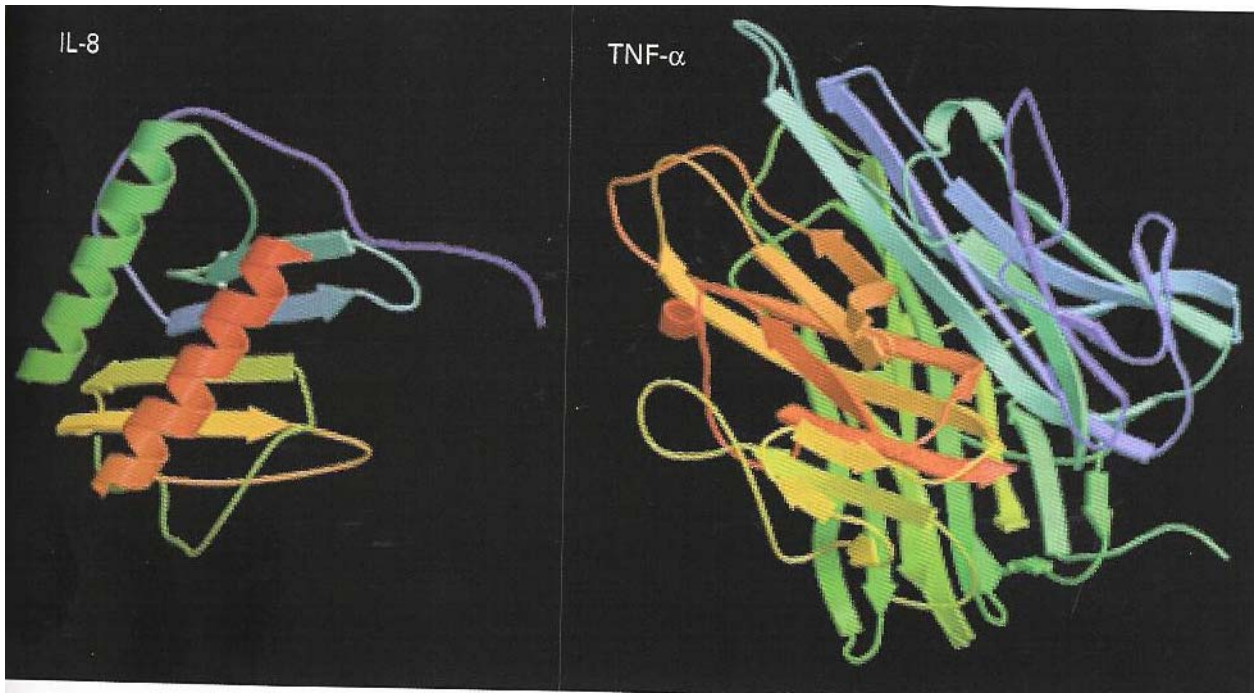

Protein folding –the mechanics of biology

Shock lung:
Note neutrophils and fluid in affected lung

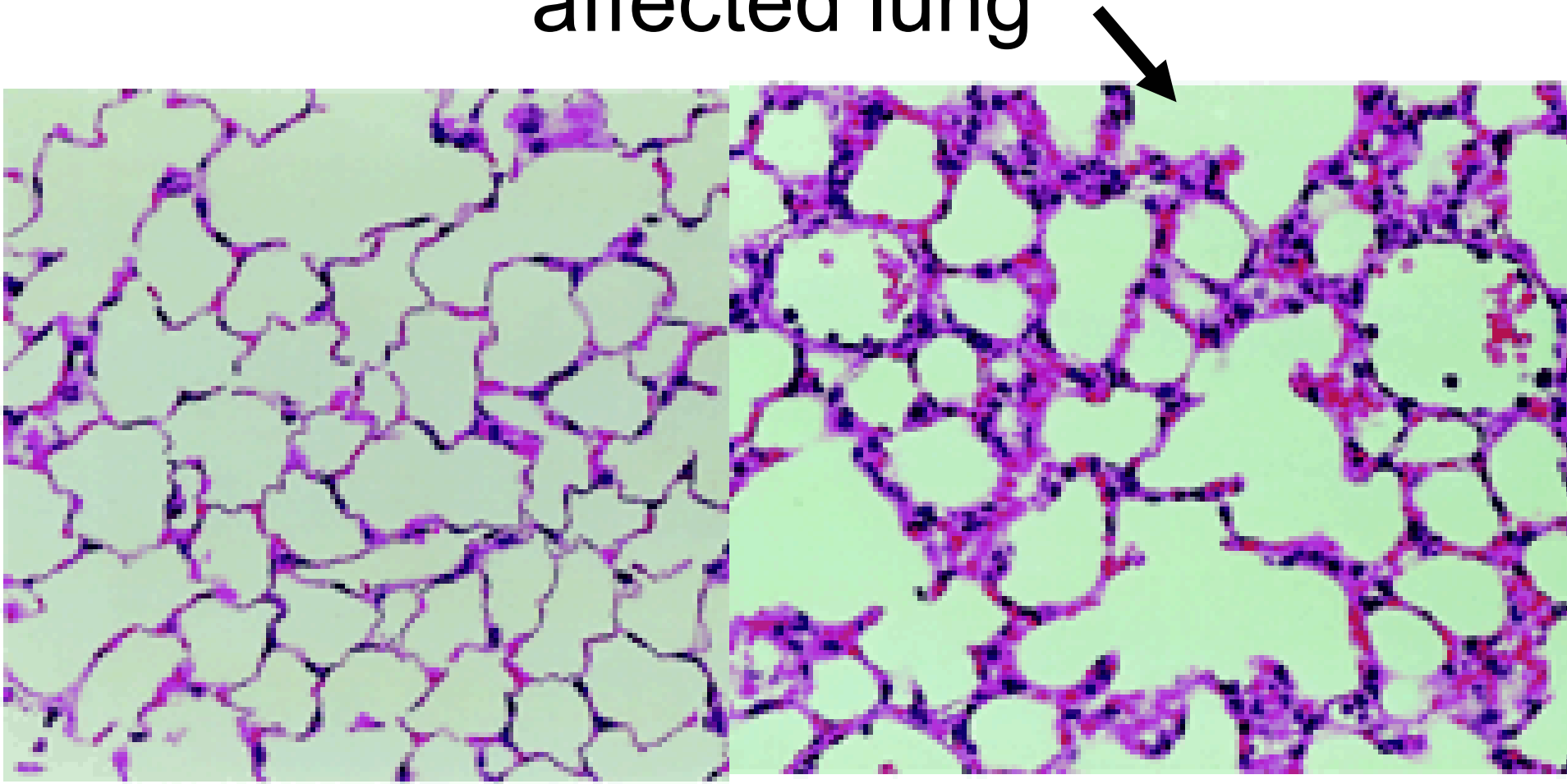

- DLK
  - Toxin to the conjunctiva and/or interface
    - Endotoxin on the keratome or blade or in solutions
  - White cells enter through gutter and are drawn towards the center

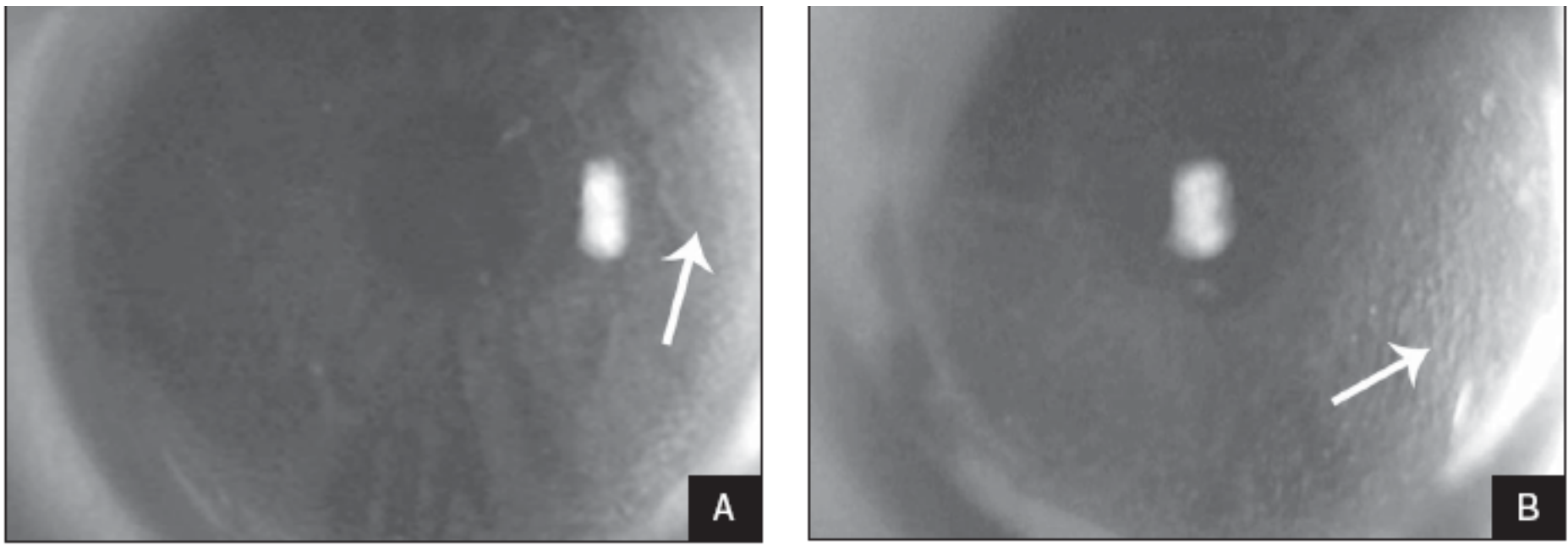

Figure 2. Slit-lamp photograph of the **A)** right and **B)** left eyes showing progression of infiltrate to the interface forming DLK (arrow).

Case 4- Day 1 AM

- Vision 20/20
- **Cells** in the inferior **LASIK interface**
  - Material consistent with neutrophils

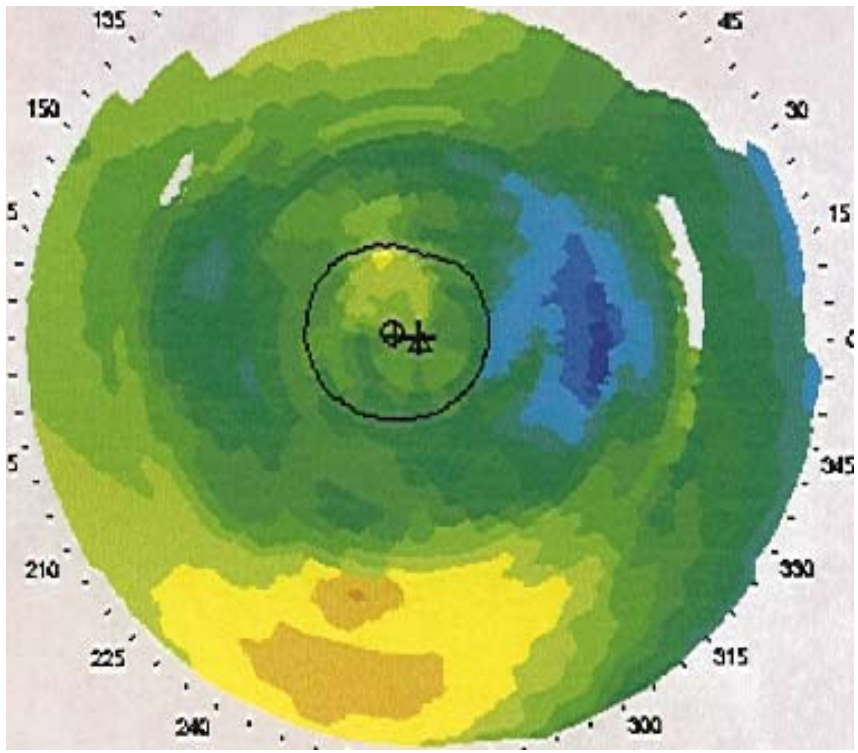

Case 4- Day 1 PM

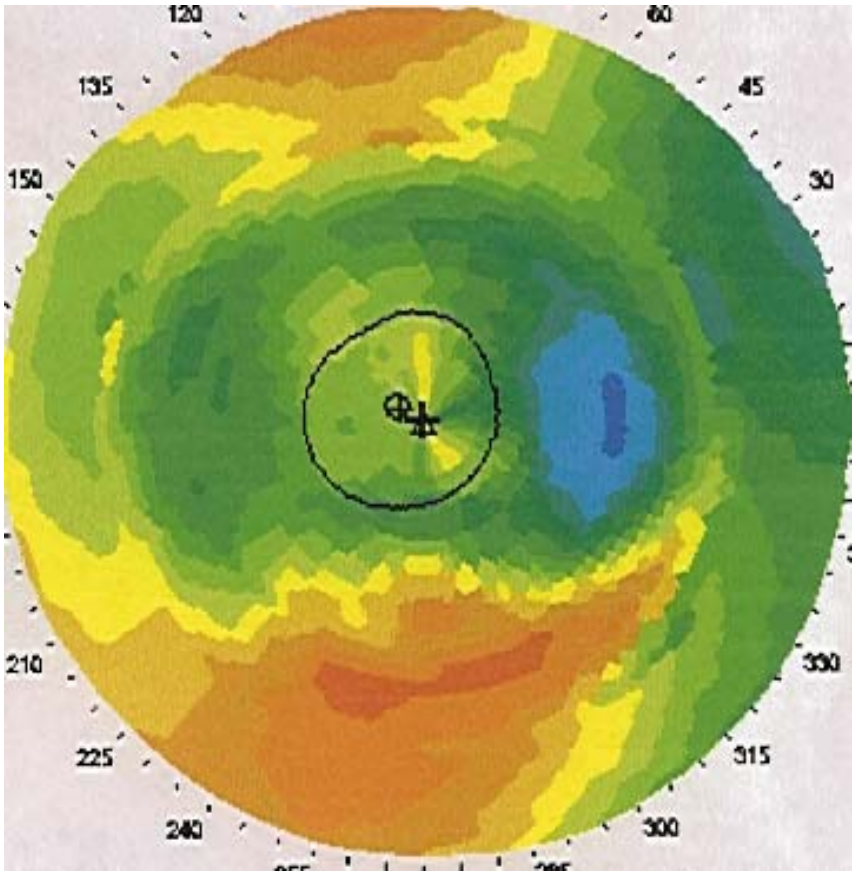

- Vision 20/30
- **Migration** of the interface **cells** into the inferior mid-peripheral interface
- **Topography** showed increased corneal thickness in the area of the shifting debris

Case 4- day 4

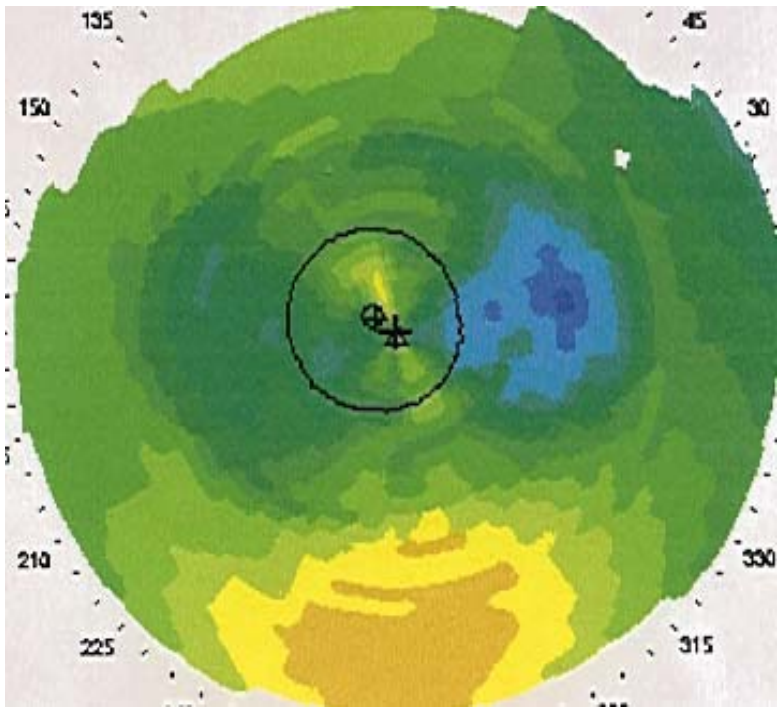

- The island is resolved
- Further migration noted
- Vision has improved to 20/25

Risk factors-Microstriae

- Thinner flap
  - 160 Hansatome keratome head has a 3.12 risk ratio compared to the 180 head
- Dry eye
- Above average correction
  - AV SE:-5.94+/-2.7D

Prevention of Microstriae and Microfolds
Mark E Johnston MD FRCSC
American Society of Cataract and Refractive Surgery
San Francisco April 2003

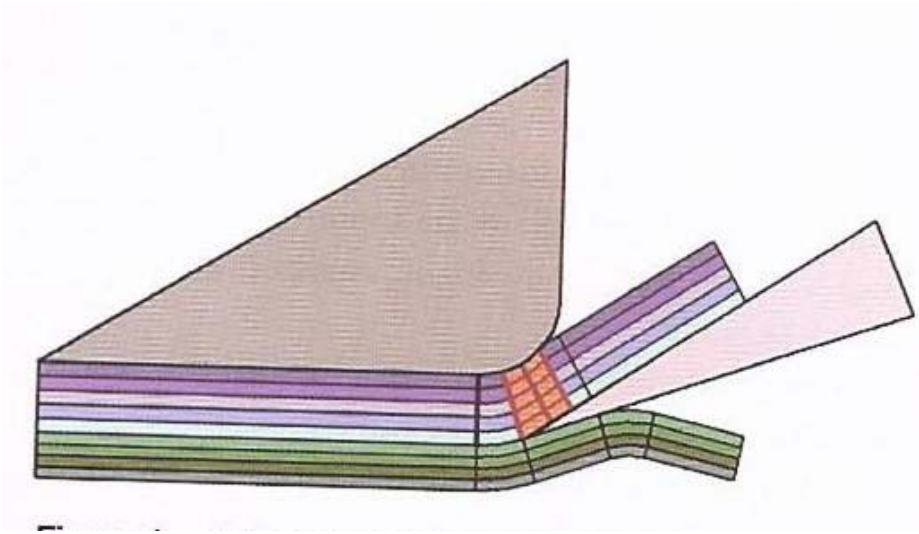

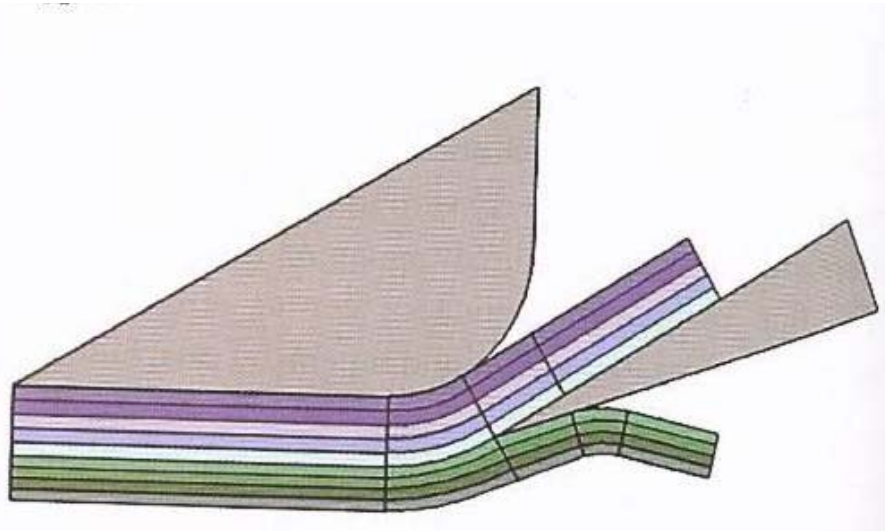

- Regular Hansatome
  - Note sharp angle of the metal plate

- Zero Compression Hansatome
  - Note flatter curvature metal plate
  - **On average cuts 20 um thinner**
  - Less epithelial defects

VHF Digital Ultrasound

- Flap thicker in the periphery
- Flap thicker in thicker cornea

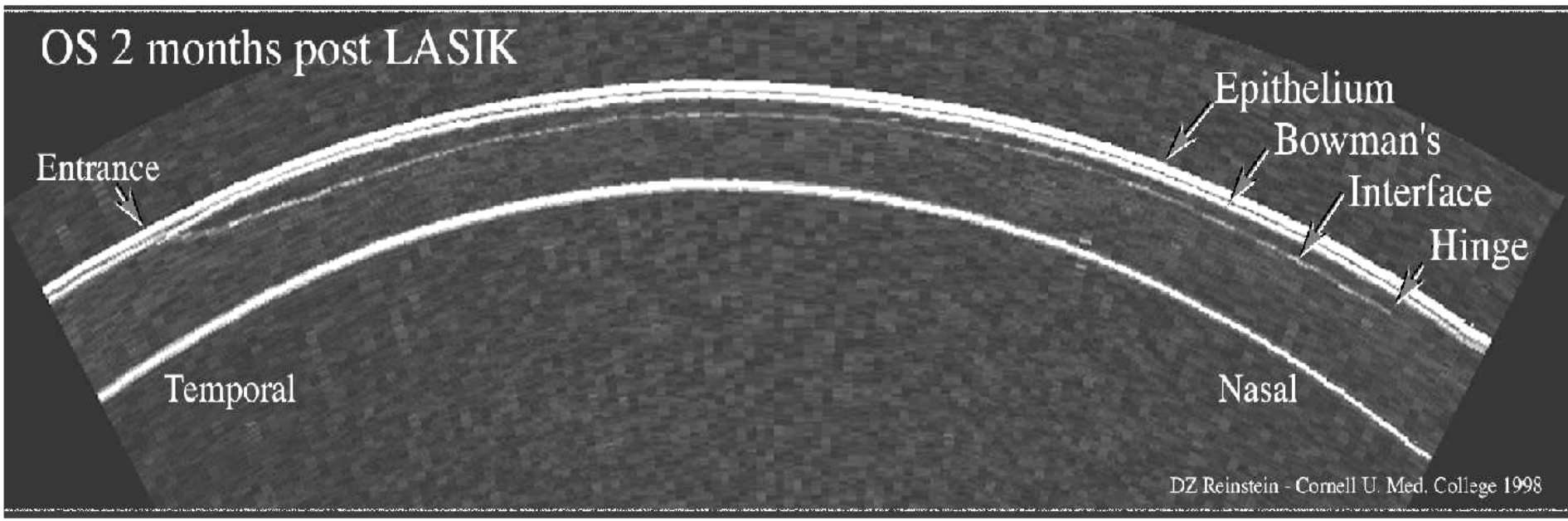

Flap is thinner in thin cornea:
We do not use 120 head on thin corneas

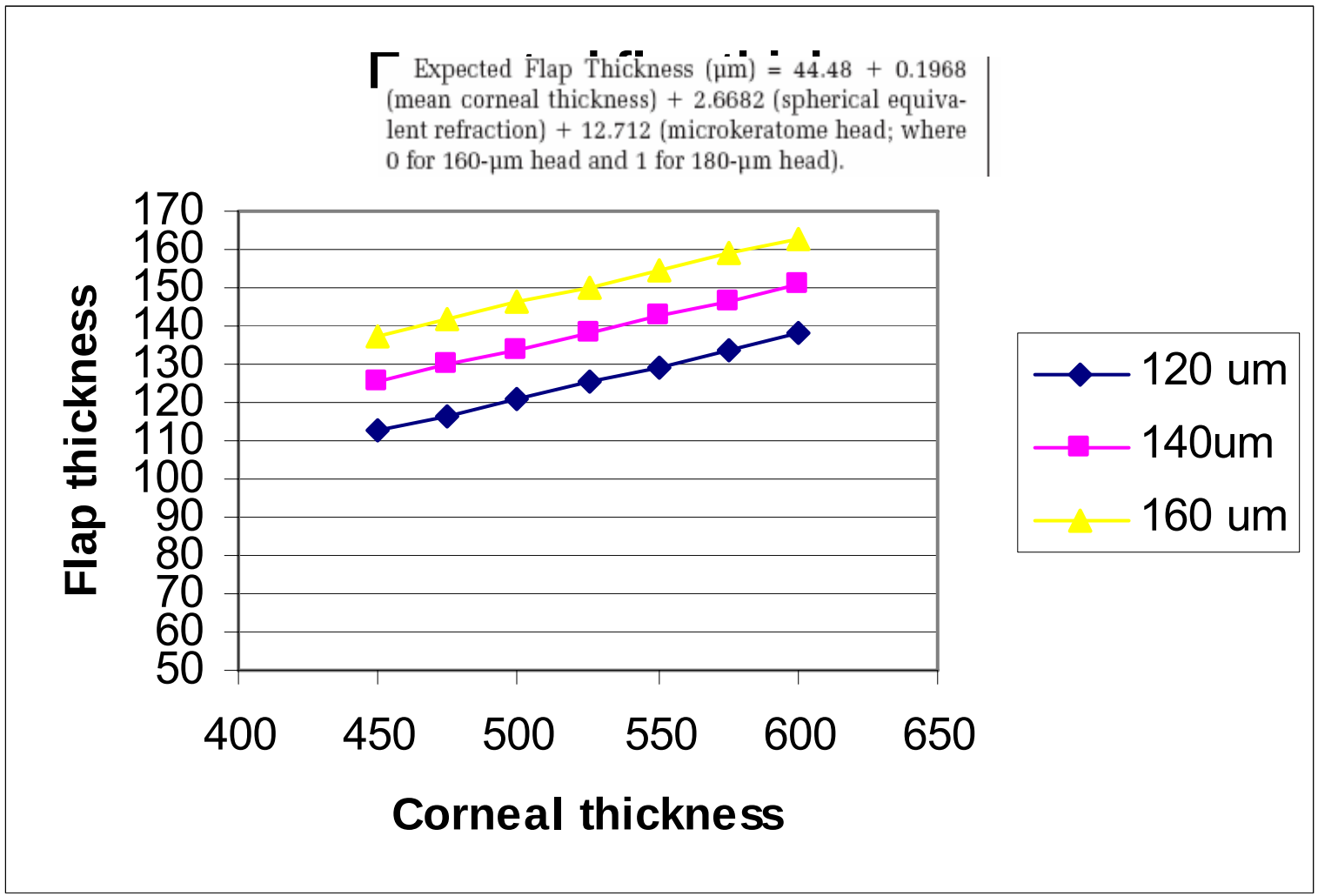

What causes microstriae ?

- Shrinkage over
  - the potential space made by the ablation
  - surgically induced stromal edema
- Flap slippage
- Thin flap or thinnest part of the flap

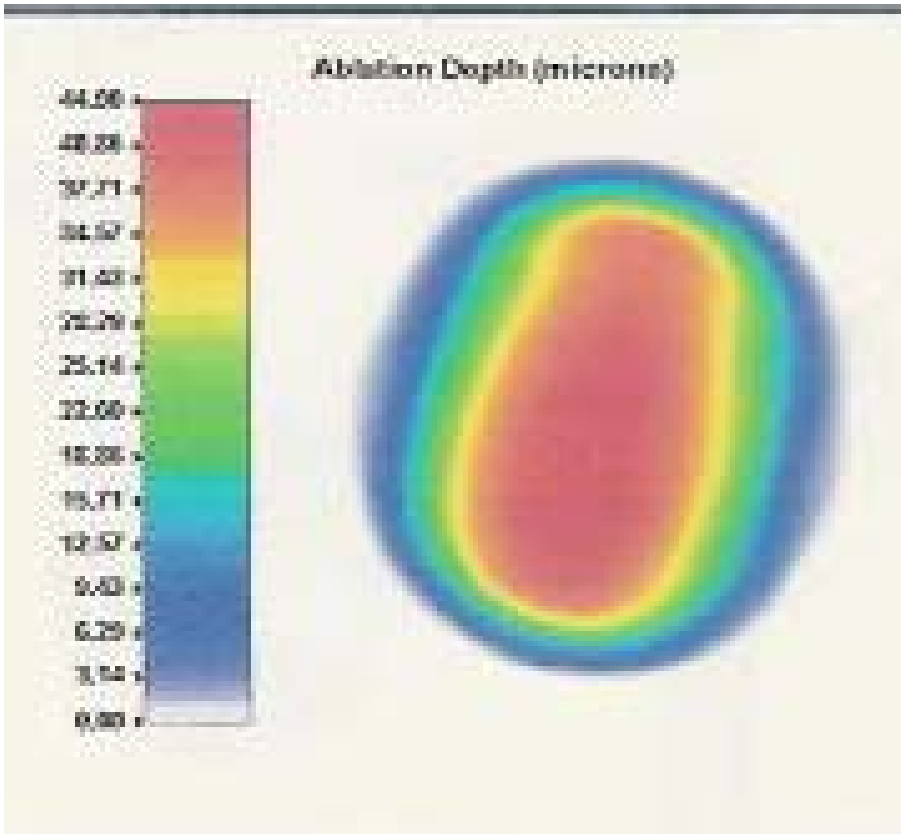

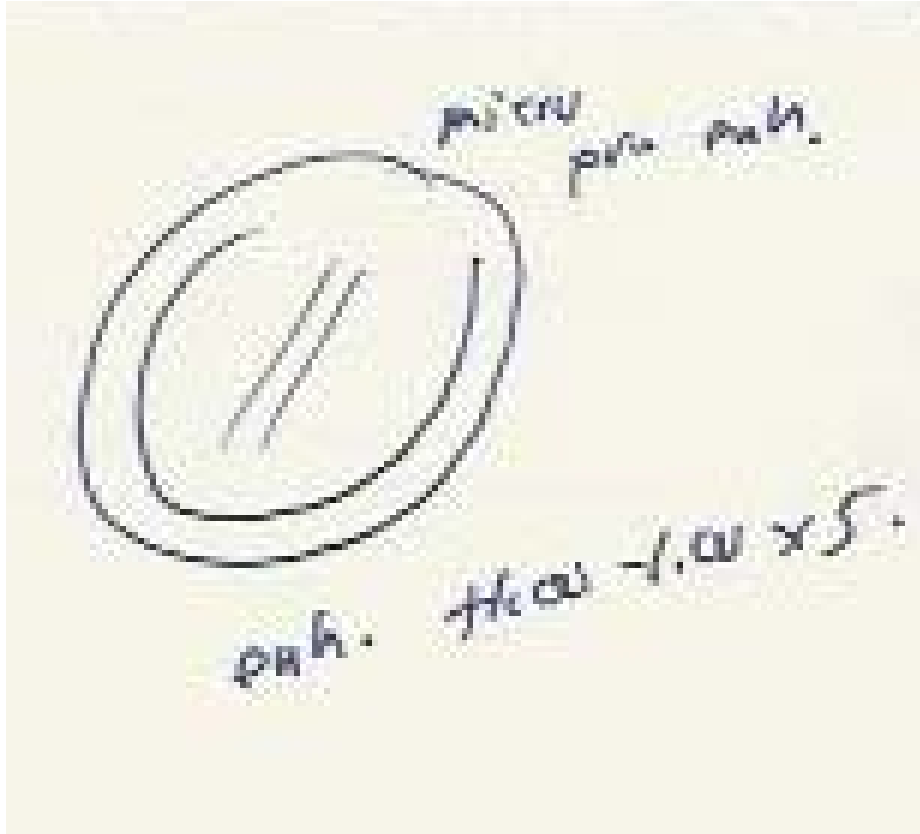

Microstriae
Related to Excess Tissue

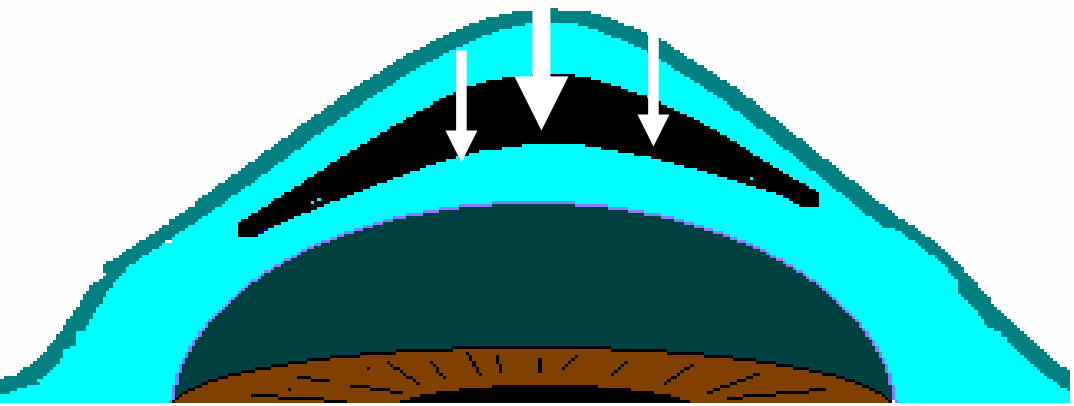

Standard teaching:

Excess tissue folds in on itself. Theory consistent with microstriae being more common after high corrections

- Does not explain the wide distribution in our patients (AV SE:-5.94+/-2.7D)

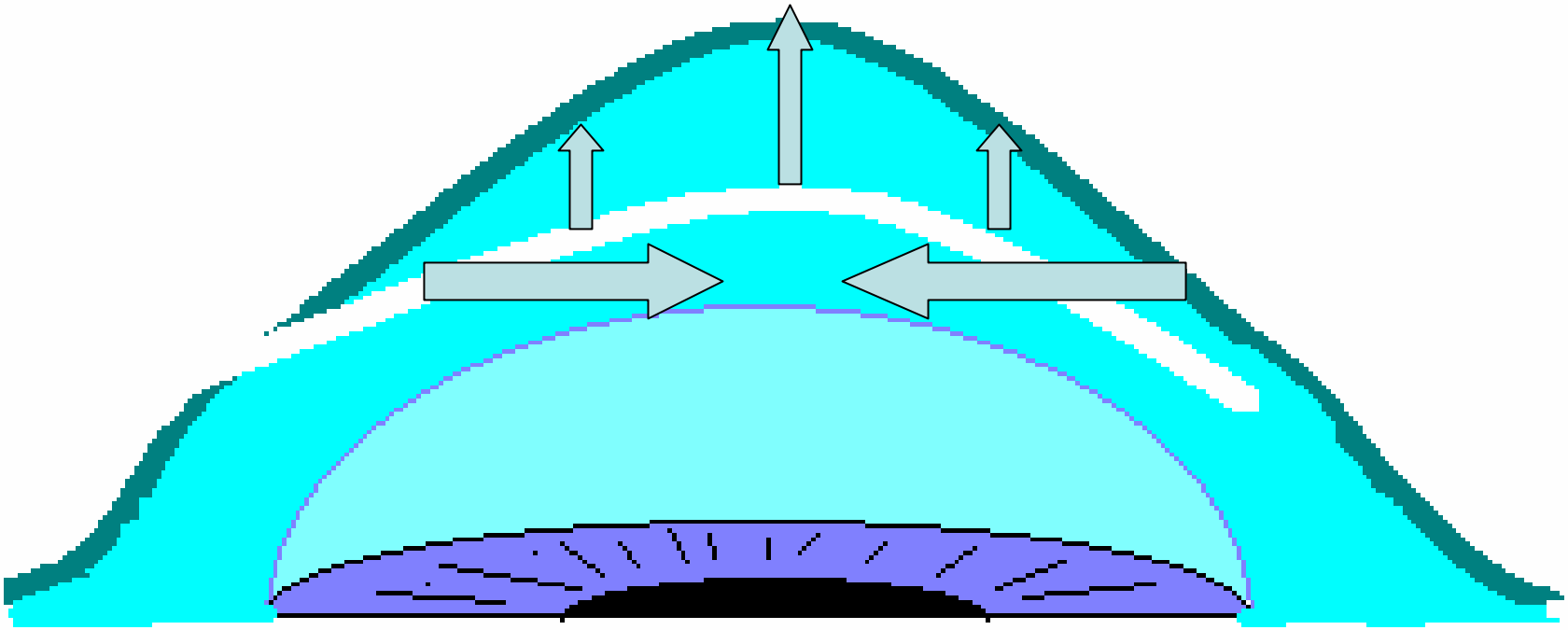

Etiology of Microstriae: excess corneal swelling

Central Microstriae: Related to over-hydration

Corneal hydrostatic pressure and aspiration of fluid and debris into the LASIK Interface, Mark E. Johnston ,Highlights ASCRS, 1999 Annual Meeting. Boston: Ophthalmology Interactive;1999.[CD-ROM]

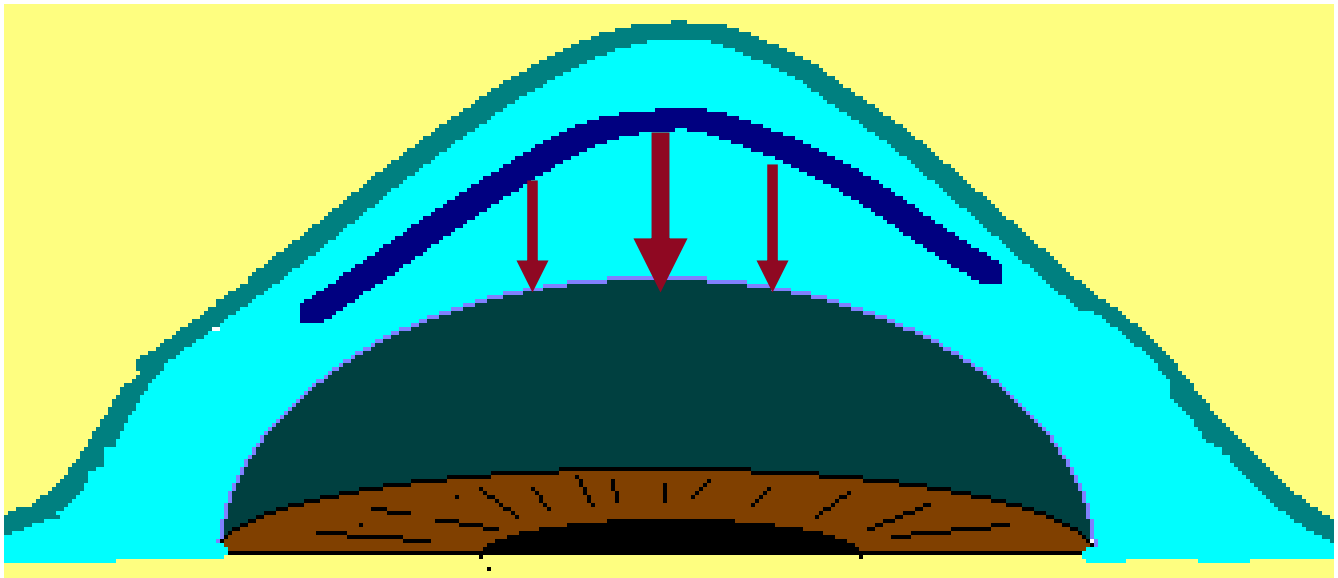

The looser posterior cornea and central cornea swell more than the tighter anterior and peripheral cornea

When the epithelium heals, the cornea dehydrates and the flap tissue infolds with secondary microstriae of the cornea.

Central Island / Microstriae formation

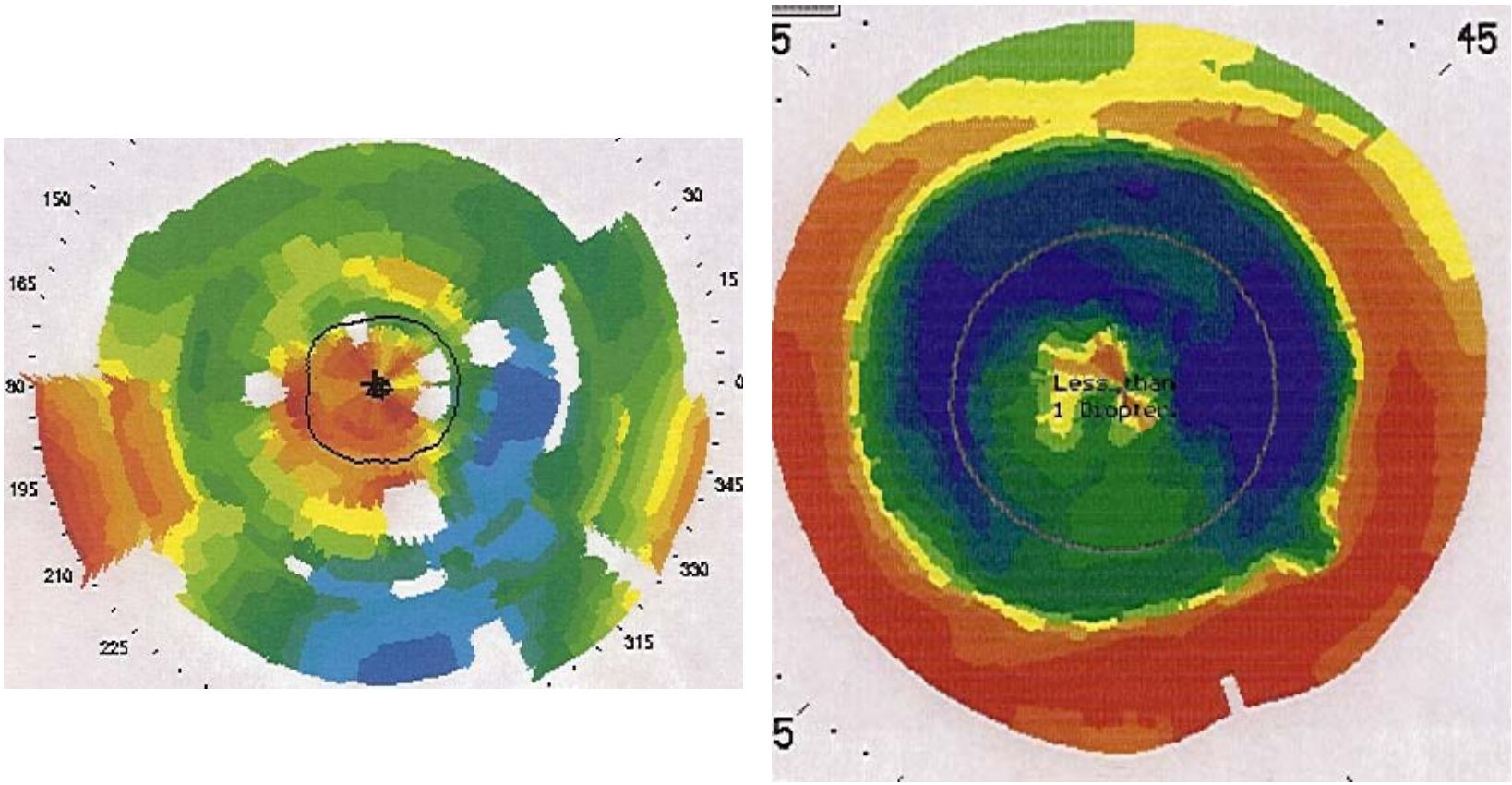

Case 5. A. Left: Thirty minutes after surgery a central island and moderate flap and deep stromal edema are noted. B. Right: Six weeks after surgery a central island and microstriae persist.

Prevention of microstriae

1. Float the flap
2. Minimize hydration
3. Use the cannula to smooth the hinge and the adjacent cornea before applying pressure over the central cornea

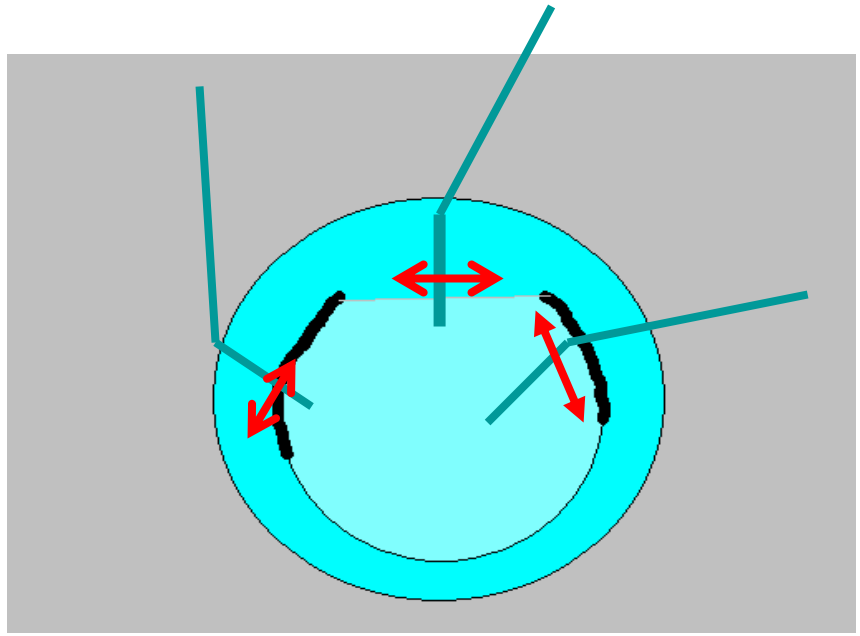

Mechanical characteristics of LASIK flap wrinkling

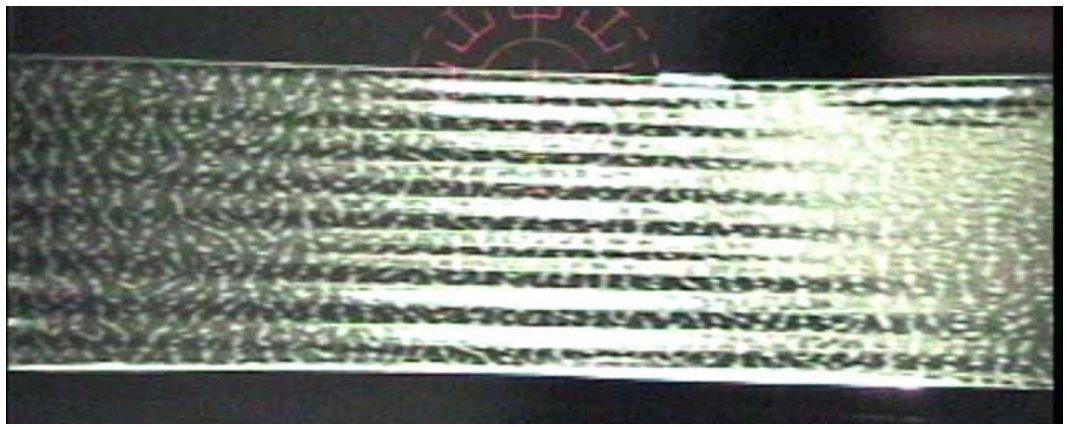

Mark E Johnston MD FRCSC

Nebraska Laser Eye Associates

Omaha NE

ASCRS 2004

johnston@nebraskaeye.com

Wrinkling of thin elastic sheets

E. Cerda, K. Ravi-Chandar, L.Mahadevan, Nature **419**,10, 579 (2002)

Föppl-Von Karman Equations

$$\lambda \sim (tl)^{1/2}/\gamma^{1/4}$$

Wavelength is proportional to the square root of the product of thickness and length divided by the fourth root of the displacement (strain)

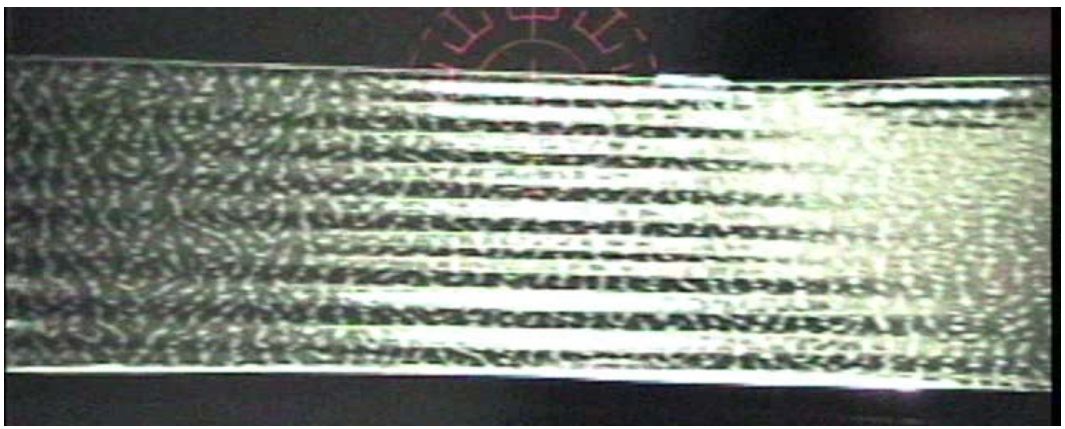

Stretched 3M Tagaderm

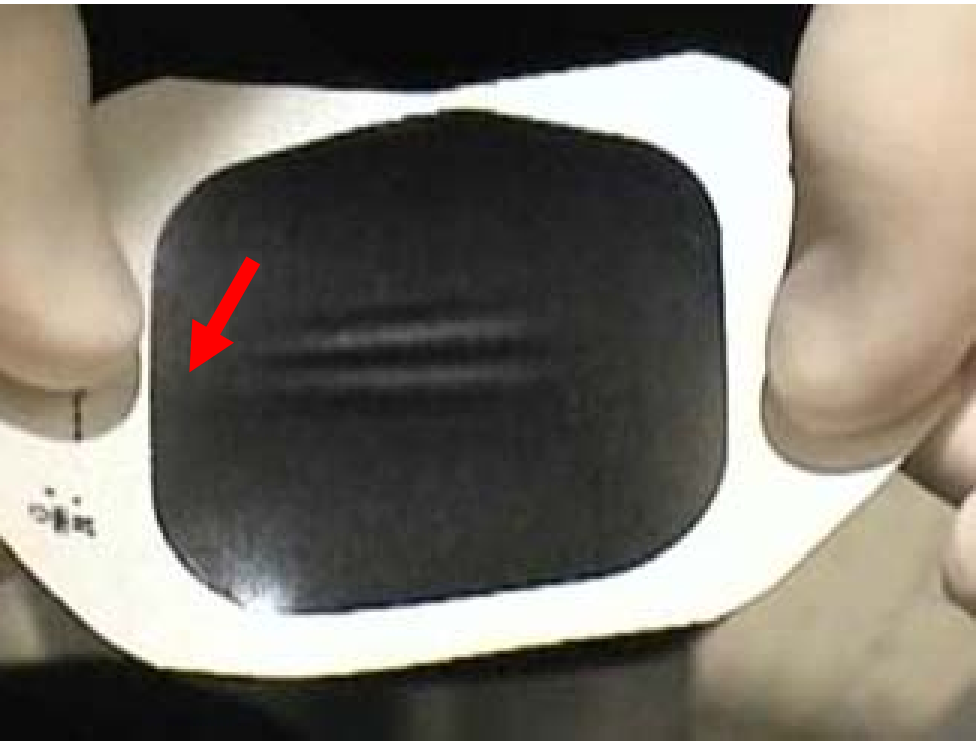

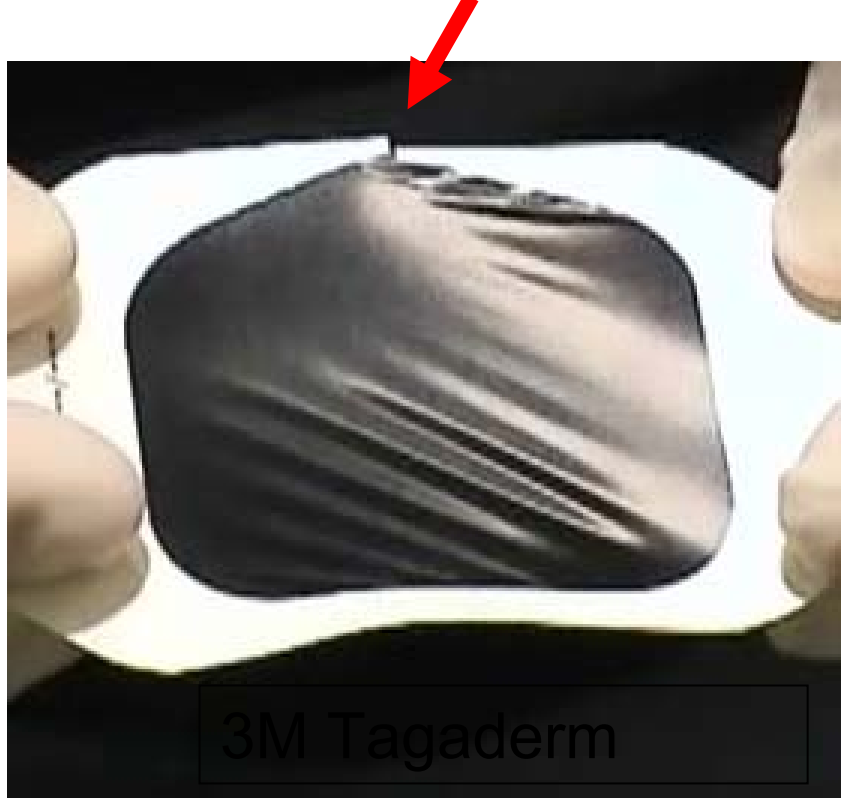

- No folds until a critical amount of displacement is achieved
- Wavelength is proportional to the fourth square root of the displacement

Wavelength ~ thickness

Reticule has 1mm marks

Six fine folds/mm ~ 160 um/fold ~ flap thickness

Corneal bending

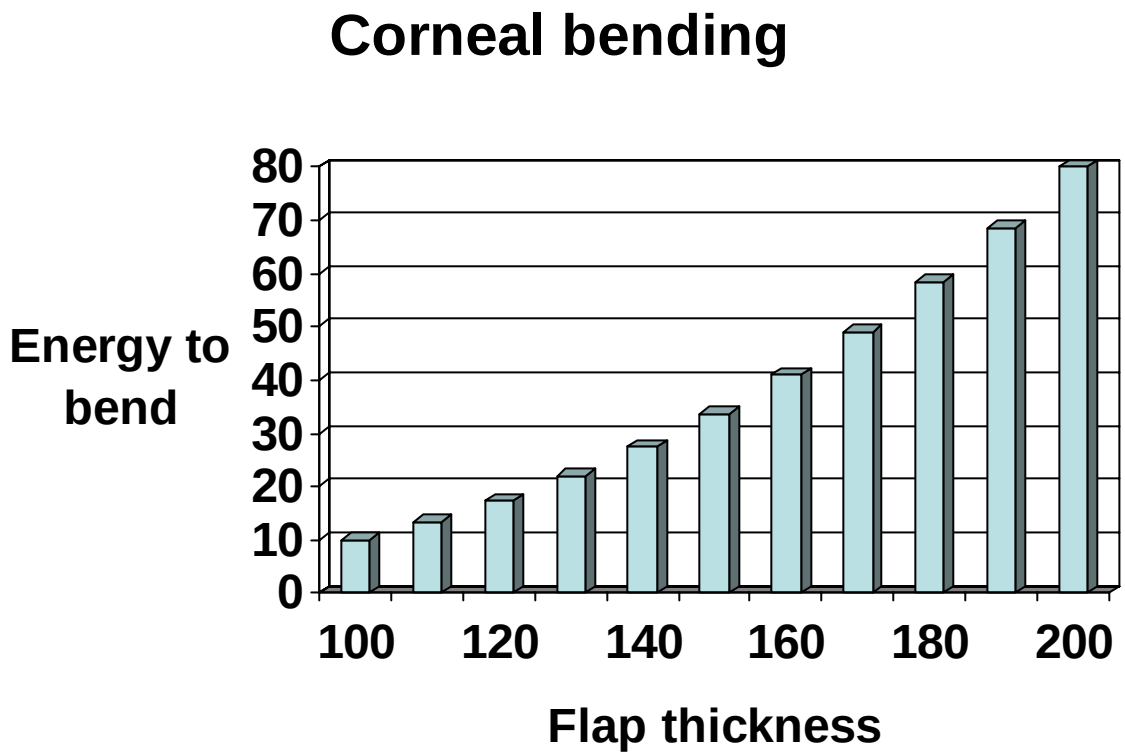

$E^B \sim k*t^3$

Energy of bending is proportional to the thickness to the third power

Doubling thickness increases the energy need to bend by a factor of eight

The energy needed to bend a 180 um flap is almost twice that required to fold a 160 um flap

Geometry and Physics of Wrinkling

E Cerda and L Mahadevan, Physical Review Letters. 90,074302-1(2003)

A: Compression wrinkles

- wavelength proportional to the thickness ($\lambda \sim 1t$)

B: Shrinkage induced wrinkles

- Wavelength a multiple of the surface thickness ($\lambda \sim 3t$)

Geometry and Physics of Wrinkling

E Cerda and L Mahadevan, Physical Review Letters. 90,074302-1(2003)

A: Compression wrinkles

- –wavelength proportional to the thickness (λ~1t)

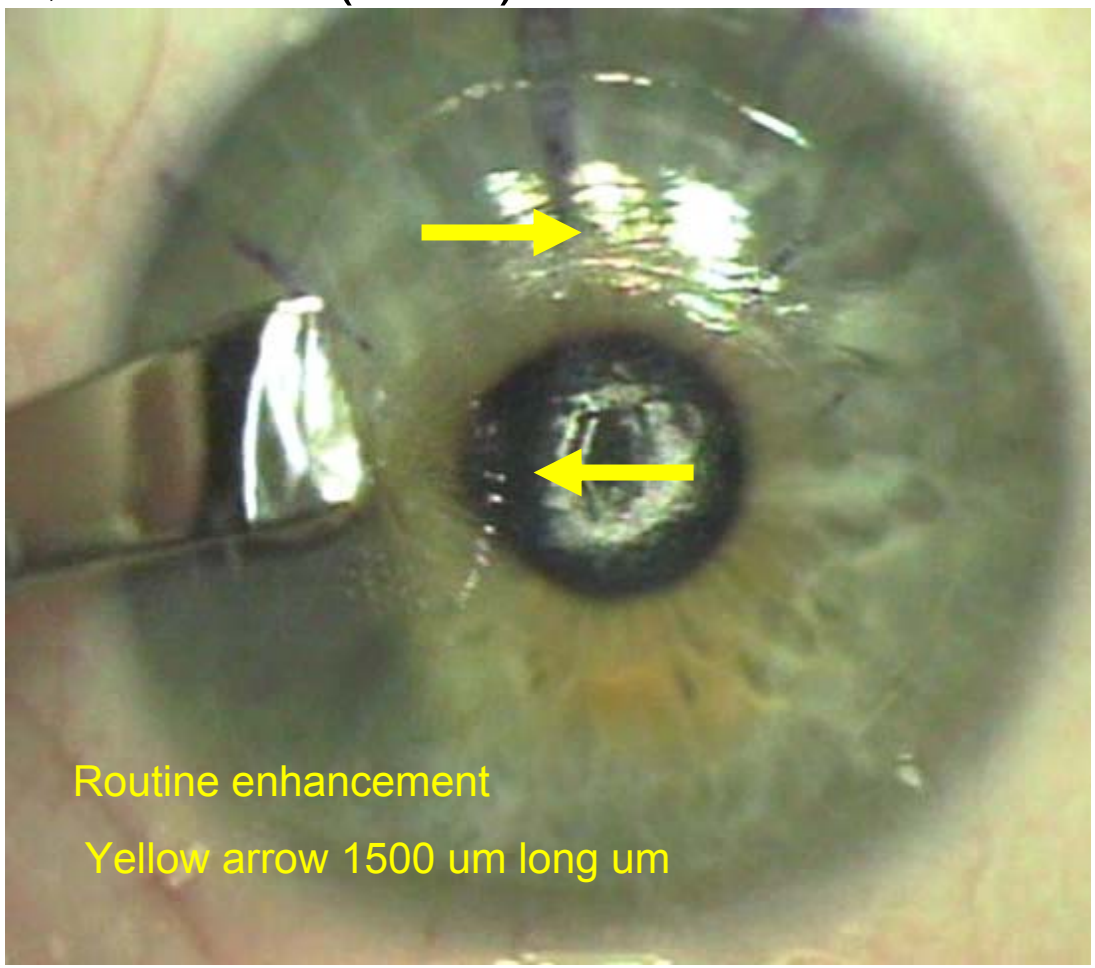

Slipped flap
compression folds less than 250 um

Red arrow 1000 um

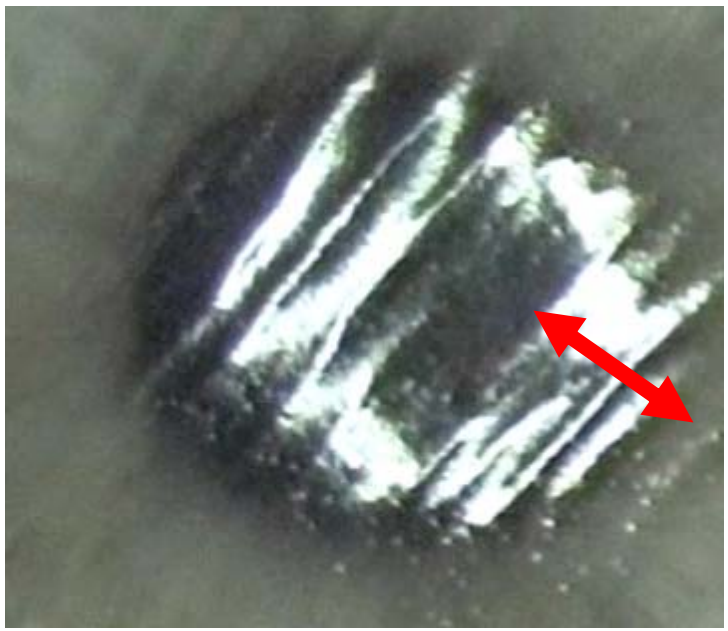

Red arrow 1000um

Folds that are spaced about the thickness of the flap are consistent with compression/displacement of the flap tissue

Slipped flap
compression folds less than 250 um

White arrow 1000 um long

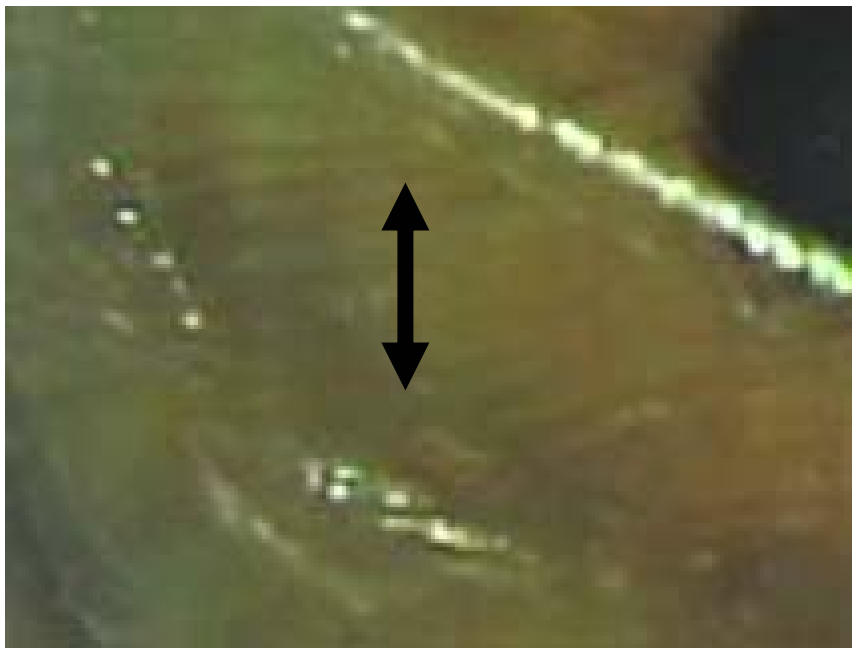

White arrow 1000 um

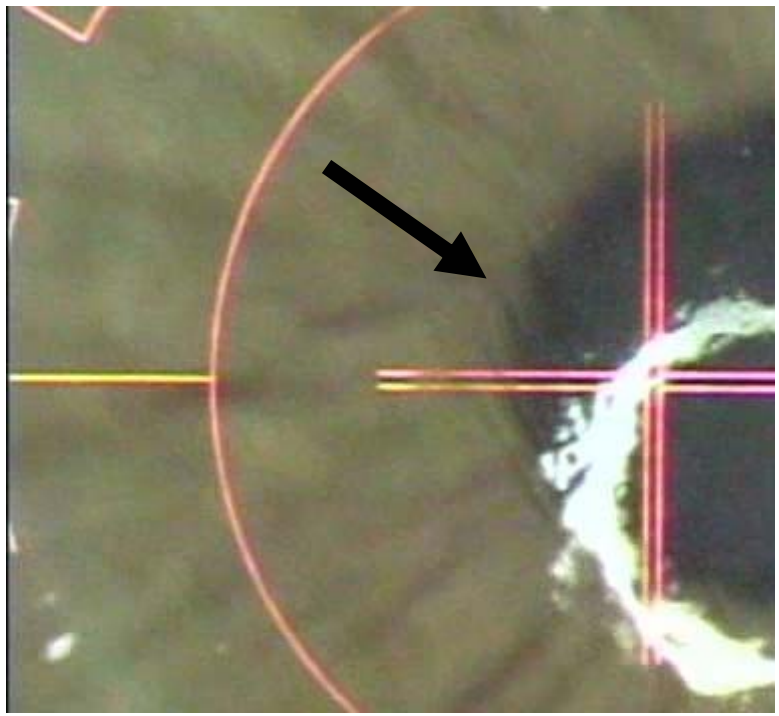

Folds that are spaced about the thickness of the flap apart are consistent with compression/displacement of the flap tissue

Geometry and Physics of Wrinkling

E Cerda and L Mahadevan, Physical Review Letters. 90,074302-1(2003)

B: Shrinkage induced wrinkles

- The wavelength is proportional to the relative ratio of the elastic modulus of the overlying membrane and the substrate times the thickness of the overlying membrane ($\lambda \sim 3t$)

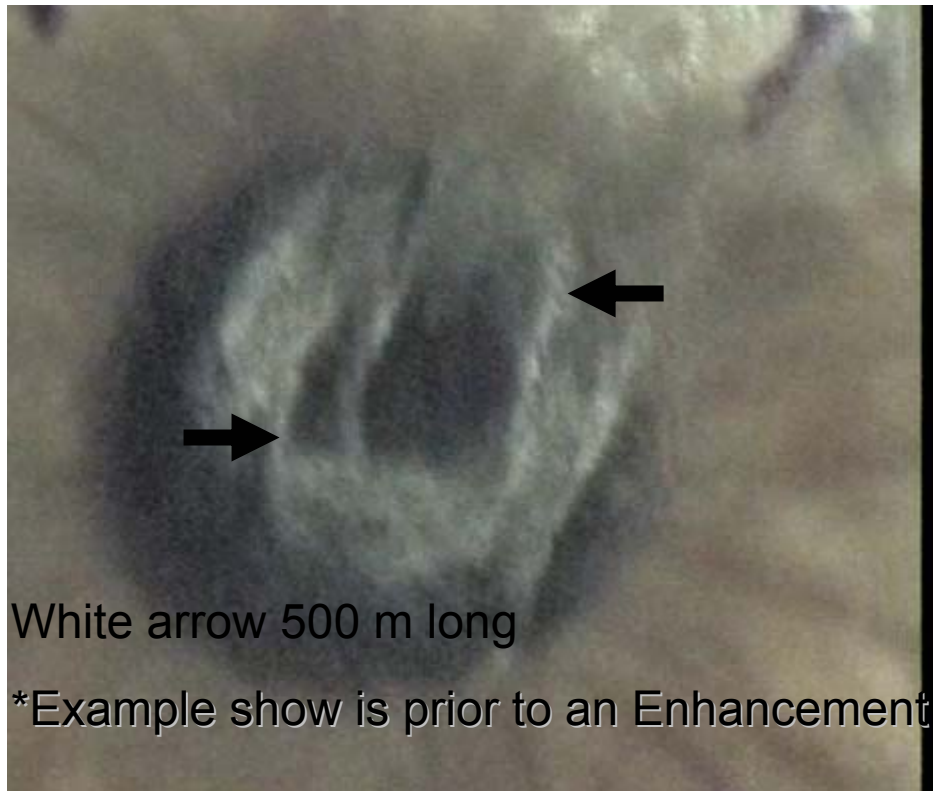

Central folds

note that the distance between major folds is about 500 um

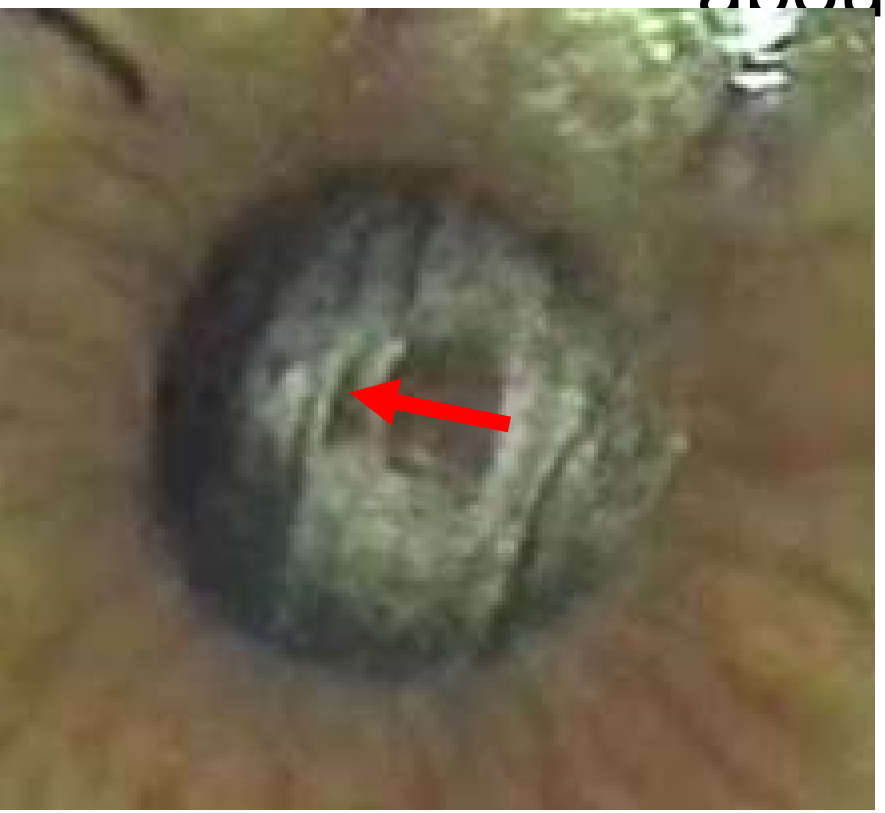

Red arrow 1000 um long

Folds that are spaced three times flap width apart are consistent with shrinkage of the underlying stromal tissue

Central Isolated folds

Folds in the bed

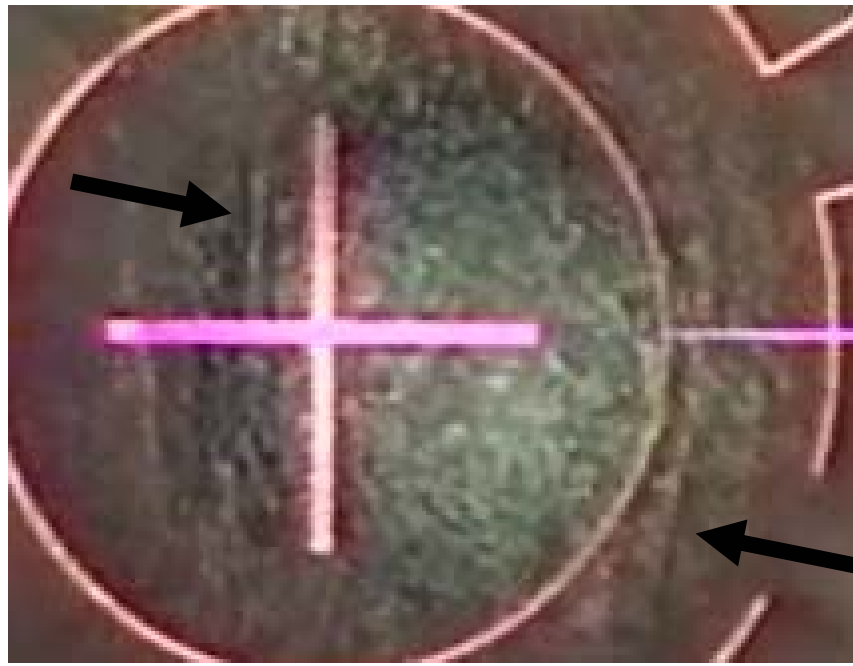

Reticule shows 1 mm

Distance between major folds is 500 um and is consistent with shrinkage of the underlying stroma

Etiology Microstriae

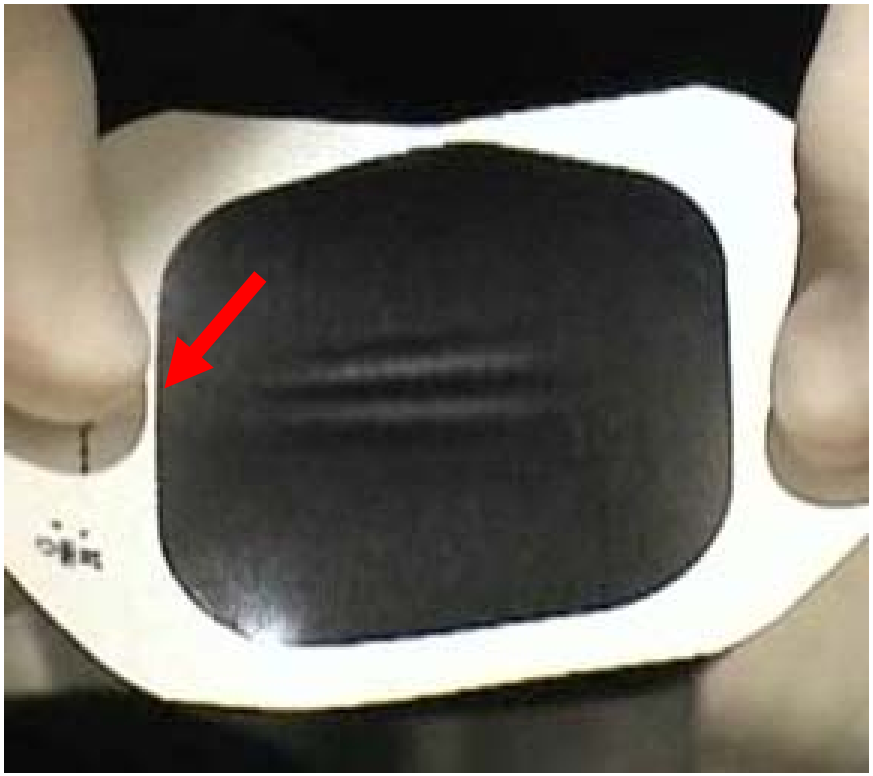

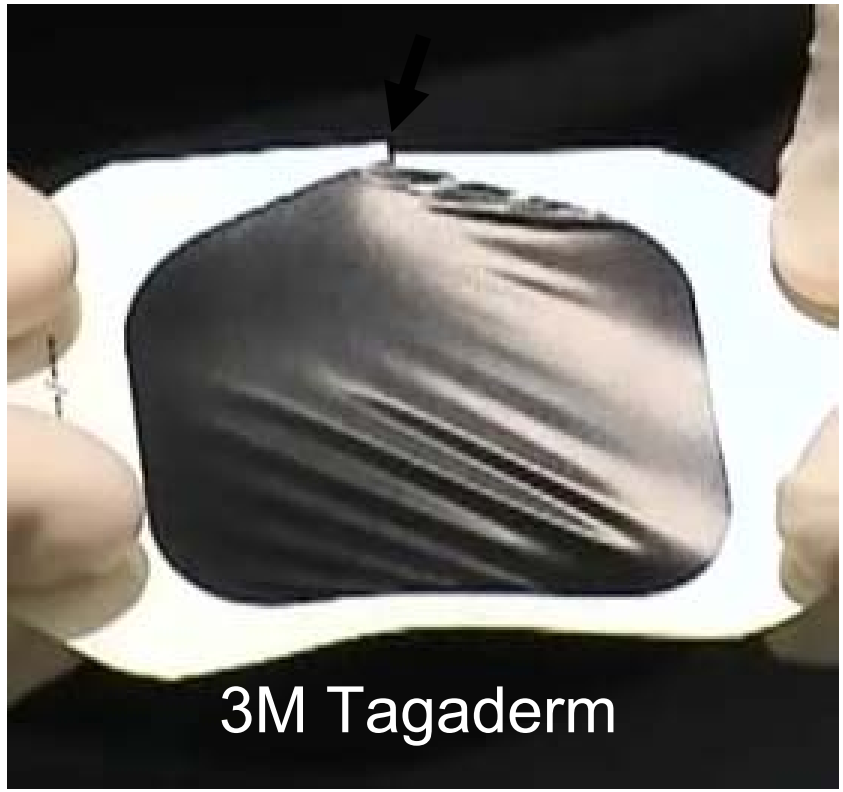

- Asymmetric tension
- Lateral displacement

Prevention of Microstriae

1. Thin flaps
   - Maximize flap thickness (both centrally and peripheral)
   - Avoid thin (and planar) flaps
2. Flap displacement
   - Premark the cornea
3. Avoid overhydration of the stromal bed

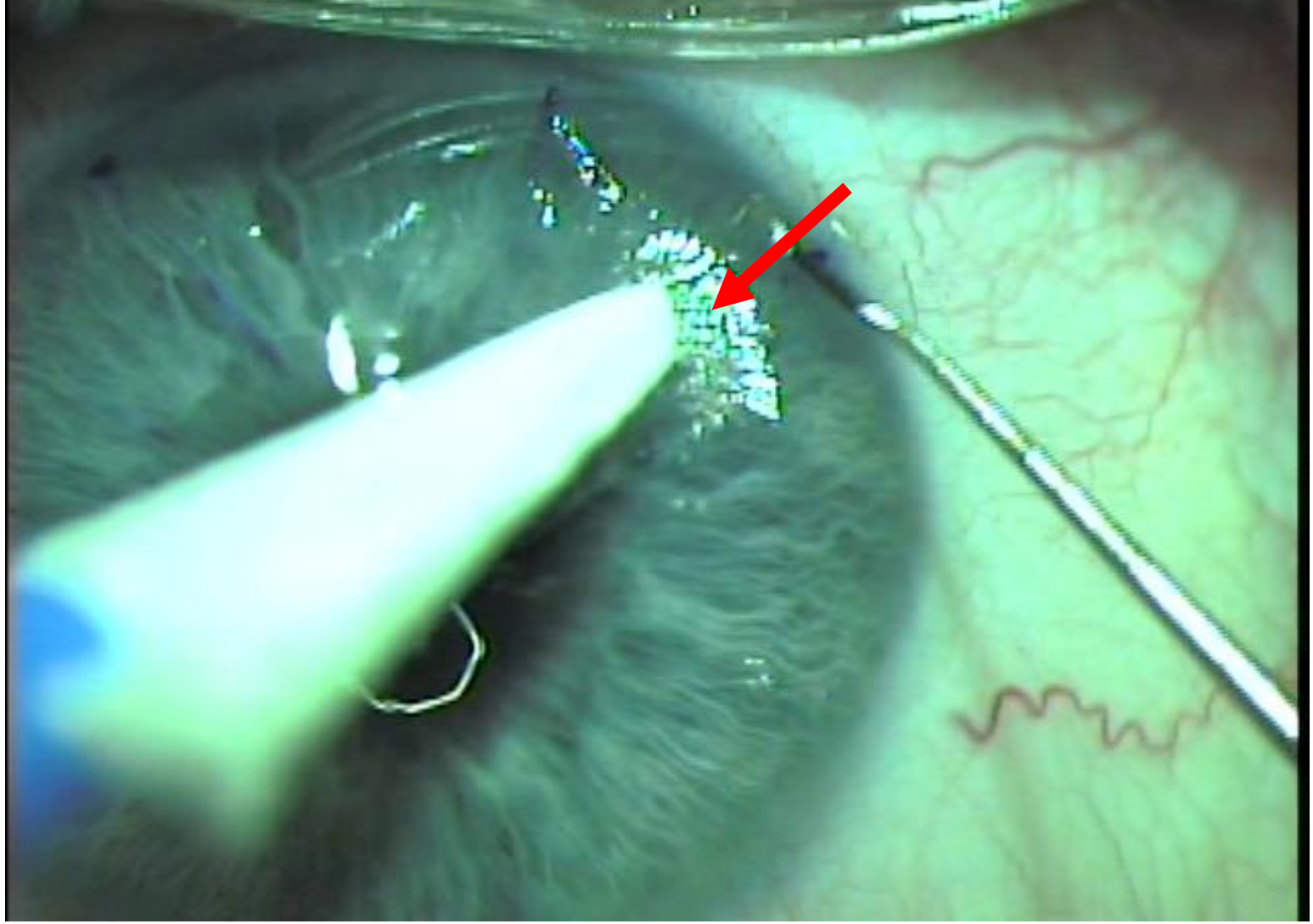

Note the microfolds to the edge of the flap
The distance between folds is proportional to the thickness of the layer

Slipped flaps

Increased incidence in 2004 related to company mislabeling keratome heads

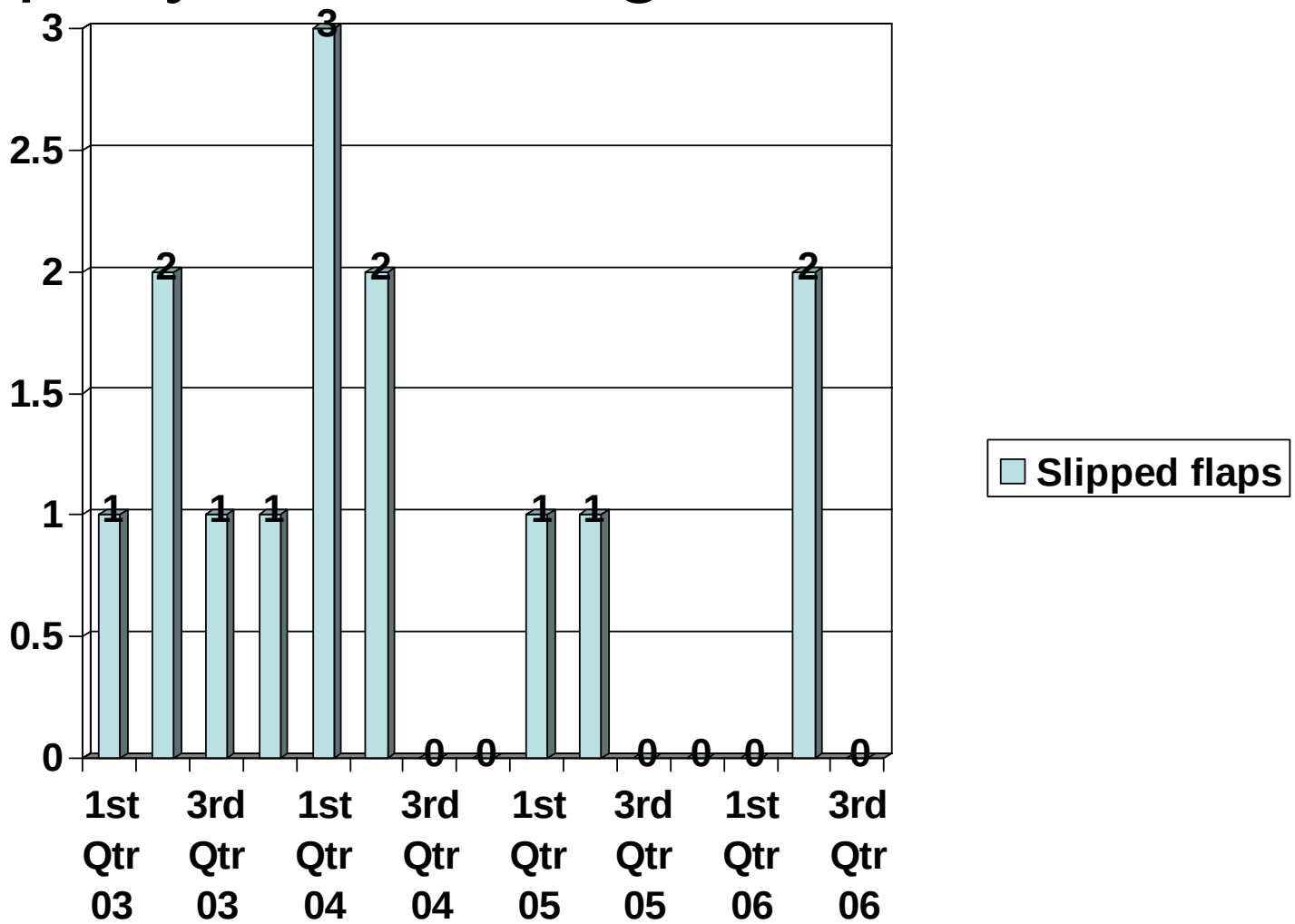

Slipped flaps: Prevention

- Avoid keratomes that cuts thin
  - Minimum targeted thickness 130 um
    - Also preventing microstriae
  - Use nomogram that takes initial corneal thickness into account
- Meniscus flap
- New blade second eye
  - Thin cornea
  - Steep cornea
  - High cylinder
- Punctal plugs
  - Routinely use:
    - 0.4 mm collagen plugs
    - superior and inferior punctum

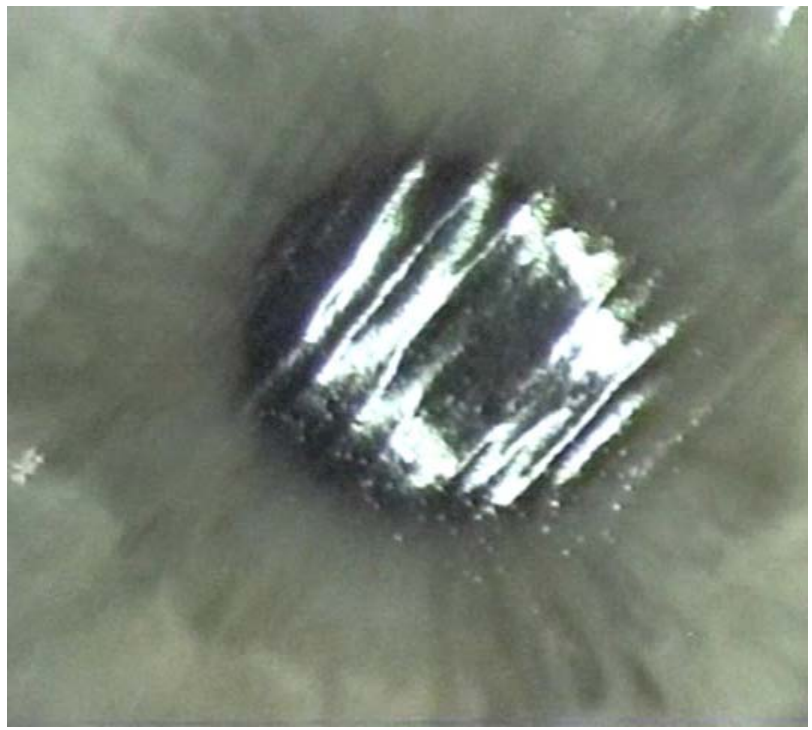

Causes of enhancement

- Increased sphere 30%
- Increased cylinder 29%
- Female 10%
- Age 5%
- Thicker flap 1%

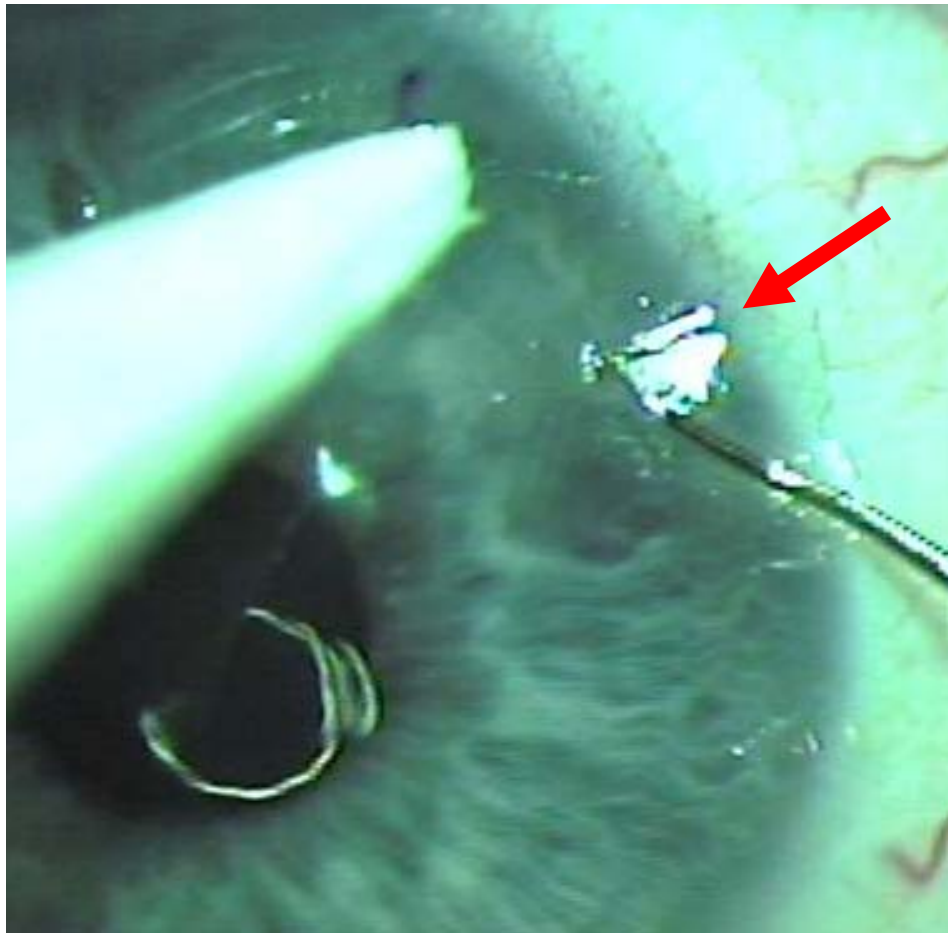

Note the folds in the peripheral cornea are further apart

More epithelial thickening with higher corrections

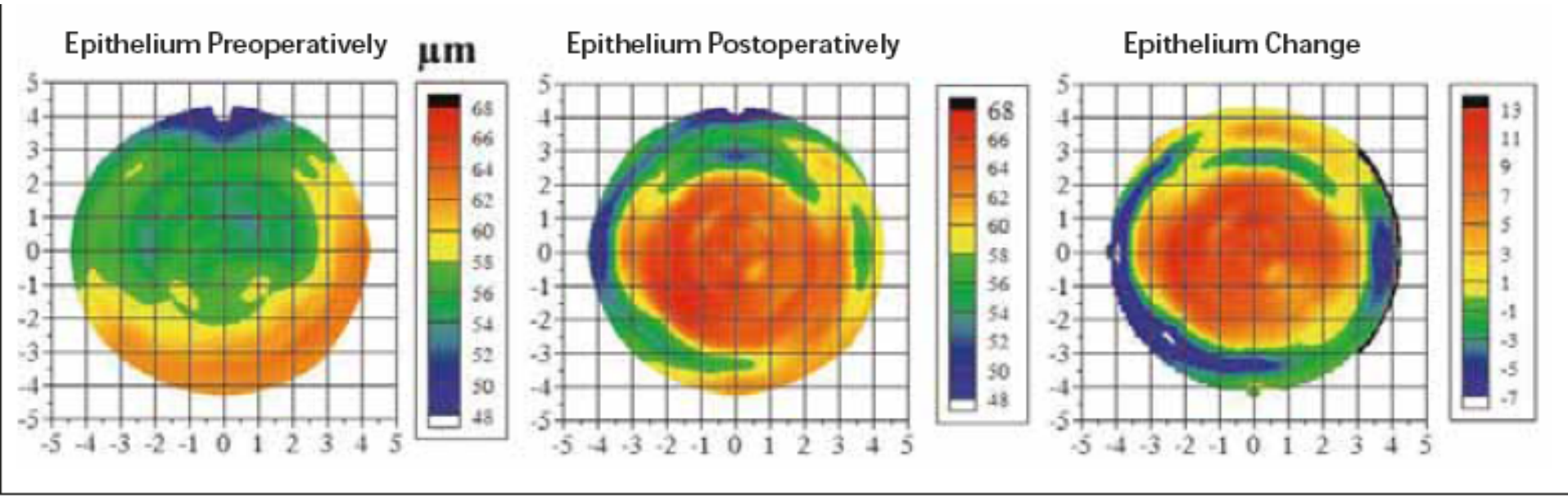

Figure 2. As evident in the epithelial thickness profile of a cornea before and after LASIK and the topographic difference map, central thickening relative to the peripheral epithelial change supports the notion that the epithelium is responsible for a regression 6 months after myopic LASIK.

Refractive Surgical Consultant ™

uses surgical outcomes to calculate laser nomograms

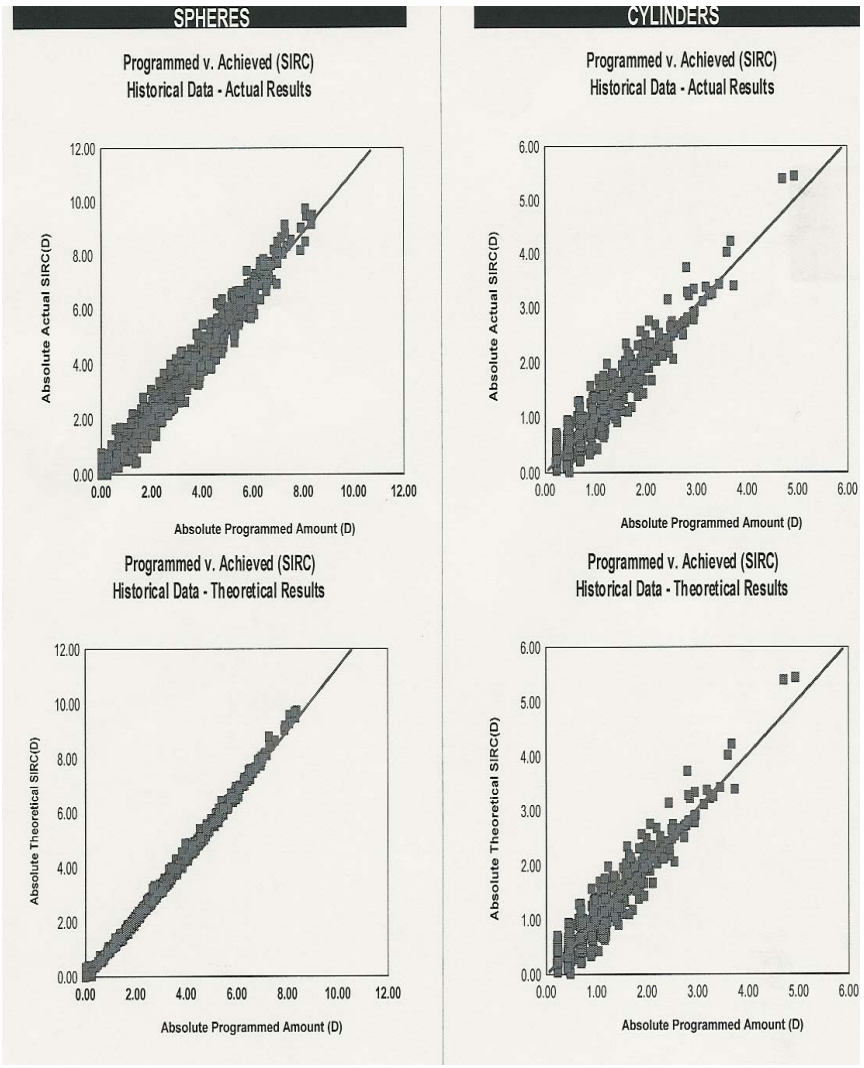

	Actual Results	Theoretical
Number Eyes	1,081	1,081
Average	0.29	0.29
Standard Deviation	0.41	0.26
Minimum	-0.99	-0.27
Maximum	1.88	1.52
+/- 0.50 D (N / %)	780 / 1,081 (72.2%)	882 / 1,081 (82.0%)
+/- 1.00 D (N / %)	1,019 / 1,081 (94.3%)	1,059 / 1,081 (98.0%)
> +/- 1.00 D (N / %)	62 / 1,081 (6.0%)	22 / 1,081 (2.0%)

	Actual Results	Theoretical
Number Eyes	860	860
Average	0.01	0.01
Standard Deviation	0.20	0.06
Minimum	-0.61	-0.10
Maximum	0.93	0.50
+/- 0.50 D (N / %)	836 / 860 (97.2%)	860 / 860 (100.0%)
+/- 1.00 D (N / %)	860 / 860 (100.0%)	860 / 860 (100.0%)
> +/- 1.00 D (N / %)	0 / 860 (0.0%)	0 / 860 (0.0%)

Developed by Dr Jack Holladay
and Dr Guy Kezirian

Biophysical modeling of cornea for

a) Residual bed thickness
   - ORB Artifact

b) Pre-op IOP
   - Not clinically significant with the RSC

c) Pre-op Corneal thickness
   - Not clinically significant with the RSC

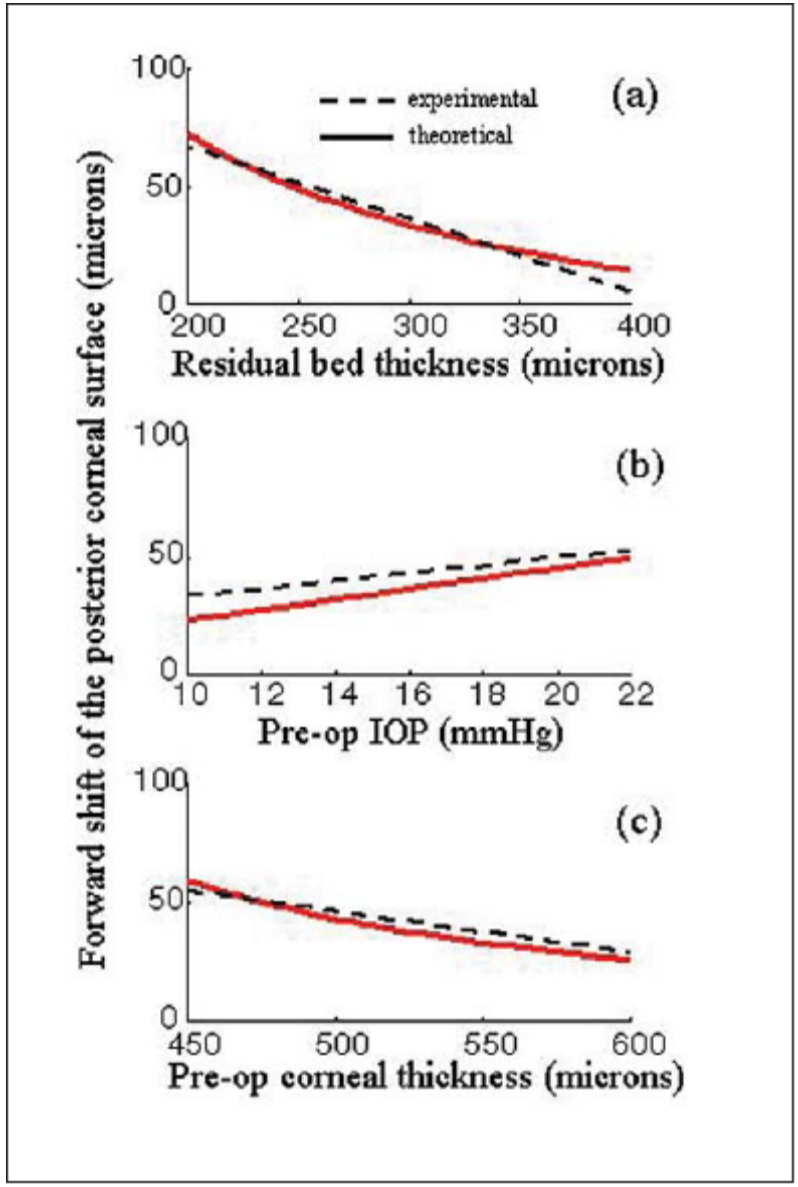

Figure 2. Forward shift of the posterior surface of the cornea after myopic LASIK predicted with our model of Eq.(2) (solid line) in comparison with the experimental curves of Baek et al[15] (dashed line). Shifts are plotted as a function of the **A**) residual bed thickness, **B**) preoperative IOP, and **C**) preoperative corneal thickness. See text and Table 1 for details on the parameters used in the model. Experimental curves are the lineal fits used by Baek et al[15] to fit 196 experimental points.

Spherical Aberration

- is greater for a steep lens
- increases with distance from the optical center

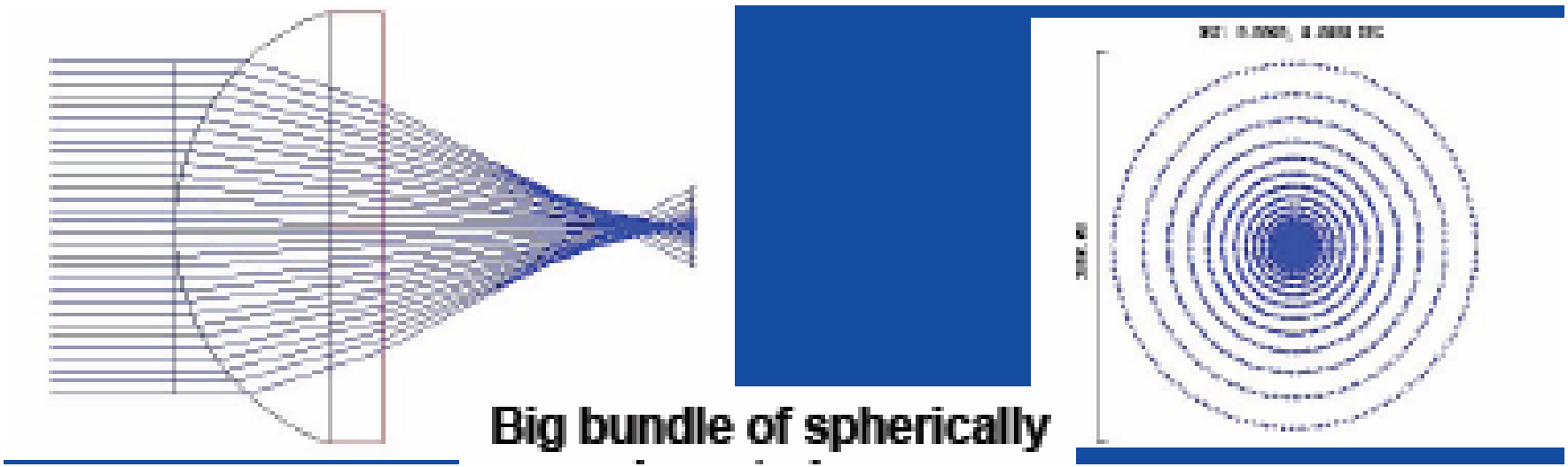

$$\delta f = ah^2 / f$$

Laser ablation profiles

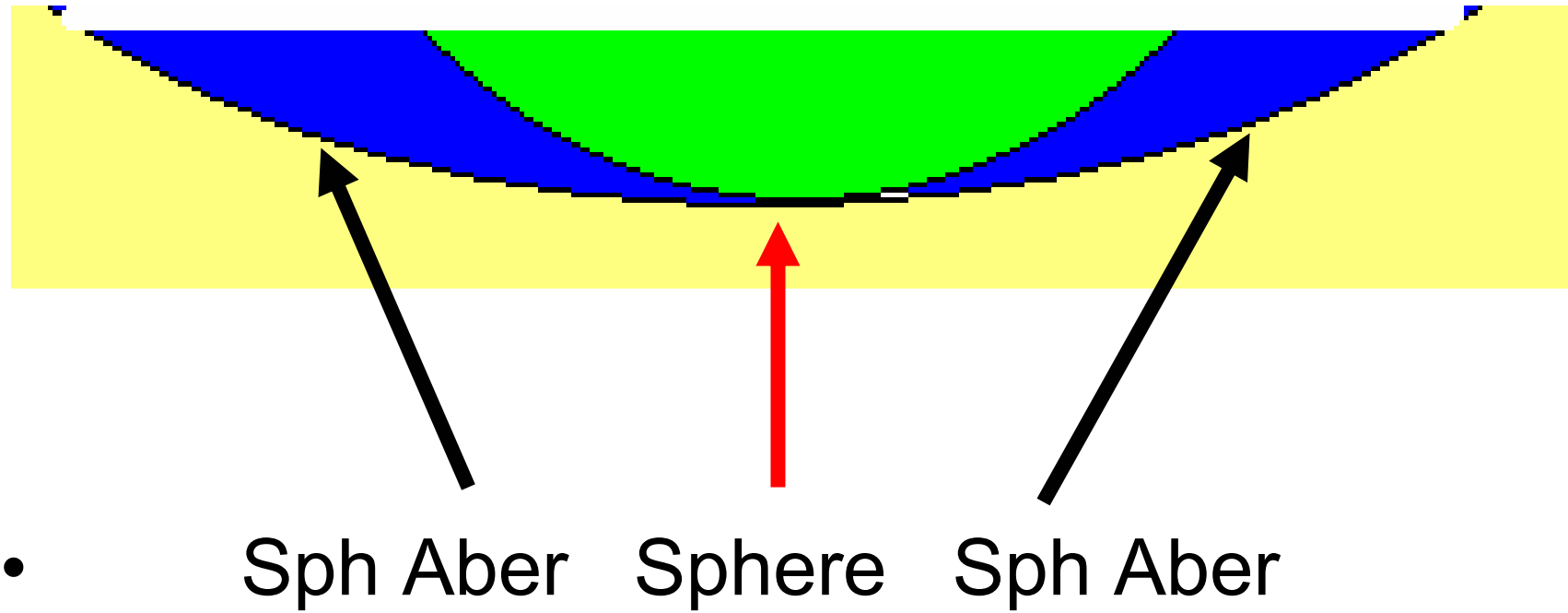

- Sph Aber Sphere Sph Aber

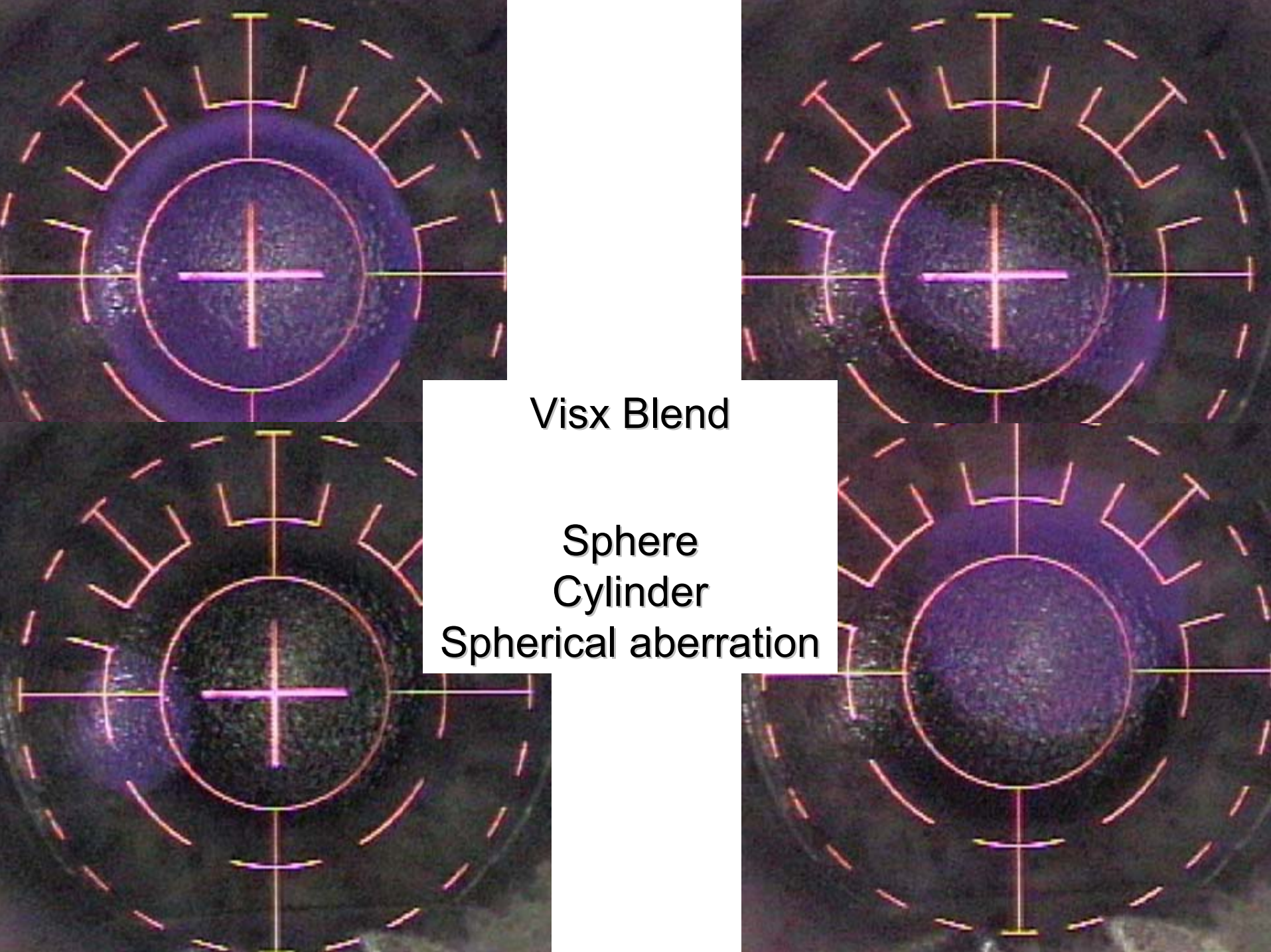
Visx Blend
Sphere
Cylinder
Spherical aberration

Overcorrection with positive spherical aberration

- Manifest is the average depth of the center of the lake:
  - can be estimated by knowing the water level and the rim height
  - Water level is like the average wavefront over the crater
  - Plus spherical aberration is proportional to the height of the rim

VISX Effective Optical Zone(EOZ) is the area within one diopter of central power

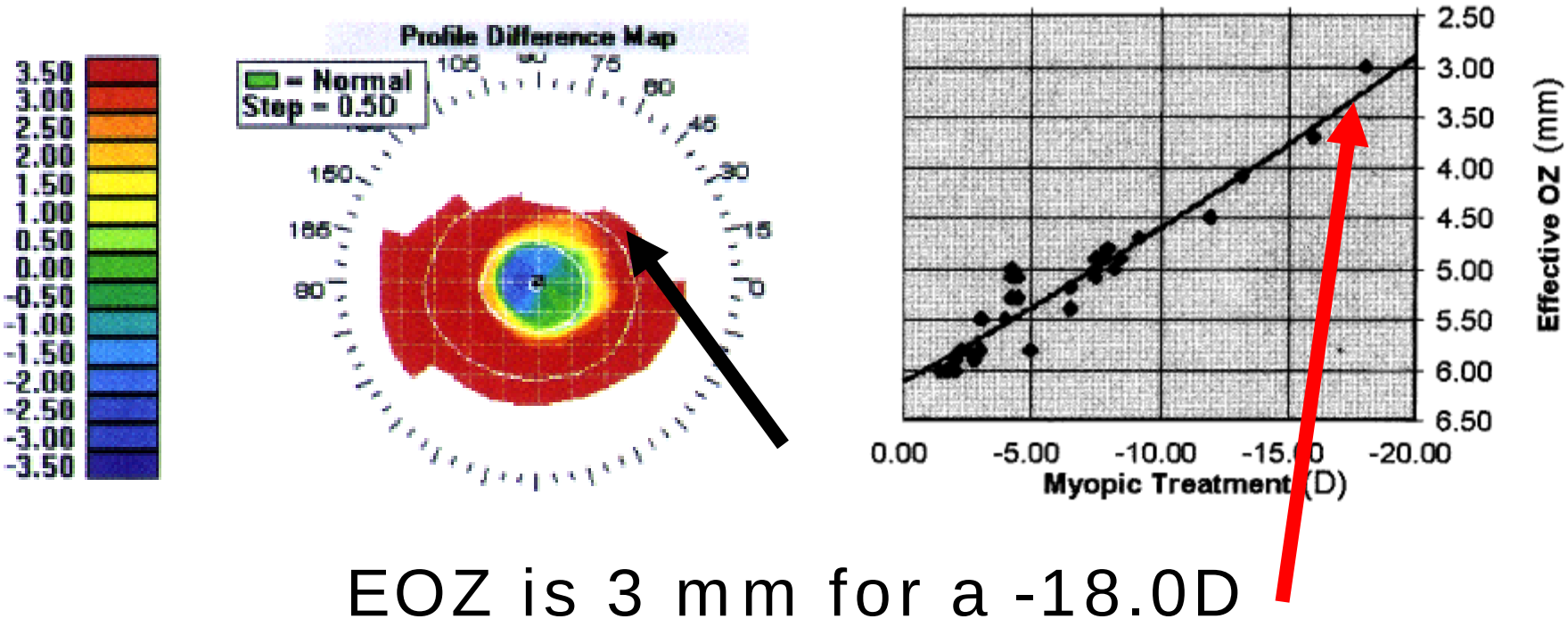

EOZ is 3 mm for a -18.0D Treatment

$Y+-0.001056x^2 + 0.0140156x + 6.11837$

Visx standard:

- Increasing spherical aberration decreases the effective optical zone
- increases the overcorrection

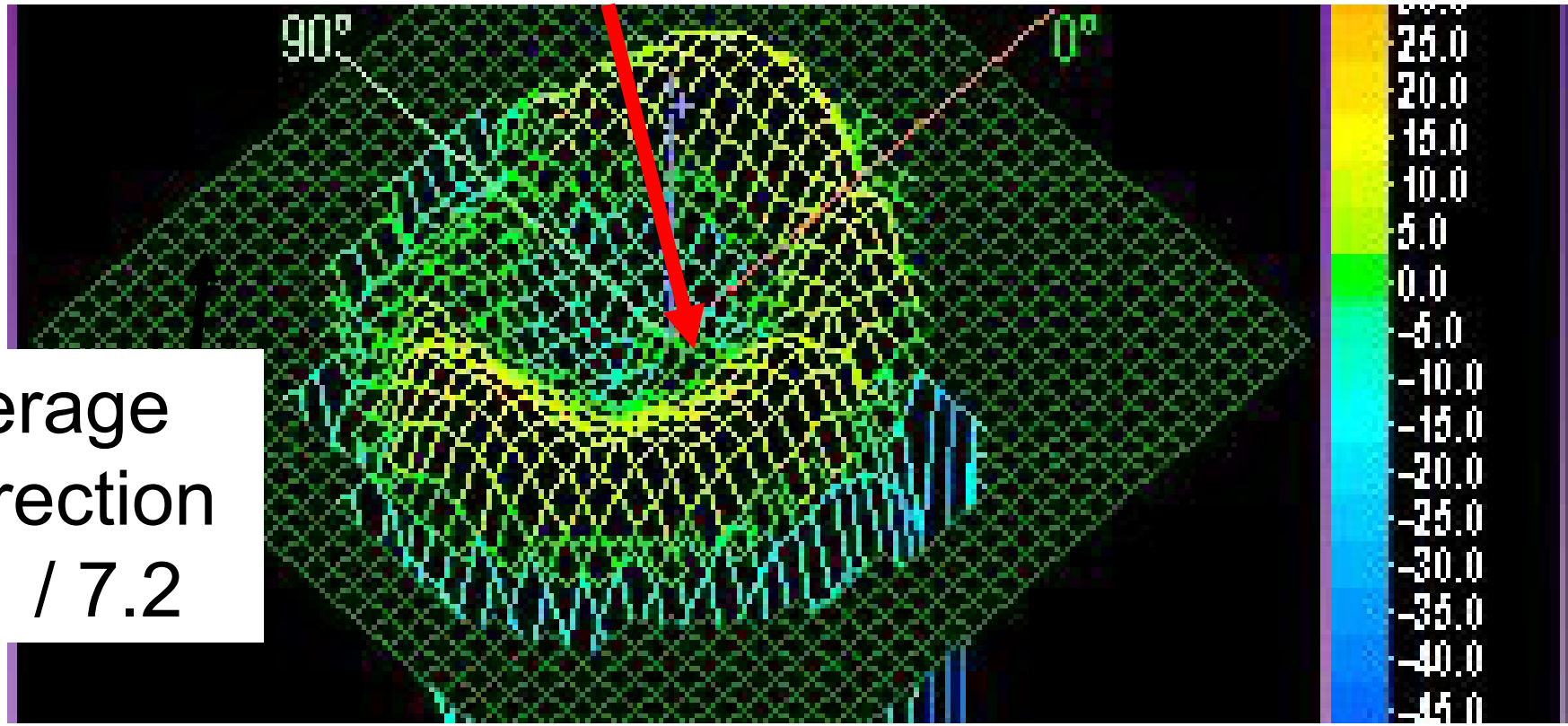

Average Correction 8.21 / 7.2

Post –op Spherical aberration (SA) compared to pre-op sphere

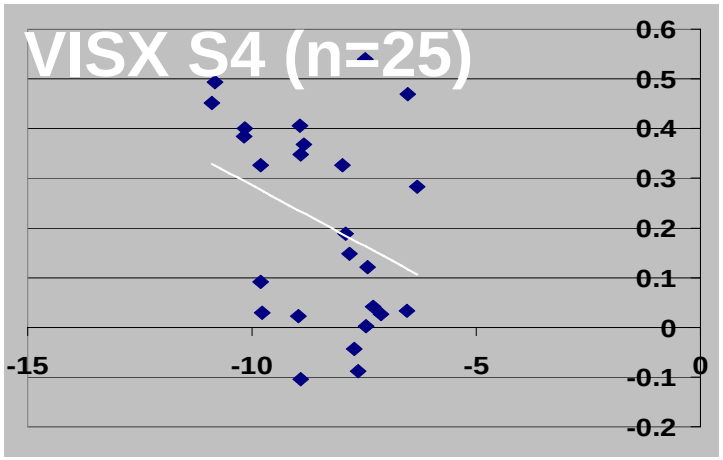

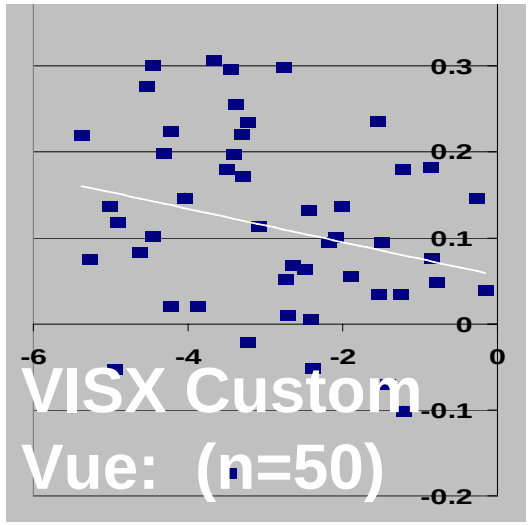

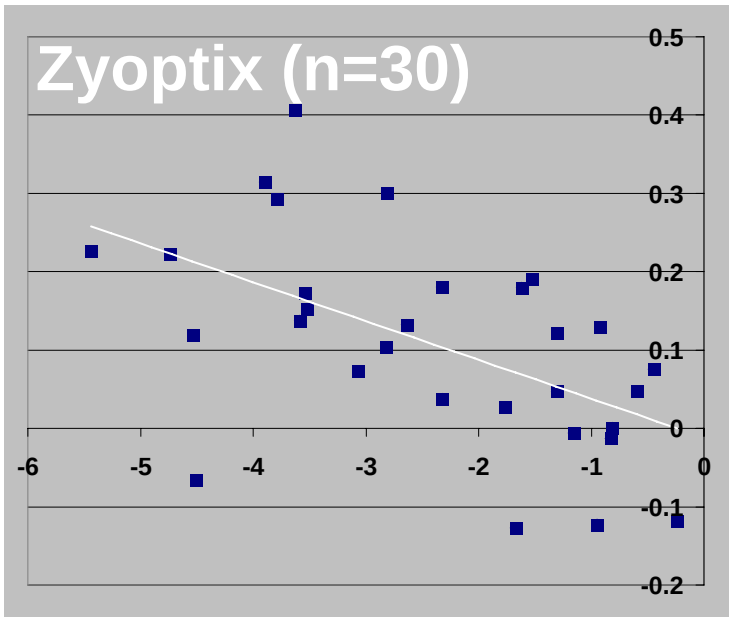

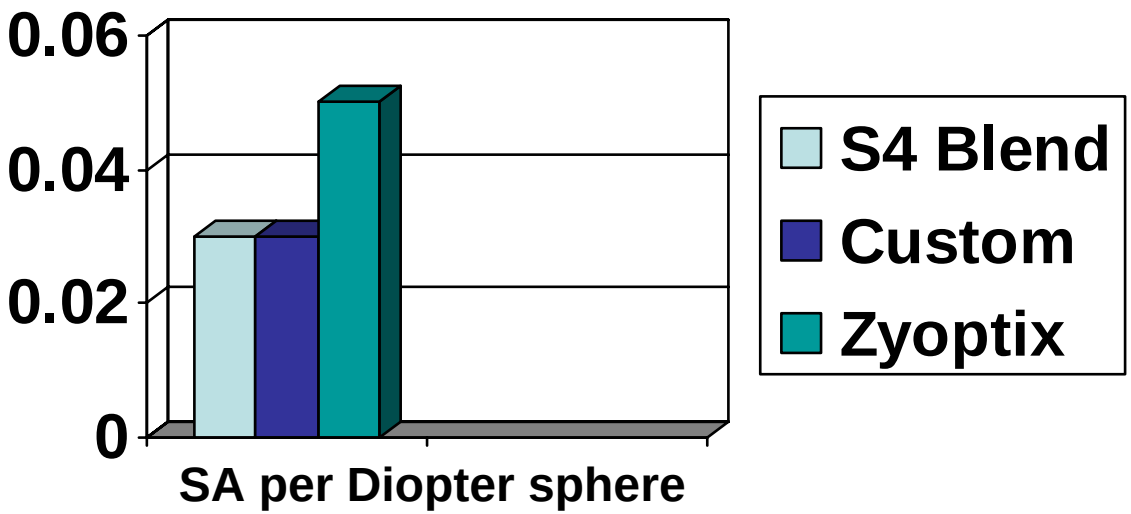

- Visx Overcorrection
  - **Standard Visx does not treat spherical aberration and atoric aberration**
  - **Increasing sphere and cylinder decreases the effective optical zone and induce overcorrection**
  - **Appropriate decrease is calculated for each treatment**

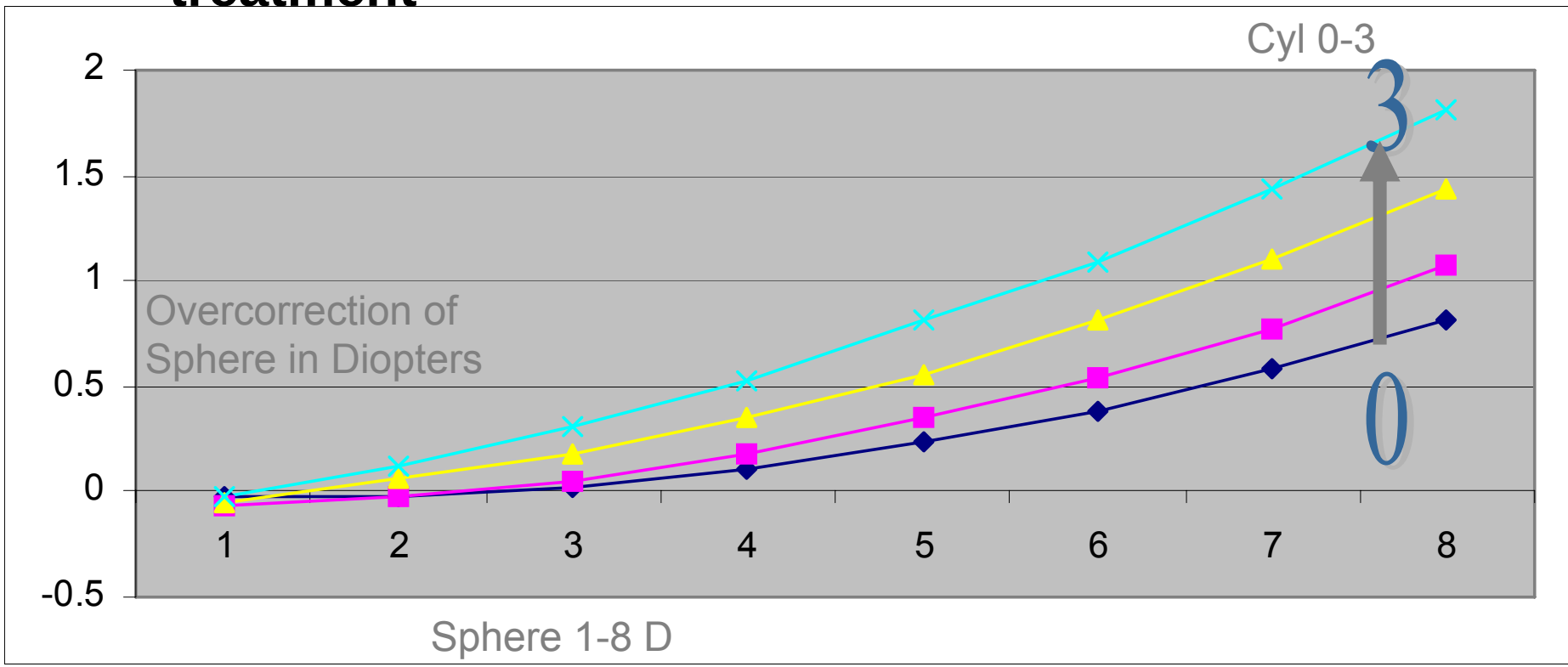

Custom Vue

Note that mid-peripheral overcorrection creates mild negative spherical aberration

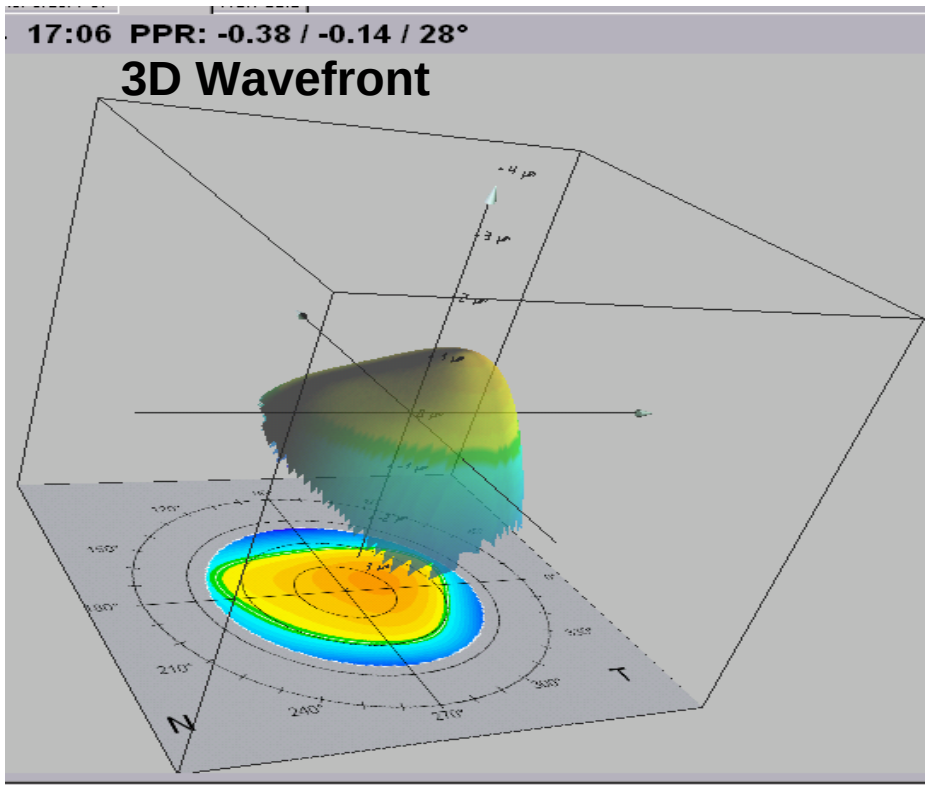

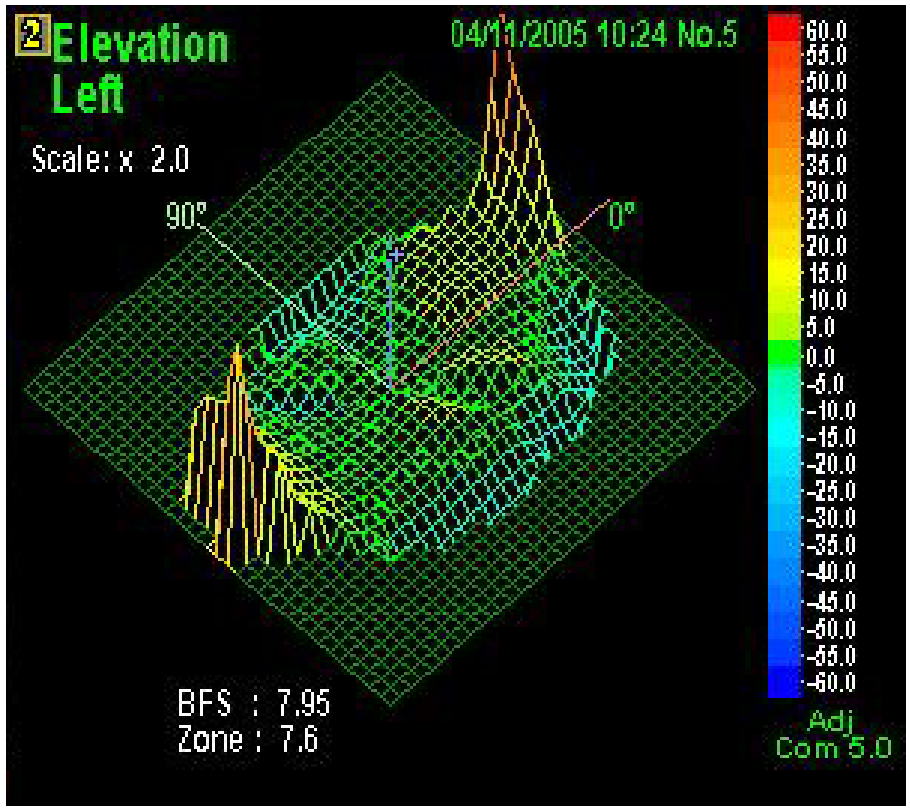

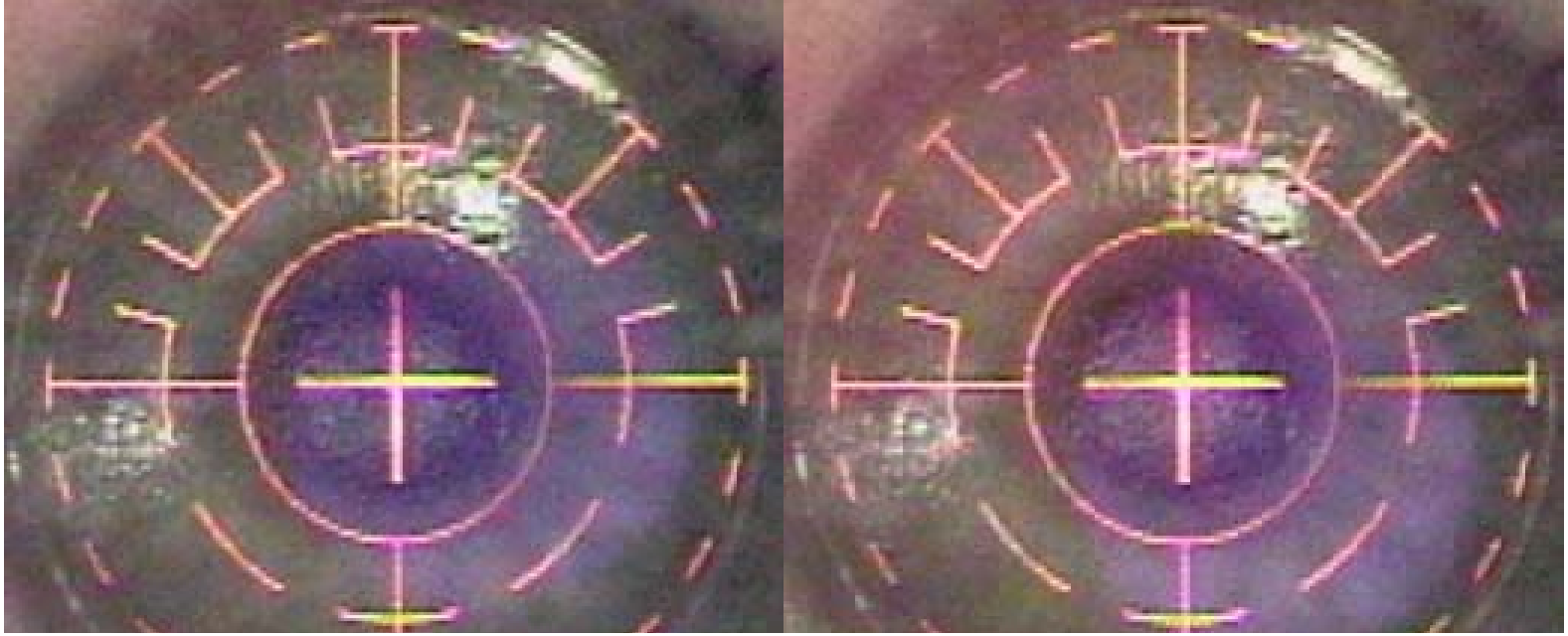

Visx Wavefront :

Note how sequential laser spot rotate around the central axis

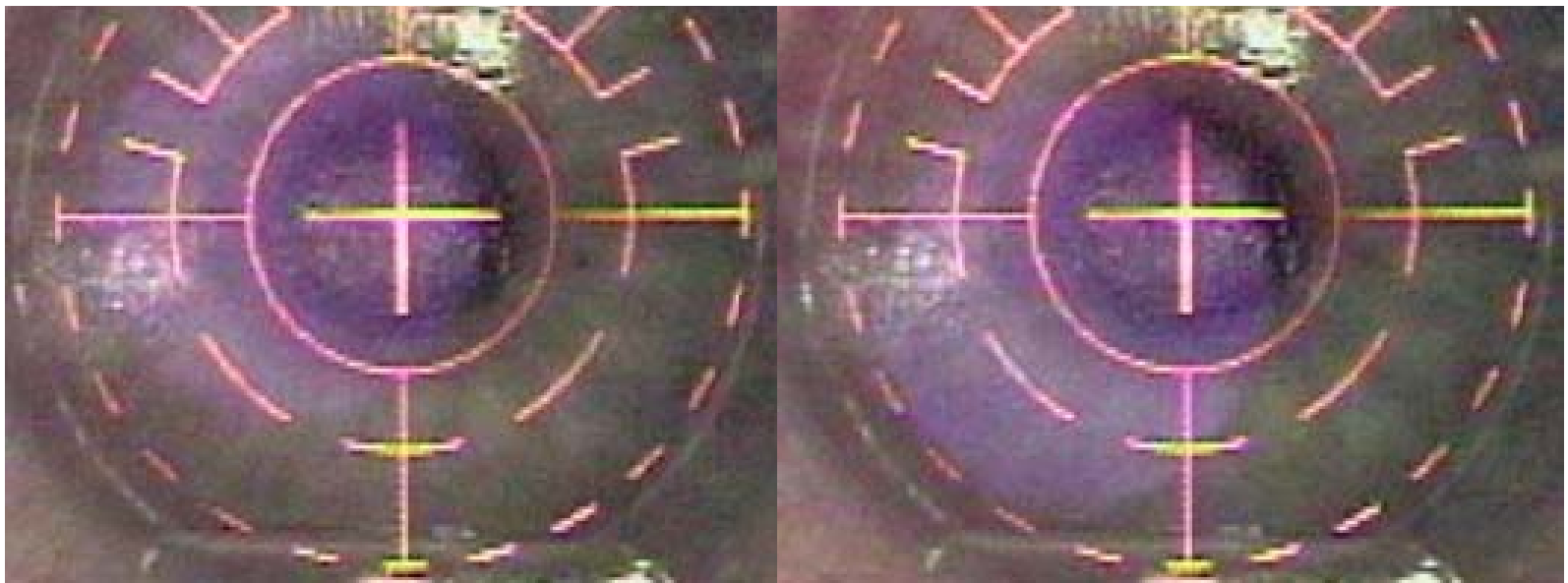

Under-correction with negative spherical aberration

- **Manifest is the average height over the center of the island:**
  - **Water level is like the average wavefront**
  - **Minus spherical aberration is like the height of the island compared to depth of the lagoon**

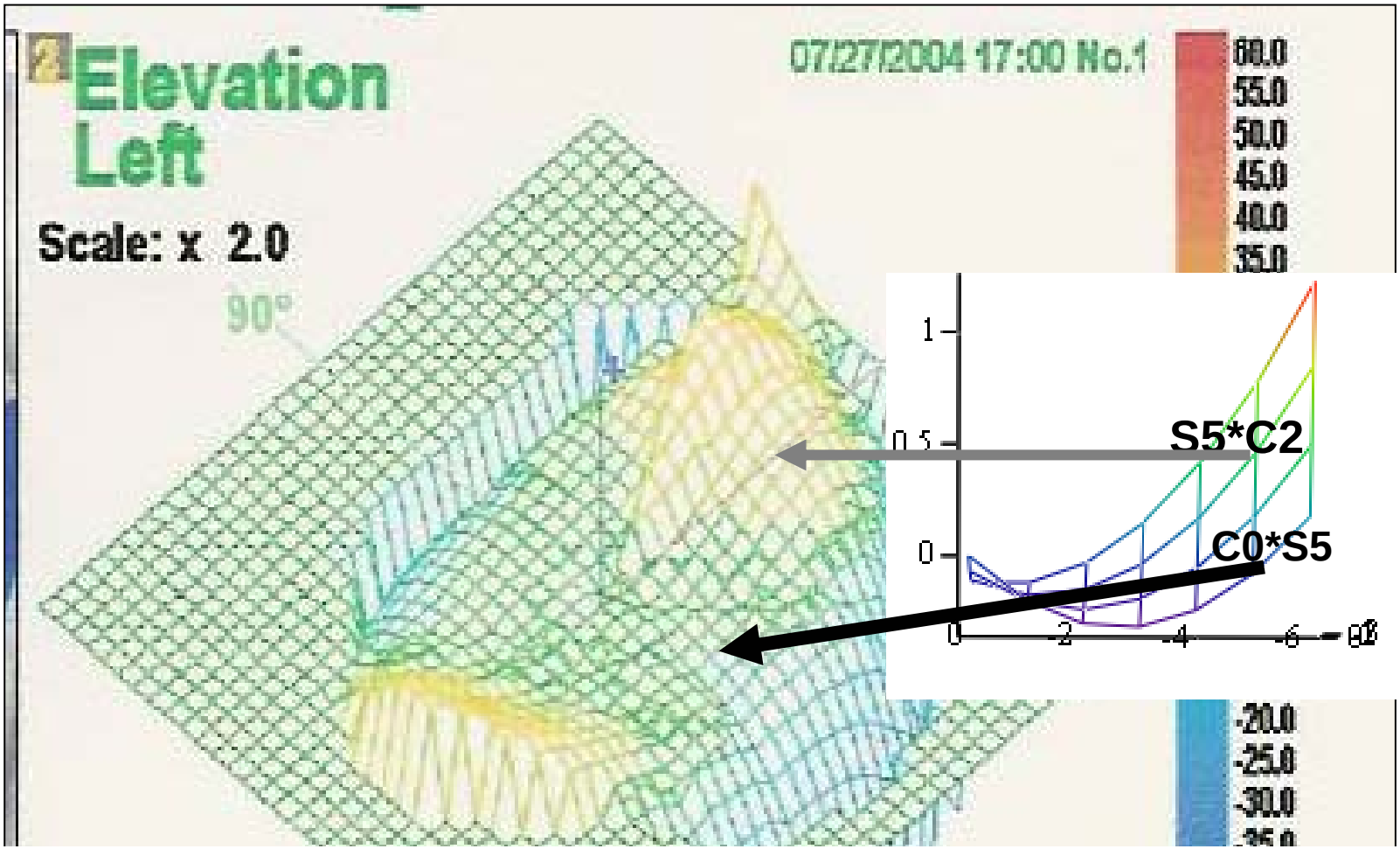

Custom Vue(2004),cylinder with the rule:

Under-treatment of the plus cylinder in the long axis S5*C0

Over-treatment in the short axis S5*C2

The curves generated using the nomogram approximate the central surface contour difference from an ideal ablation .

Visx blend with the rule:

The long axis, corresponding to the S6*C0 curve has moderate under-treatment.

The short axis, corresponding to the S6*C0 curve has mild over-treatment centrally

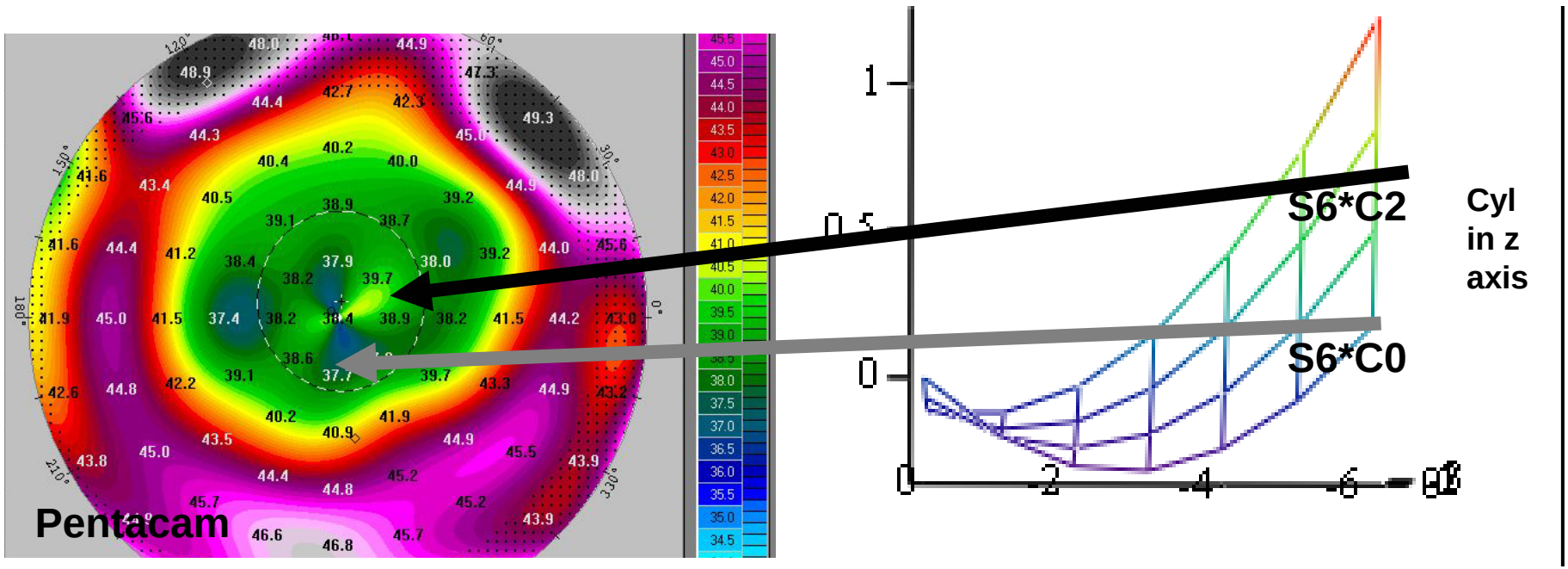

TITLE: Best fit regression modeling of excimer lasers profiles

Submitted Abstract

on September 25, 09:59 PM

for ascrsasoa2007

ABSTRACT BODY:
Purpose: To compare excimer laser ablation patterns with a best fit regression formula of postoperative refractive outcomes. To compare our results with previous studies which show that, with increasing depth of spherical (and toric) ablation, there is a decreased effective optical zone, overcorrection and increased induced spherical (and toric) aberration.

Methods: Refractive outcomes were analyzed using a commercial outcome software program, the Refractive Surgery Consultant™ (RSC), which provides a best fit regression nomogram equation for both sphere(S) and cylinder(C). Standard graphing software (Studyworks™) was used to plot the results within normal treatment profiles. Laser profiles studied were Visx Star™ with a peripheral blend (Standard); Visx CustomVue™, one to six diopters (Low-Wavefront); Visx CustomVue™, six to eleven diopters (High-Wavefront). Nomographs used to interpret the results were in minus cylinder for Standard and High-Wavefront ablations, and plus cylinder for Low-Wavefront. Surface ablation patterns were determined by reviewing surgical video and corneal topography.

Results: Results for Standard ablation (202 eyes) are $S=1.21s +0.04s^2 +0.04sc$ (r^2 0.97) and $C=0.06s +0.011 s^2 +1.18c +0.03c^2 +0.05sc$ (r^2 0.97). Results for Low-Wavefront ablation (1044 eyes) are $S=1.07s +0.01s^2 +0.17c +0.08c^2 +0.05sc$ (r^2 0.97) and $C=1.02c +0.01sc$ (r^2 0.85). Results for High-Wavefront ablation (179 eyes) are $S=1.22s +0.04s^2$ (r^2 0.98) and $C=1.32c +0.06sc$ (r^2 0.97). Standard and High-Wavefront ablations show non-linear increasing overcorrection with increasing sphere, cylinder and sphere times cylinder (coupling). Low-Wavefront ablation shows increasing sphere overcorrection with high cylinder and minimal over or under-correction of cylinder. Patients presenting for enhancement have less induced spherical aberration with Low-Wavefront (0.11u) and High-Wavefront (0.26u), than with Standard (0.52u).

Conclusion: The calculated nomograms are consistent with the previously reported association between overcorrection and imbalance between central and peripheral ablation. Newer wavefront ablation profiles require less nomogram adjustment and induce less higher-order aberrations than previous standard ablation profiles.

With the rule cylinder

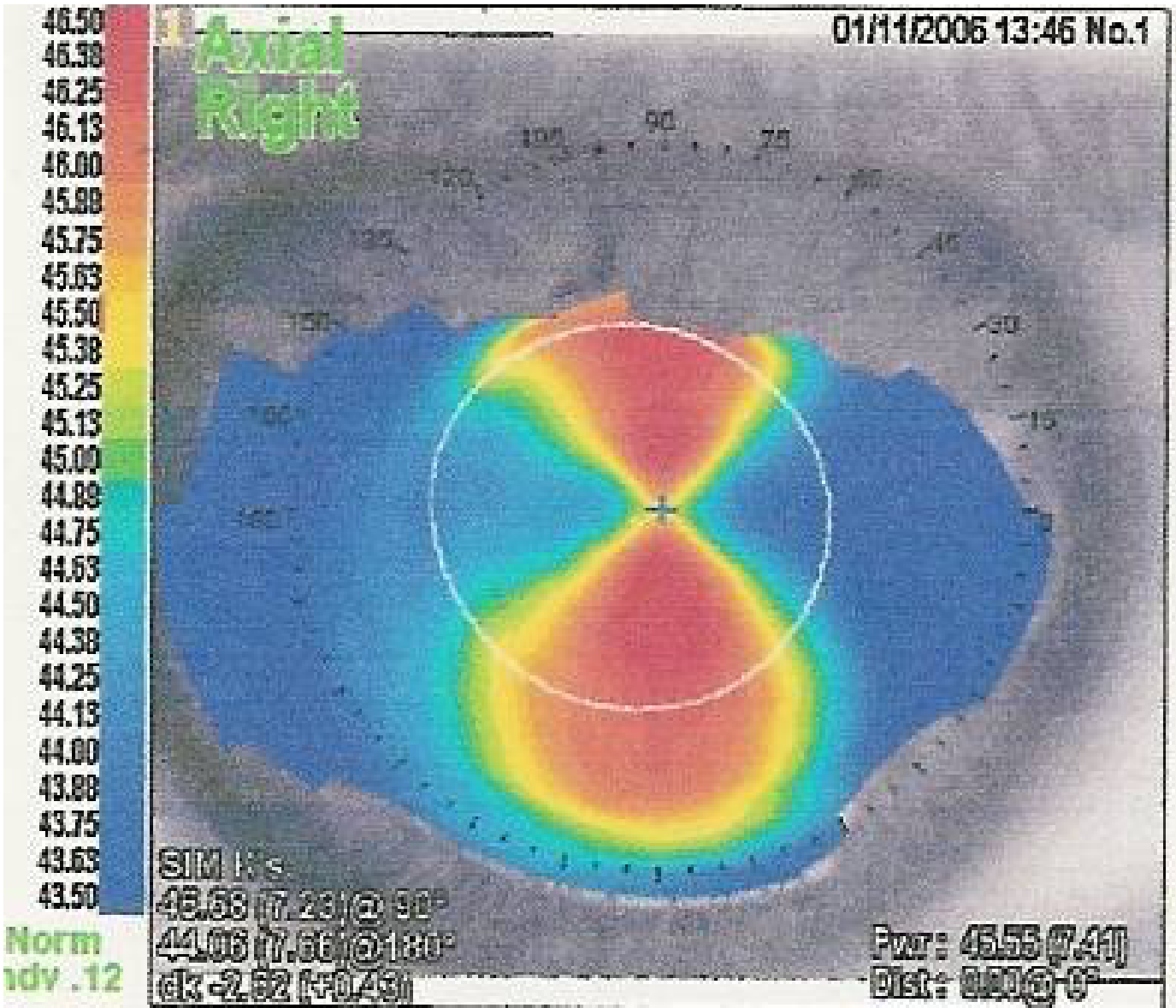

With the rule cylinder compared to a sphere

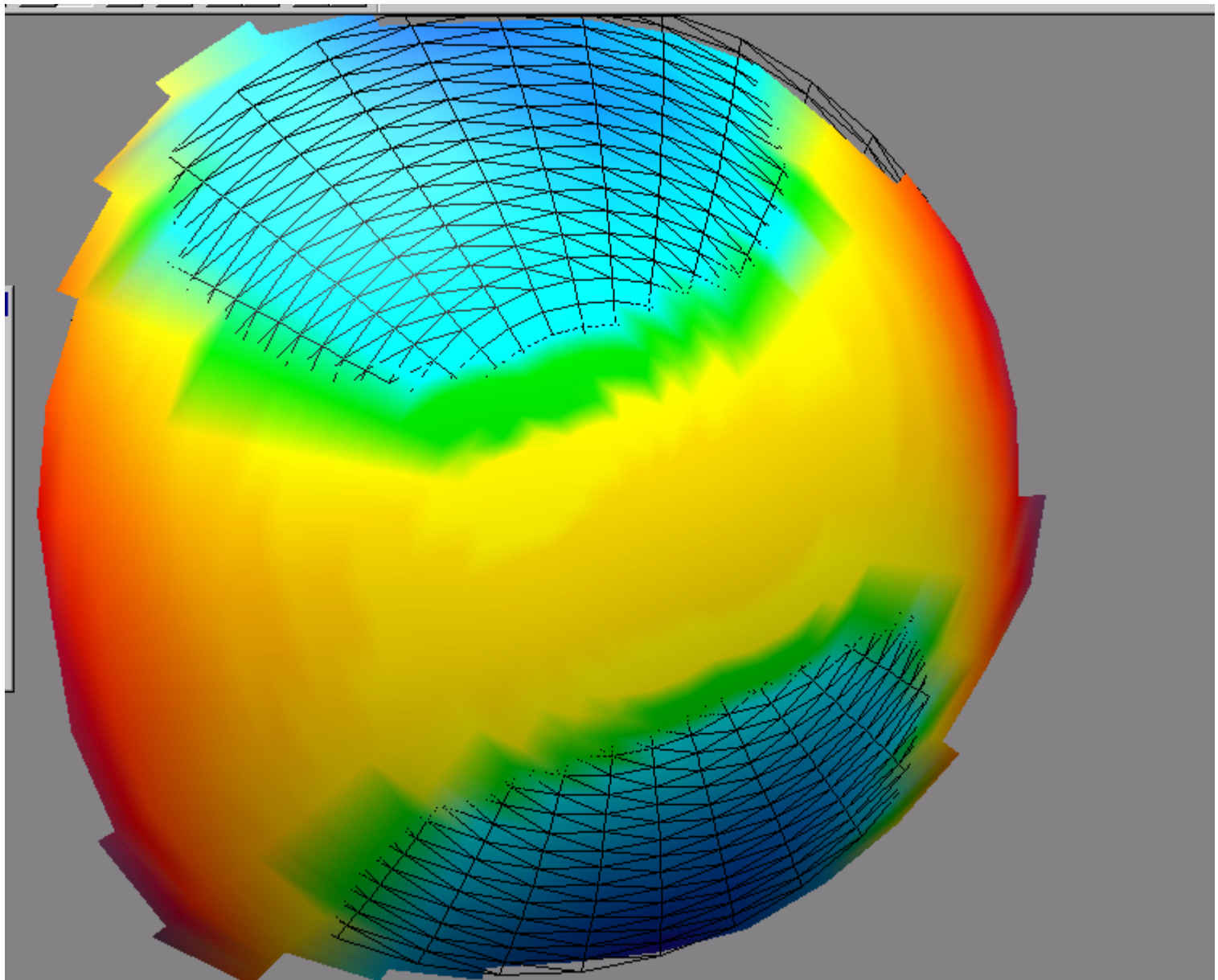

With the rule cylinder

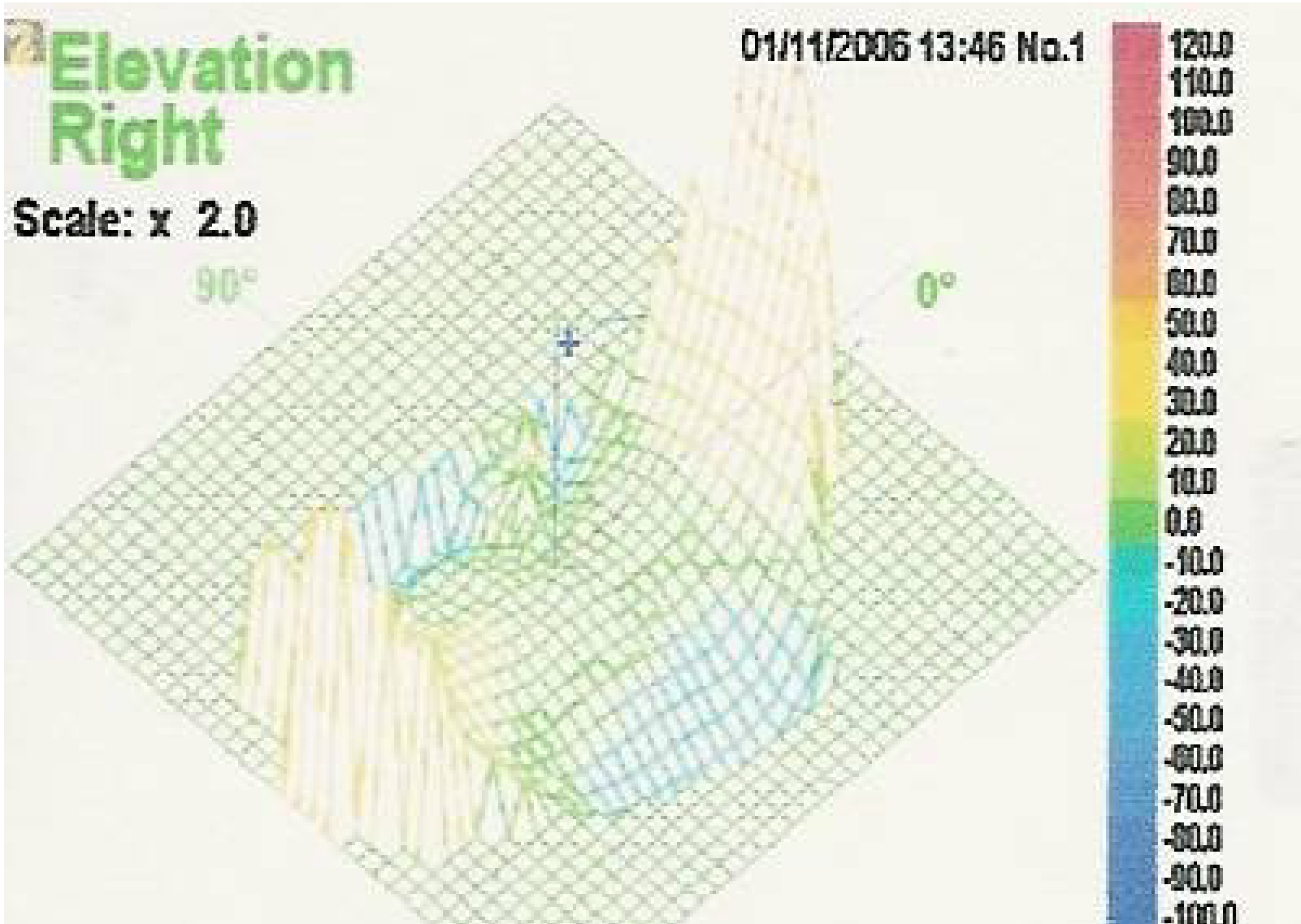

Wavefront Results 2006

Under-treatment of plus cylinder)

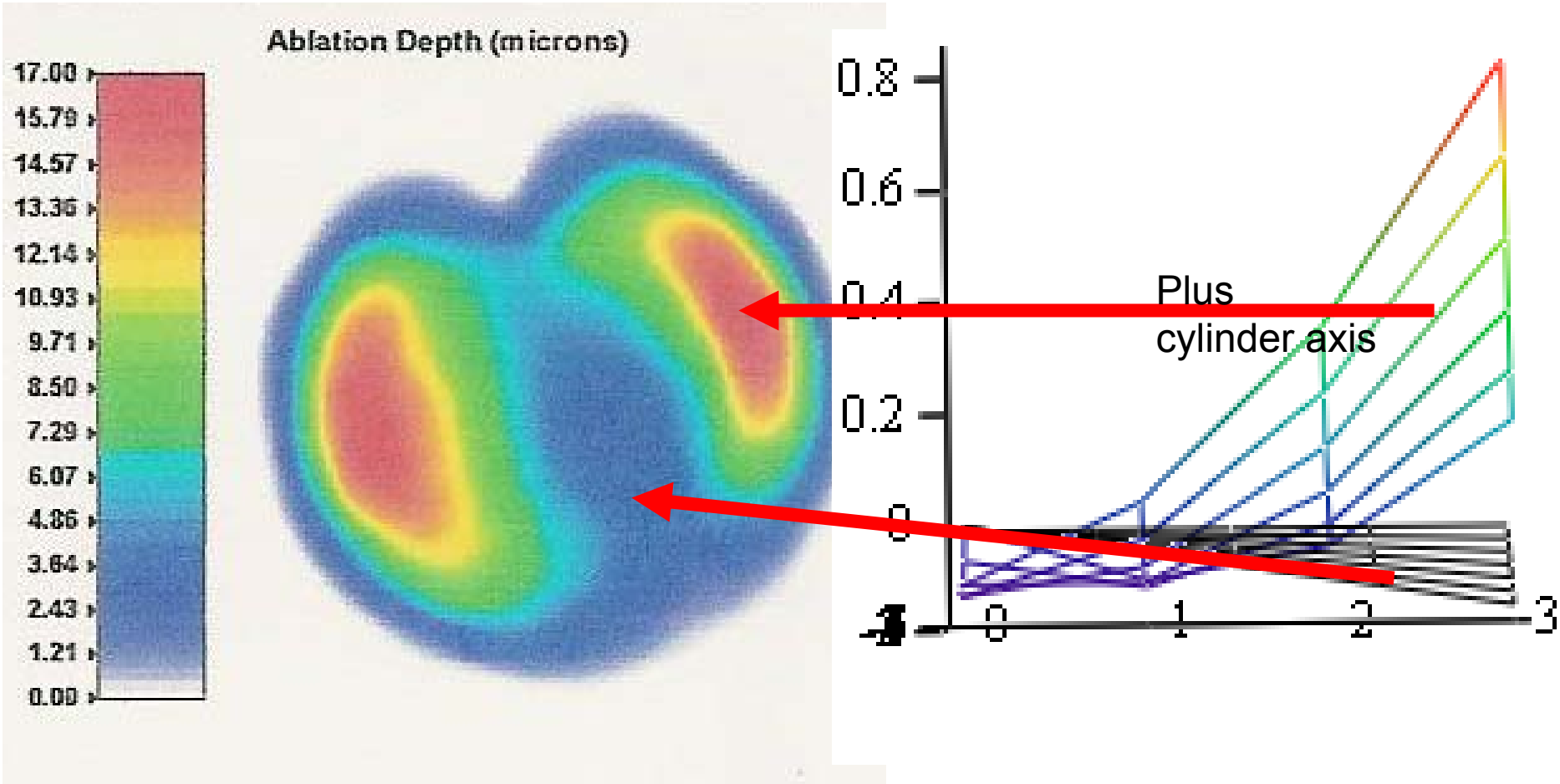

Current trial: increased peripheral blend zone

Effect of excimer laser ablation de-centration on refractive sphere, cylinder and coma

Submitted Abstract
on October 01, 10:45 PM
for ascrsasoa2007

- ABSTRACT BODY:
  Purpose: The purpose of this study is to examine postoperative sphere, cylinder and coma following excimer laser ablation. Decentration of the ablation is expected to cause under-correction of sphere, residual cylinder, and induced coma. Decentration should also theoretically reduce the effective optical zone, thereby increasing atoric aberration and inducing a relative hyperopic shift in the spherical equivalent.
-

  Methods: Sequential patients presenting for enhancement were reviewed. Laser profiles were: Visx CustomVueTM, one to six diopters (Low-Wavefront); Visx CustomVueTM, six to eleven diopters (High-Wavefront); Visx StarTM for high myopia (High-Standard). Average pre-enhancement manifest refraction was compared to the average predicted results using the Refractive Surgery ConsultantTM (RSC), a commercial outcome software program which provides a best fit regression equation for both sphere and cylinder. Increase in coma after surgery was used as a measure of ablation decentration. Within each profile, linear regression between pre- and post-operative sphere, cylinder and coma was examined.

  Results: Low-Wavefront (27 eyes, average primary sphere/cylinder(s/c) -3.49/-1.36) had an average post-enhancement coma of 0.32u and manifest s/c +0.35/-0.76 compared to a predicted RSC result of -0.06/-0.03. High-Wavefront (13 eyes, -6.85/-1.23) had coma of 0.30 with s/c of +0.04/-1.00 compared to predicted -0.10/-0.09. High Standard (18 eyes, -8.18/-1.01) had coma of 0.40 with s/c of -0.37/-0.64, compared to predicted +0.20/-0.44. Regression analysis within each laser profile show a moderate correlation between increasing residual cylinder and relative hyperopic shift in spherical equivalent: Low-Wavefront (r2 0.45), High-Wavefront (r2 0.57) and High-Standard (r2 0.41).

  Conclusion: Increased coma is consistent with decentration as an important cause of residual sphere and cylinder after excimer laser ablation. As expected, decentration with high myopia results in greater relative under-correction of sphere. Increased residual astigmatism is associated with a relative hyperopic shift in spherical equivalent consistent with decreased effective optical zone.

Coma created by tilted optics

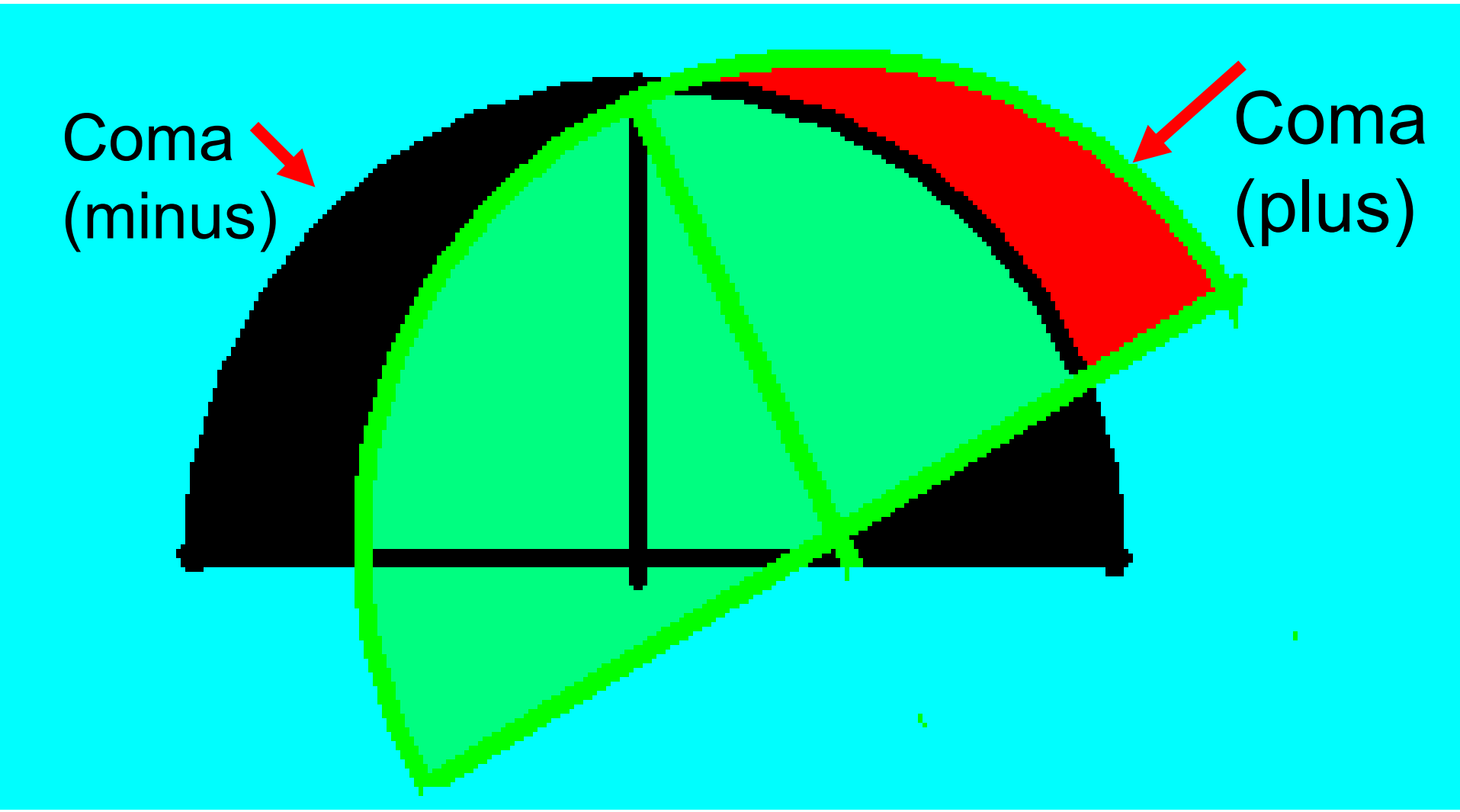

Coma from a de-centered treatment

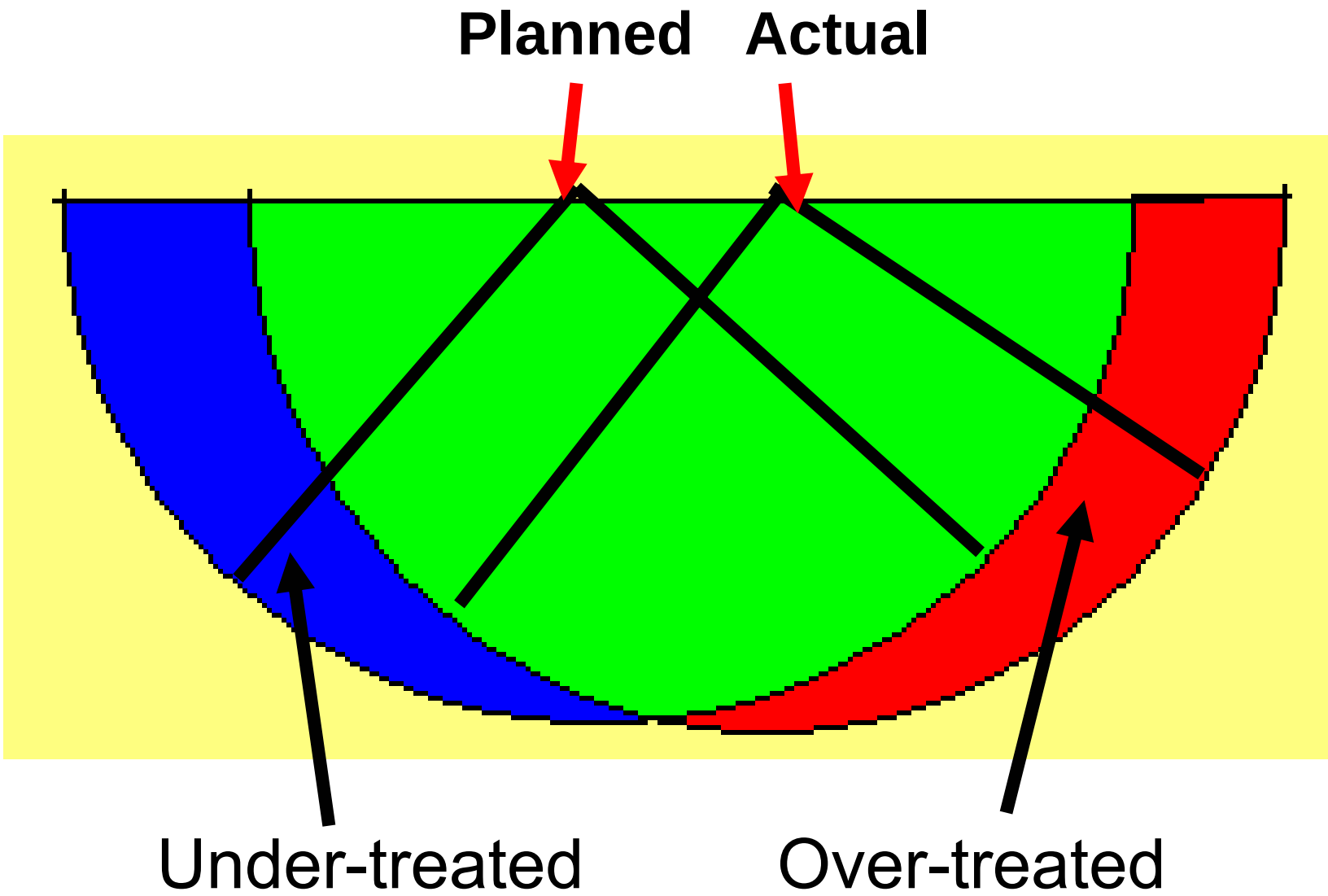

OD

+1.10 DS -1.44 DC x 131° @12.5 mm (4.00 Rx Calc)

30-Mar-2006 12:23:50 W.F. Diam (mm): **6.25** High Order: **33.4 %**

Eff. Blur (D): **0.80** Rms Err.(µ): **1.13** Quality: ✓ ✓ ✓ ✓

Acuity Map

Rms Error (µ): **1.13**

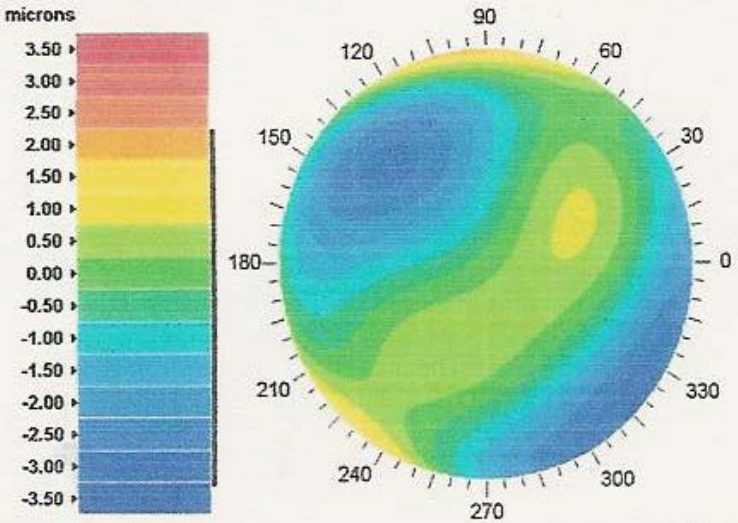

Range: -3.3 to +2.2 microns

Grid spacing: 1 mm.

Normalized Polar Zernike Coefficients (µ) — High Order Aberrations Graph

	Value	Name	0.0 — 0.66784	Axis
Z_{20}	-0.27719	Defocus		
Z_{22}	0.74925 @ 53°	Astigmatism		
Z_{31}	0.66784 @ 137°	Coma		
Z_{33}	0.16670 @ 108°	Trefoil		
Z_{40}	0.22619	Sph. Aberration		
Z_{42}	0.30856 @ 121°			
Z_{44}	0.00605 @ 56°			
Z_{51}	0.04304 @ 270°			
Z_{53}	0.07534 @ 104°			
Z_{55}	0.04483 @ 20°			
Z_{60}	0.10745			
Z_{62}	0.04893 @ 40°			
Z_{64}	0.01197 @ 78°			
Z_{66}	0.03859 @ 55°			

Wavefront High Order Aberrations

Rms Error (µ): **0.80**

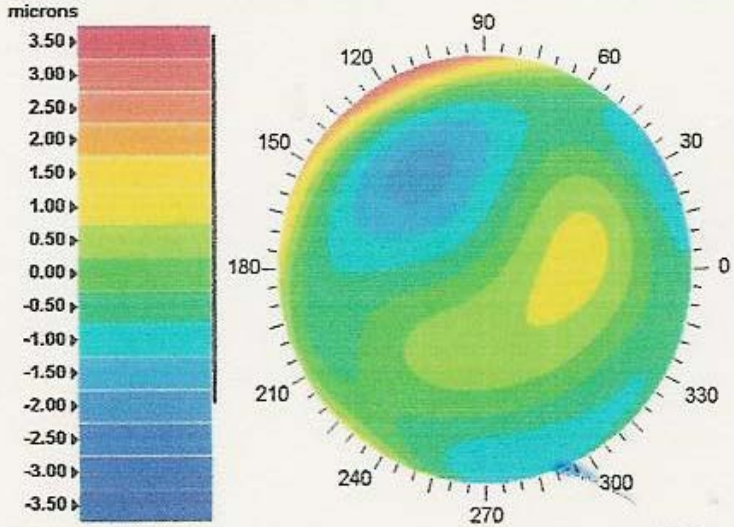

Range: -1.9 to +3.6 microns

Grid spacing: 1 mm.

Eye Image

Limbus Diam: **12.3 mm** Pupil: **8.3 x 8.1 mm @43° (avg 8.2)**

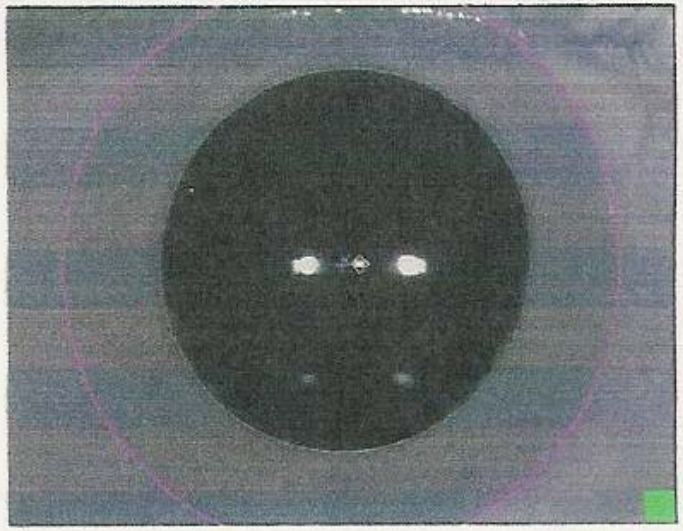

OD +1.10 DS -1.44 DC x 131° @12.5 mm (4.0 Rx Calc)

30-Mar-2006 12:23:50 W.F. Diam (mm): 6.25 High Order: 33.4 %

Eff. Blur (D): 0.80 Rms Err.(μ): 1.13 Quality: ✓ ✓ ✓ ✓

Manifest: +1.22 DS -1.48 DC x 135° @ 12.50 mm

Cycloplegic:

Auto:

Auto+Cyclo:

K1 (D): 39.09 K2 (D): 39.43 K2 Axis(°): 160

Corneal Thickness (μ): 538

Scotopic Pupil Size (mm): 6.00

Limbus Diam: 12.3 mm Pupil: 8.3 x 8.1 mm @43° (avg 8.2)

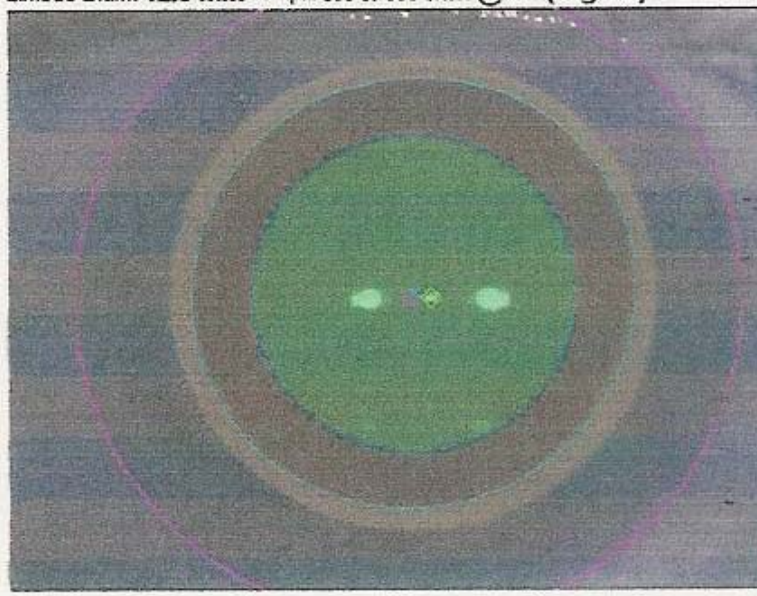

Treatment Type: LASIK Correction Type: CustomVue Nomogram Change: +0%

Physician Adjustments - SPH (D): +0.00 CYL (D): +0.00 Axis(°): VTX(mm): 0.00

Total Correction - SPH (D): +1.12 CYL (D): -1.45 Axis(°): 131 VTX(mm): 0.00

Treatment Parameters

Optical Zone (mm): 6.00

Ablation Zone (mm): 9.00

Max. Ablation Depth (μ): 16.4

No. of Tissue Pulses: 190

Treatment Time (sec): 10

Surgical Parameters

Flap Diameter (mm): 9.50

Flap Thickness (μ): 140

Residual Bed Depth (μ): 382

Additional Information

Distribution of VSS Pulse Diameters

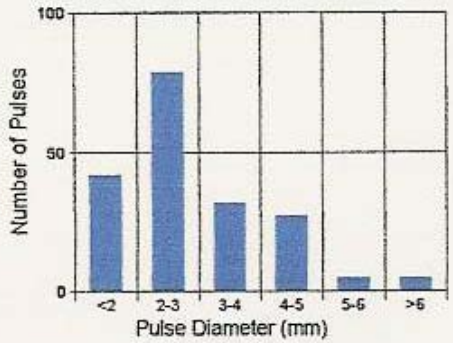

Ablation Depth (microns)

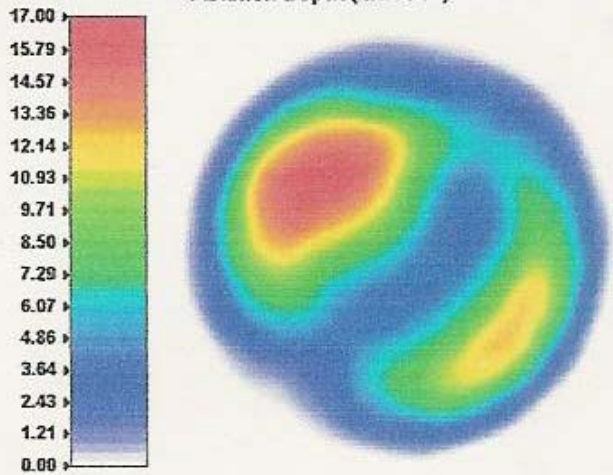

0.5 Flap

OD +1.16 DS -0.95 DC x 25° @12.5 mm (4.00 Rx Calc)

19-May-2006 12:50:49 W.F. Diam (mm): **6.75** High Order: **16.7 %**

Eff. Blur (D): **0.99** Rms Err.(μ): **1.63** Quality: ✓ ✓ ✓ ✓

Acuity Map Rms Error (μ): **1.63**

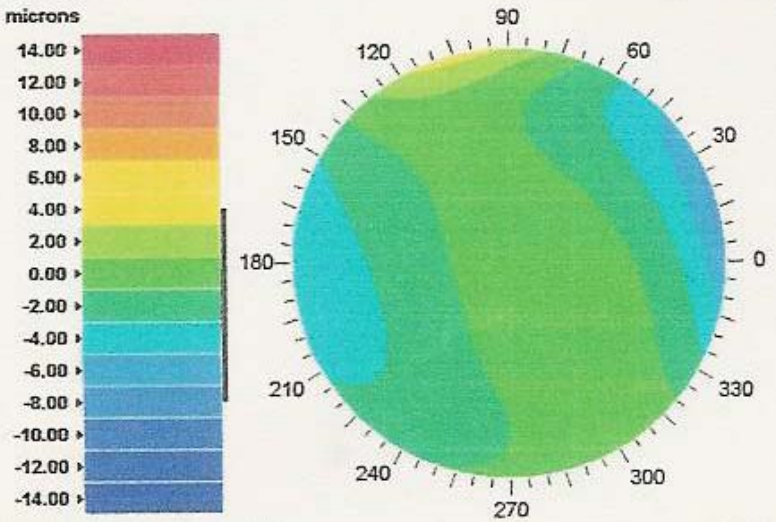

Range: -8.0 to +3.9 microns Grid spacing: 1 mm.

Normalized Polar Zernike Coefficients (μ) **High Order Aberrations Graph**

	Value	Name	0.0 0.40984 Ax
Z_{20}	-0.62230	Defocus	
Z_{22}	1.35157 @ 108°	Astigmatism	
Z_{31}	0.40984 @ 174°	Coma	
Z_{33}	0.36325 @ 95°	Trefoil	
Z_{40}	0.18417	Sph. Aberration	
Z_{42}	0.25398 @ 84°		
Z_{44}	0.11709 @ 29°		
Z_{51}	0.03441 @ 121°		
Z_{53}	0.09901 @ 77°		
Z_{55}	0.06946 @ 33°		
Z_{60}	0.00846		
Z_{62}	0.06351 @ 86°		
Z_{64}	0.00818 @ 50°		
Z_{66}	0.04962 @ 50°		

Wavefront High Order Aberrations Rms Error (μ): **0.66**

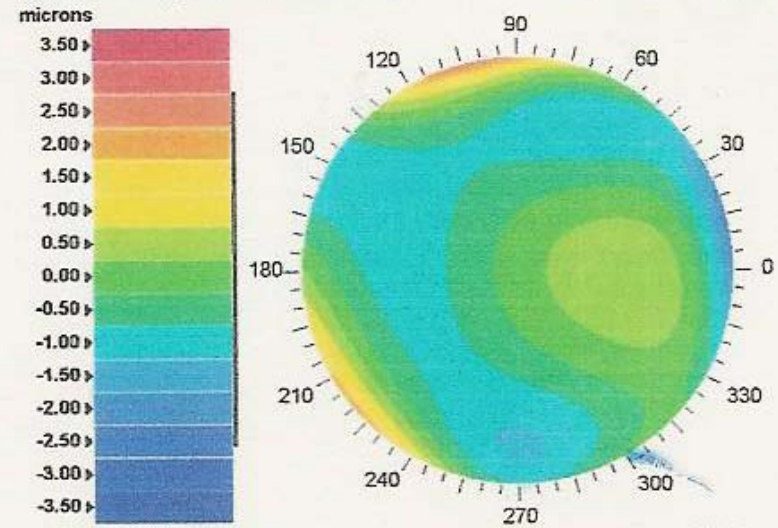

Range: -2.6 to +2.8 microns Grid spacing: 1 mm.

Eye Image Limbus Diam: **12.7 mm** Pupil: **8.4 x 8.1 mm @123° (avg 8.2**

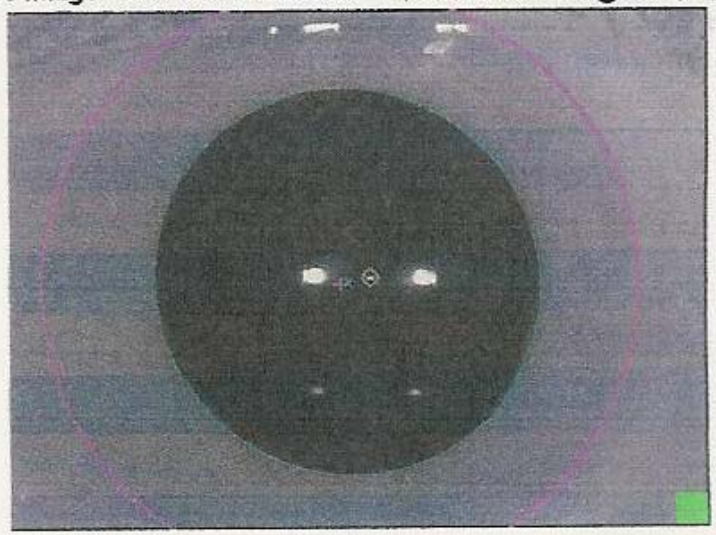

Nebraska Laser Eye Assoc.

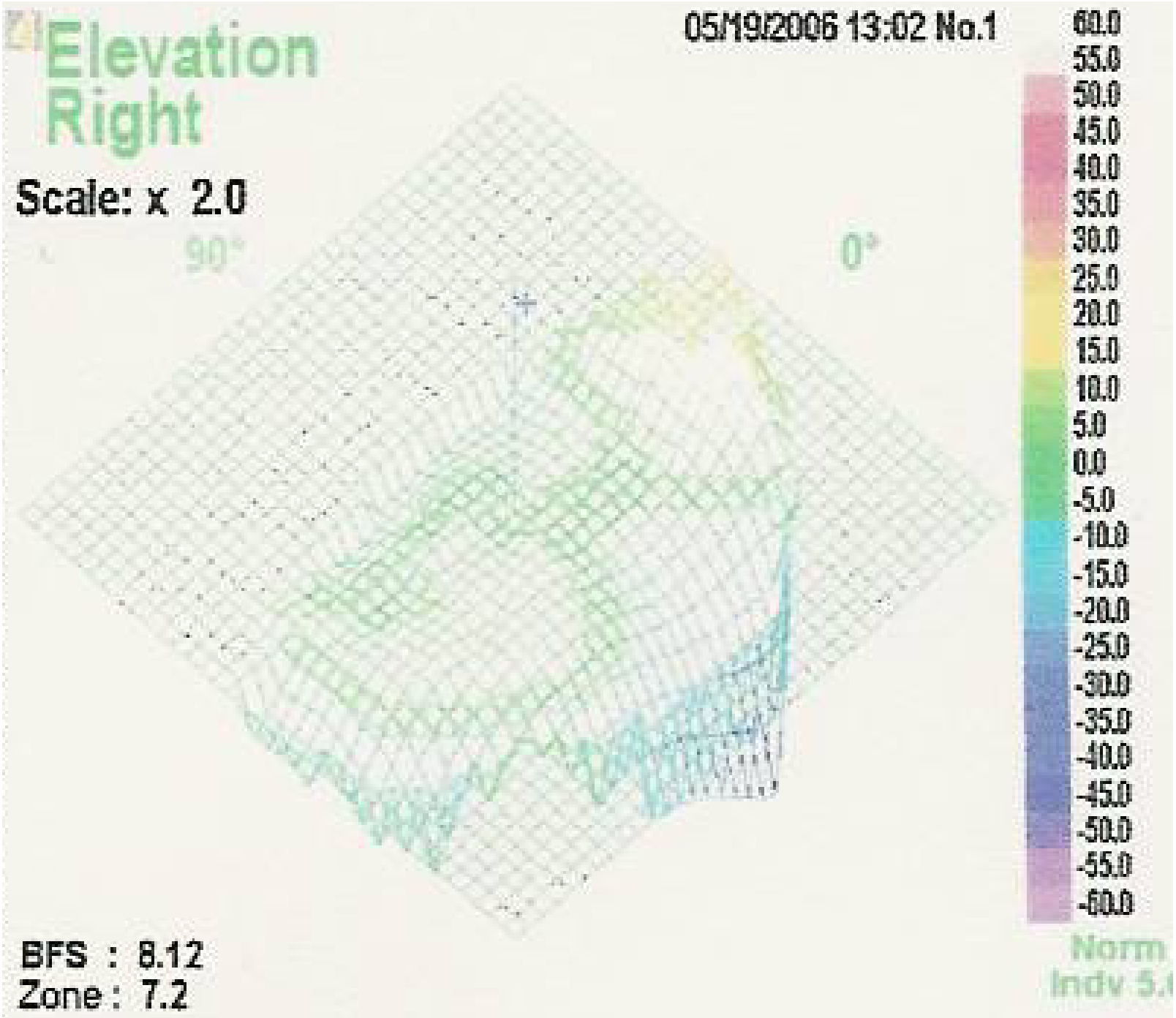
Elevation
Right
05/19/2006 13:02 No.1
Scale: x 2.0
90°
0°
60.0
55.0
50.0
45.0
40.0
35.0
30.0
25.0
20.0
15.0
10.0
5.0
0.0
-5.0
-10.0
-15.0
-20.0
-25.0
-30.0
-35.0
-40.0
-45.0
-50.0
-55.0
-60.0
BFS : 8.12
Zone : 7.2

Decentration Induces Hyperopic Cylinder

Under-treated coma

Over-treated coma

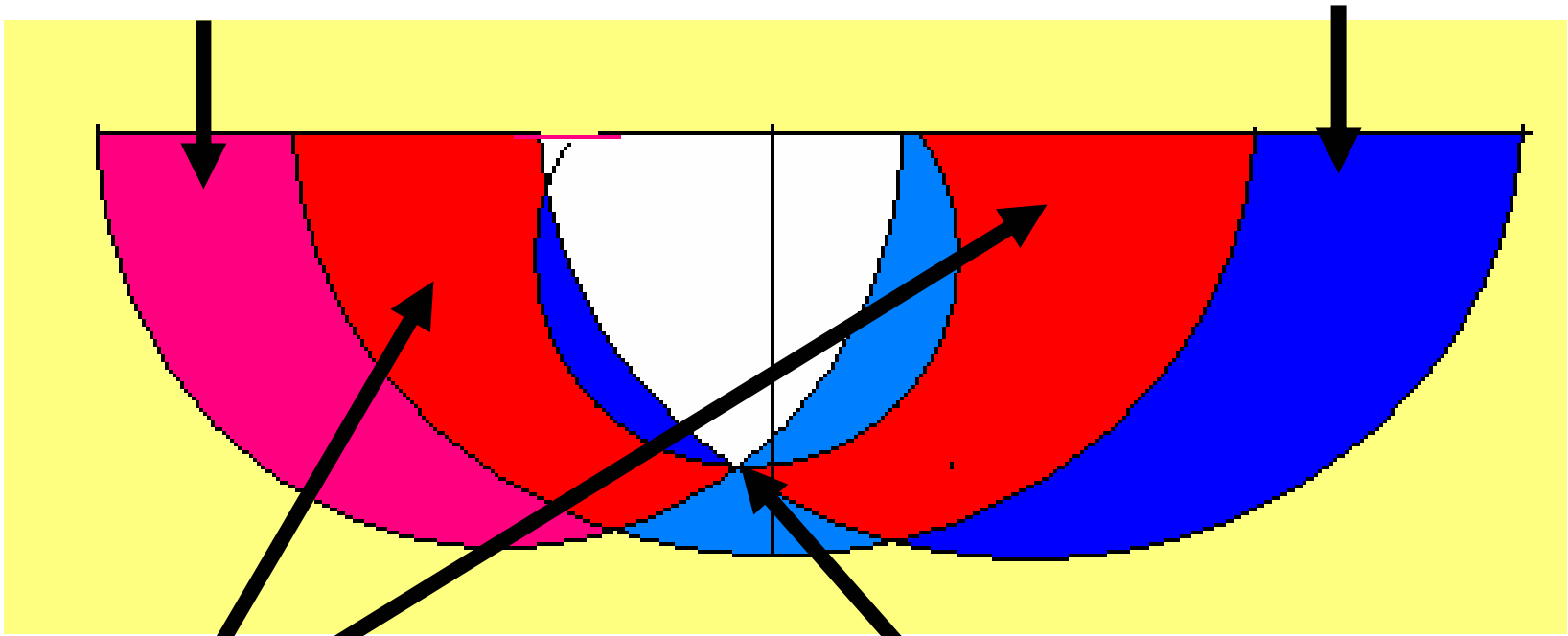

Induced plus cylinder

Best fit sphere to visual axis

OD

+1.16 DS -0.95 DC x 25° @12.5 mm (4.0 Rx Calc)

19-May-2006 12:50:49 W.F. Diam (mm): **6.75** High Order: **16.7 %**

Eff. Blur (D): **0.99** Rms Err.(μ): **1.63** Quality: ✓ ✓ ✓ ✓

Manifest: **+1.04 DS -0.85 DC x 28° @ 12.50 mm**

Cycloplegic:

Auto:

Auto+Cyclo:

K1 (D): **41.41** K2 (D): **42.45** K2 Axis(°): **15**

Corneal Thickness (μ): **477**

Scotopic Pupil Size (mm): **6.00**

Limbus Diam: **12.7 mm** Pupil: **8.4 x 8.1 mm @123° (avg 8.2)**

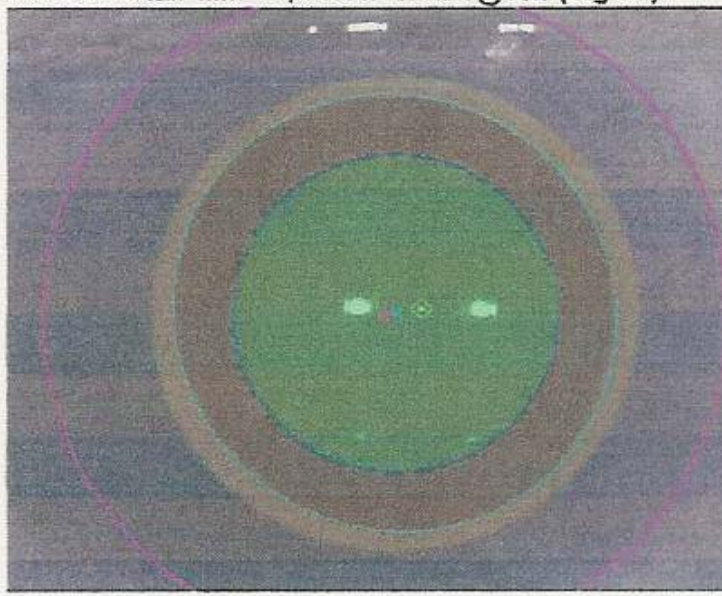

Treatment Type: **LASIK** Correction Type: **CustomVue** Nomogram Change: **+0%**

Physician Adjustments - SPH (D): **+0.00** CYL (D): **+0.00** Axis(°): VTX(mm): **0.00**

Total Correction - SPH (D): **+1.18** CYL (D): **-0.96** Axis(°): **25** VTX(mm): **0.00**

Treatment Parameters

Optical Zone (mm): **6.00**

Ablation Zone (mm): **9.00**

Max. Ablation Depth (μ): **16.6**

No. of Tissue Pulses: **244**

Treatment Time (sec): **12**

Surgical Parameters

Flap Diameter (mm): **9.50**

Flap Thickness (μ): **140**

Residual Bed Depth (μ): **320**

Additional Information

Distribution of VSS Pulse Diameters

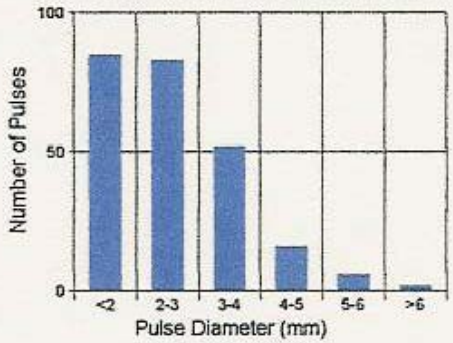

Ablation Depth (microns)

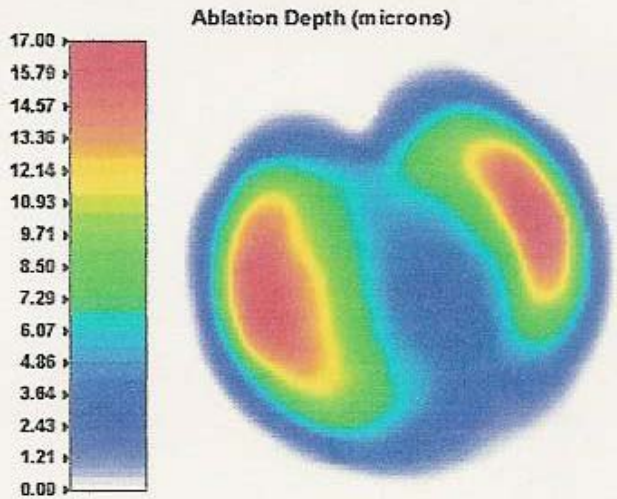

Nebraska Laser Eye Assoc.

ActiveTrak™ : 3-D Eye Tracking

- Infrared cameras
  - Dual side-mounted
- Oblique IR Lighting
  - Does not interfere with surgeon lighting preferences

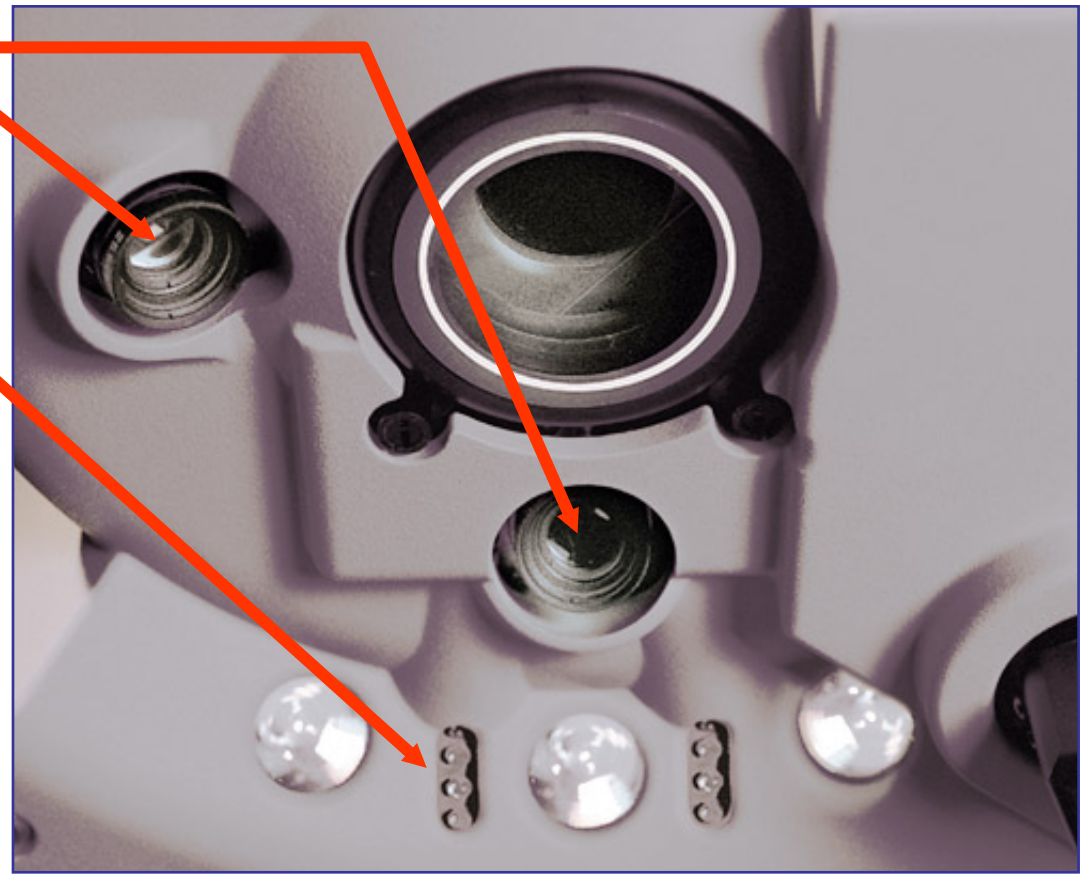

Centroid shift
mesopic:registration photophic:treatment

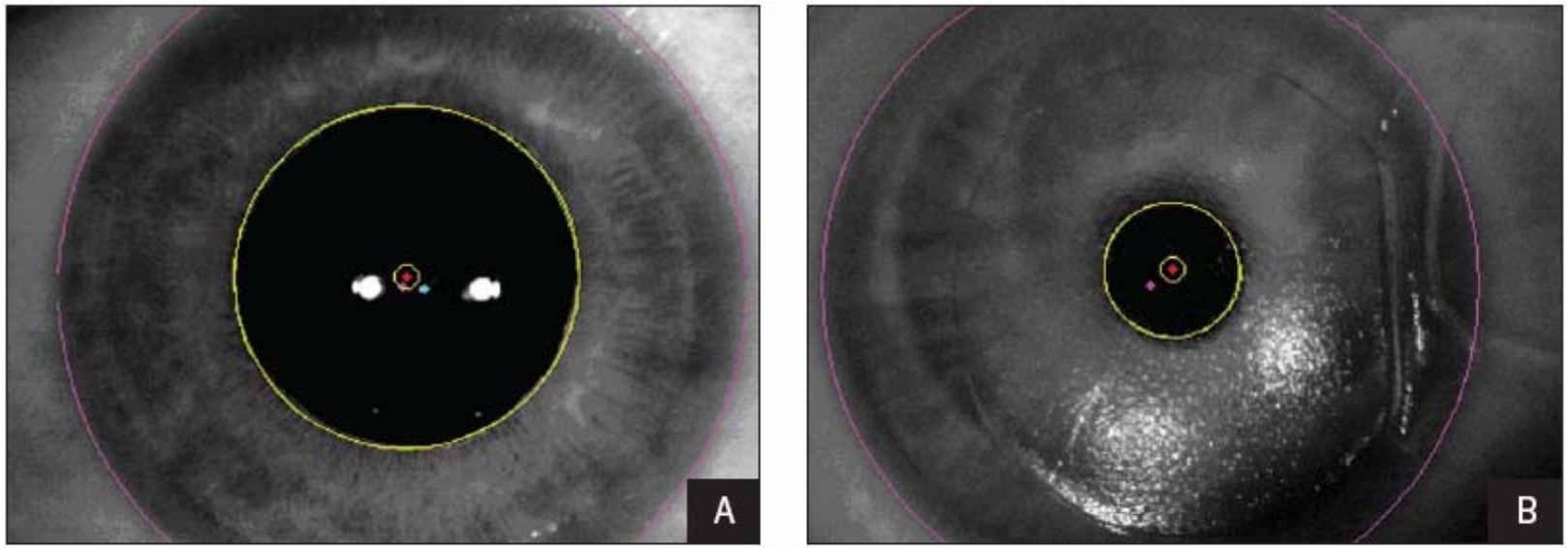

Figure 3. Images of the right eye of patient 1104. **A**) Image taken with the WaveScan camera under mesopic conditions. **B**) Image taken by the laser camera under photopic conditions. In both images, the red dot marks the center of the pupil, which was found using a circle-fit method (circle is denoted by the green line). The yellow "o" marks the center of the pupil, which was found using an elliptical-fit method (ellipse is denoted by the yellow line); the magenta dot marks the center of the iris (iris is denoted by the magenta line). Finally, the cyan dot shows the position of the first Purkinje image in the WaveScan picture. The images show how the pupil center changes as the pupil changes size. The iris center and boundary do not alter with changes in lighting conditions. Note the change in pupil center in relation to the iris center.

Centroid shift-nasal mesopic:registration photophic:treatment

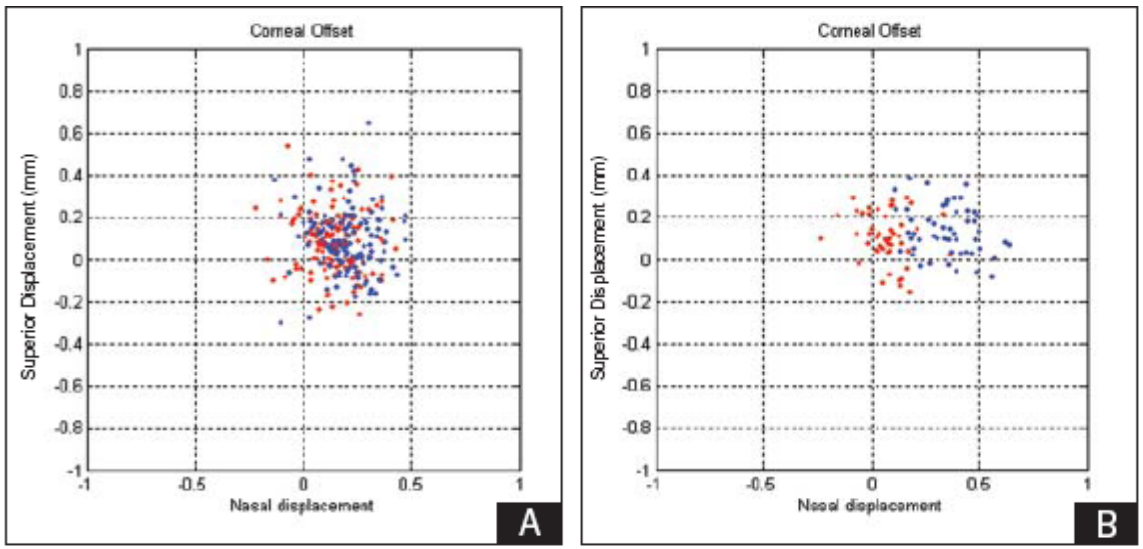

Figure 5. The pupil center relative to the iris center under mesopic and photopic conditions. **A**) Data collected from 130 eyes (Courtesy of Yang et al[3]). **B**) Data collected from 52 eyes measured on the WaveScan instrument under mesopic conditions, and from the laser's on-board camera taken under photopic conditions. The lighting conditions are color coded, with blue representing photopic and red representing mesopic or scotopic conditions. Positive x-axis values represent nasal displacement from the center of the iris in millimeters.

Iris Registration

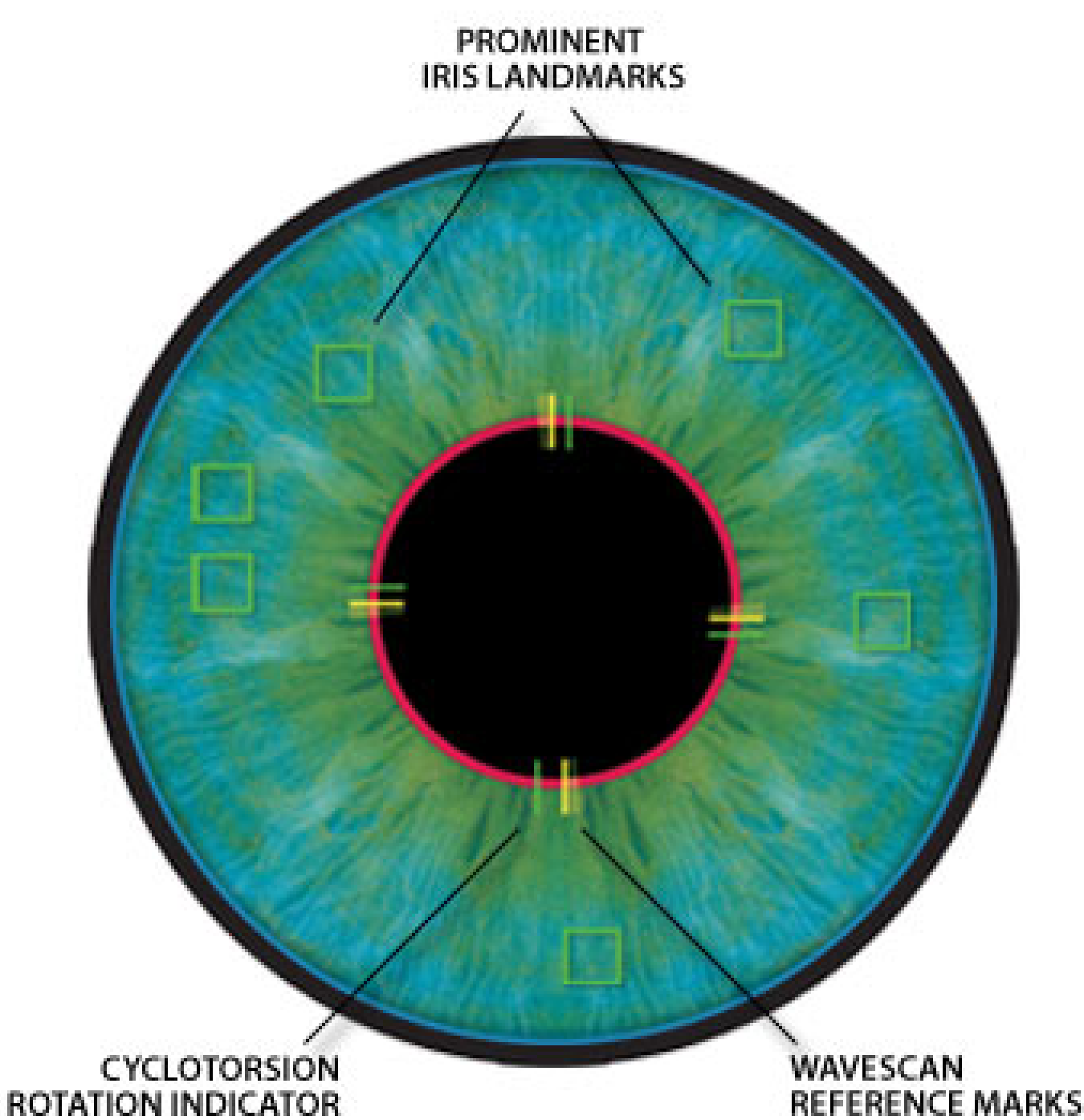

Limbus, and therefore the pupil center, not properly recognized